LUND UNIVERSITY

Moisture permeability of mature concrete, cement mortar and cement paste

Hedenblad, Göran

1993

[Link to publication](#)

Citation for published version (APA):
Hedenblad, G. (1993). *Moisture permeability of mature concrete, cement mortar and cement paste.* [Doctoral Thesis (monograph), Division of Building Materials]. Division of Building Materials, LTH, Lund University.

Total number of authors:
1

Moisture Permeability
of Mature Concrete,
Cement Mortar and Cement Paste

Göran Hedenblad
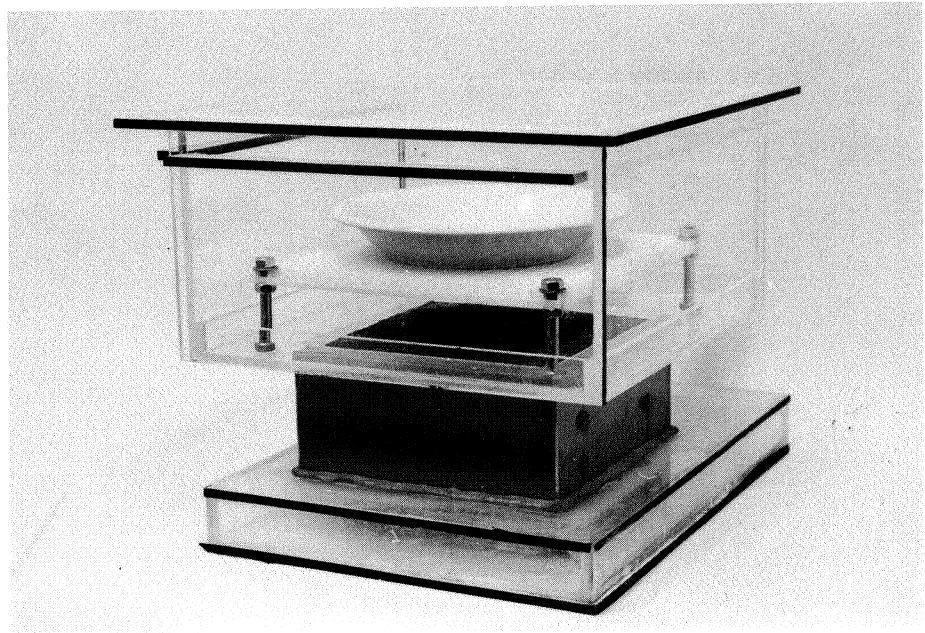
Division of Building Materials
Lund Institute of Technology

To Jenny
   Rikard
   my parents

C O N T E N T S

PREFACE

Moisture research has been performed at the Division of Build-
ing Materials, Lund Institute of Technology (LTH) since its
start in 1964. Both theoretical and experimental research have
been carried out. This thesis is mainly an experimental study.

The Moisture Research Group at the Lund Institute of Technology
(LTH) was established in 1981 to augment the moisture research.
The group consists of researchers from the divisions of
Building Physics, Building Materials and Building Science, all
at LTH. The members of the Moisture Research Group have
provided many valuable suggestions for this work.

I would like to express my sincere gratitude to all those who
have assisted me in this study.

First of all I would like to thank Professor Arne Hillerborg,
who initiated this project about 1985. At that time he was head
of the Division of Building Materials at the Lund Institute of
Technology. His patience and constructive advice have been of
great help to me. I also thank Professor Göran Fagerlund, head
of the Division since 1989, for his advice and for giving me
the opportunity to finish the thesis.

The manufacturing of the specimens and the experimental equip-
ment has been carried out by Bo Johansson, Ingemar Larsson and
Sture Sahlén. They have also had ideas about solving many
practical problems.

The experimental work has been carried out with extreme exacti-
tude by Agneta Ohlsson. I express my sincerest thanks to her.

Constructive discussions have been held with Dr. Johan Claesson
and Jesper Arfvidsson who has furnished me with computer
programs for moisture transport.

I am grateful to Britt Andersson who has drawn the figures, and
to Anni-Britt Nilsson who has polished the typescript.

SUMMARY

The purpose of the investigation was to find moisture transport coefficients for mature concrete which are applicable in realistic situations, and also to analyse the mechanisms of moisture transport.

The main test series comprised specimens of concrete, cement mortar and cement paste. The results are given in Chapters 7, 8 and 9. All specimens had exposed areas of about 0.2*0.2 m. The depths varied from 0.063 to 0.150 m. The influence of varying amounts of aggregate and of air was also studied.

The specimens had their bottom side in water or in moist air and their upper side in 33 % relative humidity (RH). The distribution, at equlibrium, of the relative humidity within the specimens was measured, as well as the amount of transported water. Great emphasis was placed on the avoidance of errors and on making corrections for possible causes of errors.

Theoretical models were applied in connection with the evaluation and analysis of the test results. The model by Gilliland et al (1958) proved very useful for the analysis of moisture transport at very high humidities, where the measurement of the relative humidity gives uncertain results. A composite model may explain the influence of aggregate and of air on the moisture permeability of concrete.

The evaluated moisture permeabilities of concrete are given in TABLE 7.1 and TABLE 7.2 and are summarized in TABLE 16.1. The moisture permeability for cement paste, cement mortar and concrete is nearly constant between about 33 to 70 % RH. Between about 70 to 90 % RH the moisture permeability increases with increasing RH. Above about 90 % RH the moisture permeability

increases strongly with RH. All the test results are given in
APPENDIXES.

NOTATIONS

Symbol	Definition	Dimension
A	area	m^2
A	water sorption coefficient	$kg(m^2s^{1/2})$
B	water penetration coefficient	$m/s^{1/2}$
b	width of the masked edge	m
C	cement content	kg/m^3
D	water vapour diffusion coefficient in the air	m^2/s
D_w	moisture diffusivity	m^2/s
d	thickness	m
f_i	number of ions per salt molecule	1
f	fraction of molecules, which have diffuse reflections	1
G	flow rate	kg/s
G_s	adsorbed layer flow rate	
g	density of moisture flow rate	$kg/(m^2s)$
$\vec{g}$	vector density of moisture flow rate	$kg/(m^2s)$
g_l	density of moisture flow rate which depends on pure liquid transport	$kg/(m^2s)$
g_v	density of moisture flow rate which depends on pure diffusion	$kg/(m^2s)$
h	height of specimen	m
i	number	1
k	a constant in Eq. (13.7)	
L	length	m
M	molar weight	kg/mole
M_w	molar weight of water	0.018 kg/mole
m	$m = 1/B^2$	s/m^2

m_s	mass divided by area of sorbed water from a water surface	kg/m^2
n	number	
n_s	number of mole of salt ions	
n_w	number of mole of water	
P	porosity	%; 1
p	pressure in liquid	Pa
p_v	gas-phase pressure	Pa
p_v	partial water vapour pressure	Pa
p_{vs}	partial water vapour pressure at saturation	Pa
p_w	partial water vapour pressure over pure water	Pa
p_1	partial water vapour pressure over salt solution	Pa
R	general gas constant	8.134 j/(mol k)
r	radius	m
RH	relative humidity	%; 1
S	variable in Eq. (4.3)	
s	pressure difference between the pore water pressure and ambient total pressure	Pa
T	absolute temperature	K
t	time	s
u	moisture content mass by mass	kg/kg
v	humidity by volume	kg/m^3
v_{ref}	humidity by volume at a reference level	kg/m^3
v_s	humidity by volume at saturation	kg/m^3
w	moisture content mass by volume	kg/m^3
w_e	evaporable moisture content mass by volume	kg/m^3
w_n	non-evaporable moisture content mass by volume	kg/m^3
w_o	mixing water	kg/m^3
w_e^∞	eqilibrium moisture content mass by volume	kg/m^3
w_{es}	evaporable moisture content at saturation	(kg)

w_o/C	water-cement ratio	kg/kg
X	surface concentration (in principle w or u counted from a reference level)	
x	coordinate	m
z_v	moisture resistance with regard to humidity by volume	s/m
α	degree of hydration	1
ϵ_2	variable in Eq. (4.4)	
δ_p	moisture permeability with regard to partial vapour pressure	kg/(msPa)
δ_v	moisture permeability with regard to humidity by volume	m^2/s
δ_{v1}	transport coefficient for pure diffusion in a material	m^2/s
δ^s	moisture permeability dependent on suface flow	m^2/s; g/(mhmmHg)
$\delta_v^{mean,1}$	mean moisture permeability between water and 33 % RH	m^2/s
$\delta_v^{mean,2}$	mean moisture permeability between moist air and 33 % RH	m^2/s
η	dynamic viscosity	Ns/m^2
ν	mean velocity	m/s
λ	mean free path	m
λ_m	moisture conductivity	kg/(msPa)
λ_{m1}	transport coefficient for pure capillary suction	kg/(msPa)
ρ	density of air	kg/m^3
ρ_a	mean density of the adsorbate	kg/m^3
ρ_1	density of the liquid	kg/m^3
ρ_w	density of water	kg/m^3
σ	standard deviation	
ϕ	relative humidity (RH)	%; 1
ψ	fundamental flow potential	kg/(ms)

1 INTRODUCTION

1.1 **Moisture in concrete, cement mortar and cement paste**

Moisture in cement-based materials is one condition for the cement to hydrate. In concrete the cement is mixed with water and aggregate (sand and gravel). Some of the mixing water is chemically bound to the cement. The amount (w_n) which is bound to the cement is approximately

$$w_n = 0.25\alpha C \hspace{6cm} (\ 1.1\ )$$

w_n = chemically bound water $\hspace{3cm}$ (kg/m^3)
α = degree of hydration $\hspace{3.7cm}$ (1)
C = cement content $\hspace{4.3cm}$ (kg/m^3)

For concrete with a water-cement ratio (w_o/C) of more than about 0.4, α is able to reach the value 1, but it can take several years.

In "normal" concrete much more water is used at the mixing than can be chemically bound. Some of the water is physically bound to the structure of the cement paste. The amount which is fixated ($w_{e\infty}$) depends on whether the material is under rewetting (absorption) or under drying (desorption) and on the relative humidity (RH). The connection in principle between the moisture content, which is physically bound, and RH is given in FIG 1.1.

1

Equilibrium moisture content, $w_{e\infty}$

Desorption

Scanning curves

Absorption

0   50   100 RH(%)
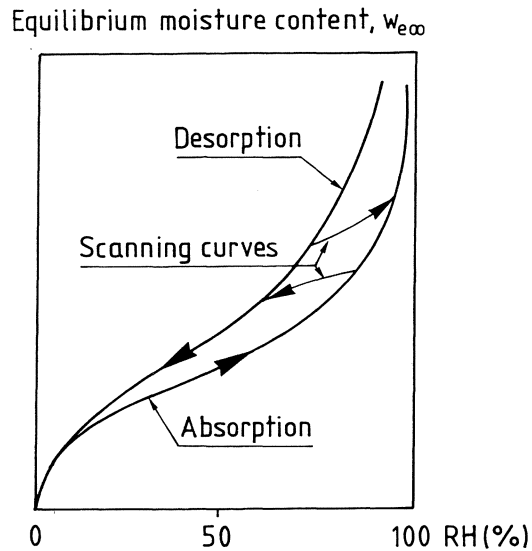
FIG 1.1   Sorption isotherms in principle.
           Nilsson (1980).

The material at drying follows the desorption isotherm, whereas
at rewetting the absorption isotherm is followed. If the
material is first dried out to some extent and then rewetted, a
scanning curve is followed. In concrete, which can have
different degrees of hydration, more water is physically bound
to the structure at a higher degree of hydration within the RH
range 0-45 % but less water in the range 45 to 100 %.

If the whole material does not have the same RH, at constant
temperature, moisture is transported from one part of the
material to another. Moisture can also be transported to or
from the material. The moisture transport is described
by means of moisture transport coefficients. The transport
coefficients can have different potentials, but it is possible
to relate the moisture transport coefficients with different

2

potentials to each other; see Chapter 2. The moisture transport
coefficients are not constants; they depend on the moisture
content or the relative humidity of the material; see FIG 1.2.
For the definition of δ_v, see Eq. (2.1).

$$\delta_v \; (m^2/s)$$

0   100 RH (%)
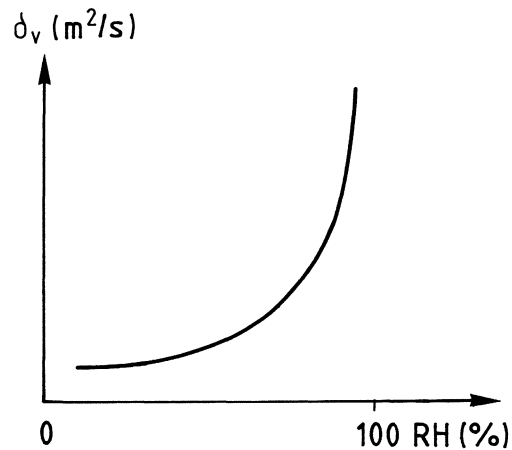
FIG 1.2 Moisture permeability (with the humidity by volume as
          potential) as a function of the relative humidity.
          In principle.

The moisture transport coefficients for cement-based materials
also depends on the degree of hydration and probably also on
whether the material is under absorption or desorption. The
temperature could also have an influence on the moisture
transport coefficients.

According to Fick's first law, which is valid for steady state
calculations, we can write

$\vec{g} = -D_w * grad \; w_e$ (1.2)

$\vec{g}$ = vector density of moisture flow rate $(kg/(m^2s))$
D_w = moisture diffusivity (m^2/s)
w_e = evaporable moisture content mass by volume (kg/m^3)

3

When a material is under non-steady conditions such as drying, Fick's second law is used. In one dimension it is written

$$\partial w_e / \partial t = - \partial /(g)/\partial x = \partial(D_w * \partial w_e / \partial x)/\partial x \qquad (\ 1.3 \ )$$

$$t = time \qquad\qquad\qquad\qquad\qquad (\ s \ )$$

Fick's laws can be used for cement products, when there is no, or very small, hydration going on.

1.2 **Literature survey**

Pihlajavaara (1965) showed the diffusivity for cement mortar with w_o/C 0.56 and with maximum particle size of the aggregate 1.4 mm. He used prisms 4*4*16 cm which were membrane cured for about 10 months before the drying was started. The drying was unidimensional and occurred from the short sides of the prisms. The drying took place in two different climates, namely 40 % RH, 20°C and 70 % RH, 20°C. Seven prisms in each climate were allowed to dry for different periods of time. After 68, 179, and 293 days of drying, prisms from each climate were taken out and the moisture distribution of the prisms was determined. The diffusivity was determined as a function of the moisture content of the specimens, see FIG 1.3.

C in FIG 1.3 refers to the moisture content by volume in the cement mortar. C^{cp} indicates the moisture content by volume in the cement paste (kg moisture in cement mortar by m^3 cement paste in cement mortar).

$$k = k_e(1 + bu^n)$$

Curve N:o	b	n
①	2.51	2.60
②	4.90	4.09
③	11.2	5.22

k $10^{-11}\ \frac{m^2}{s}$

u →   0   0.2   0.4   0.6   0.8   1

$\varphi = 40\%$ C → 60 80 100 120 140 160 kg
C^{cp} → 200 300 400 m^3

$\varphi = 70\%$ C → 90 100 110 120 130 140 150 160 170 kg
C^{cp} → 200 300 400 m^3
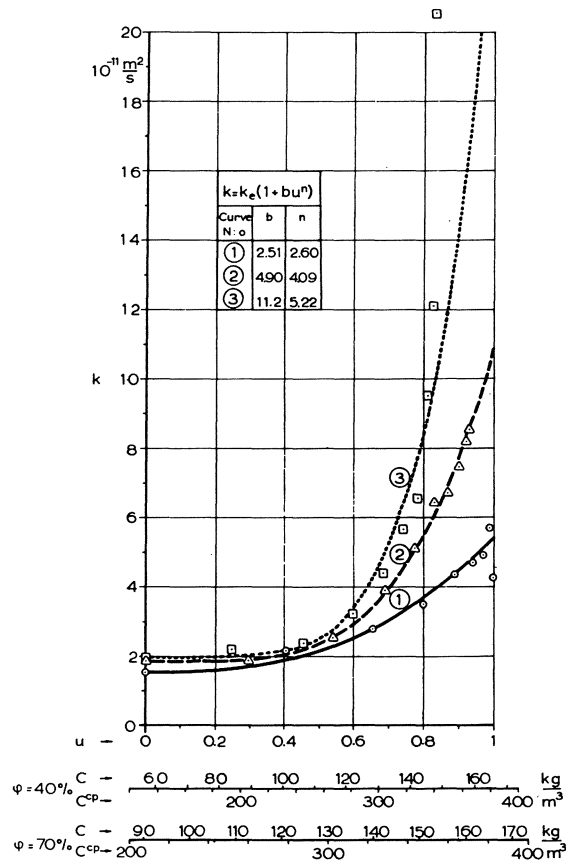
FIG 1.3   Diffusivity as a function of the moisture content
of cement mortar. Pihlajavaara (1965).

Curves 1, 2 and 3 in FIG 1.3 represent the diffusivities after
68, 179 and 293 days of drying. In FIG 1.3 it is shown that D_w
depends both on the drying time and the drying climate. If D_w
should be shown as a function of the moisture content by volume
(C in FIG 1.3), six curves were obtained. Pihlajavaara pointed
out that at high moisture content the evaluation of the
relationship between the diffusivity and moisture content is
unreliable.

Pihlajavaara's measurements of the moisture content in the
prisms have been used in section 14.4 to compare calculated
drying, with moisture transport coefficients according to this
thesis, with measured drying.

Băzant & Najjar (1972) mathematically analysed some measurements that were reported in the literature. They arrived at the conclusion that the diffusivity should have the general appearance shown in FIG 1.4.
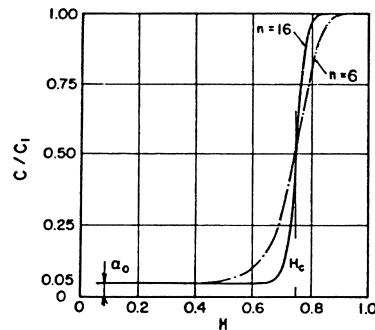
FIG 1.4   Variation of relative diffusivity as a function
          of relative humidity.
          Bažant & Najjar (1972).

H in FIG 1.4 is the relative humidity and C/C_1 is the diffusivity at a certain RH expressed as a function of the maximal diffusivity.

At low RHs (below 60 to 70 %), the diffusivity is only 5 % of the maximal value. At 75 % RH, C/C_1 is 0.5. At about 80 to 90 %, RH the maximal value is reached. In most of the calculated cases the curve n=16 is used, which means that the maximal diffusivity is obtained at about 80 % RH. Băzant & Najjar assumed that the desorption isotherms were straight lines.

Nilsson (1980) measured the moisture permeability of three cement mortars with different w_o/C, namely 0.4, 0.6 and 0.8. The measurements where made with the cup method, in a special way, so that the moisture permeability was obtained as a function of the relative humidity. The specimens had a thickness of 5 and 10 mm, and the maximal size of aggregate was 1 mm. The specimens were cured in water for a month before they

were placed in the cups. The measurements lasted about half a
year. Nilsson calculated the diffusivities from the moisture
permeabilities, and D_w is shown in FIG 1.5.

$D(10^{-11} m^2/s)$
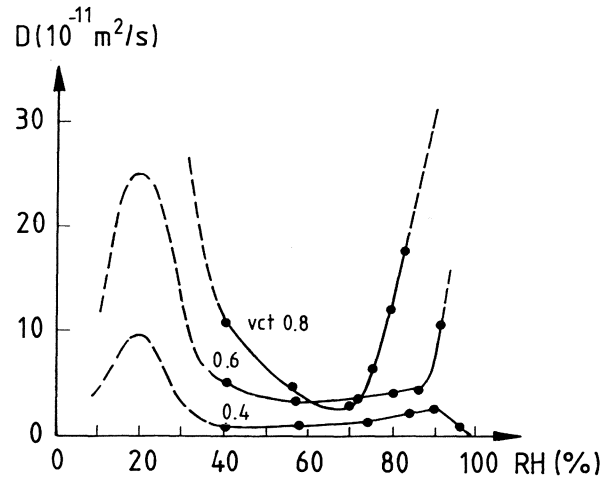
FIG 1.5 Diffusivities as functions of the relative humidity
          for cement mortar with w_o/C 0.4, 0.6 and 0.8.
          Nilsson (1980).

The three different cement mortars have different shapes and
not the general shape that is shown in FIG 1.4. The diffusivity
for w_o/C 0.4 decreases for RH over 90 %. For w_o/C 0.6, there is
a stronger increase in the diffusivity at about 90 % RH.

Sakata (1983) has made drying experiments with concrete prisms
10*10*L cm, where L was 8, 16, 24, 32 and 40 cm. The drying was
unidimensional and occurred from the 10 * 10 cm sides of the
prisms. Ordinary portland cement was used. The diffusivities
for concrete with w_o/C 0.48 are shown as functions of the
moisture content w_e/w_e^{max} in FIG 1.6. The diffusivity 0.1
cm^2/day corresponds to $11.6 * 10^{-11}$ m^2/s.

7
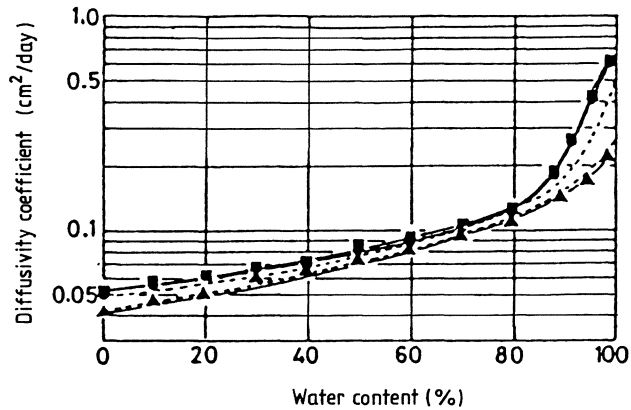
FIG 1.6 Diffusivities as functions of the moisture content
w_e/w_e^{max}. Concrete with w_o/C 0.48.
Sakata (1983).

FIG 1.6 shows that the diffusivity depends on the moisture
content of the concrete. The diffusivities increase with
increasing moisture content. The quotient between maximal and
minimal diffusivity is about 10.

When FIG 1.3 to FIG 1.6 are compared, it is seen that,
for most of the figures, the higher the moisture content or RH,
the higher the diffusivities. When FIG 1.4 is compared with
FIG 1.5, it is seen that in FIG 1.5 there is not a general
shape of the diffusivities as shown in FIG 1.4. In FIG 1.3 the
diffusivities start to increase when the relative moisture
content is about 0.5, and in FIG 1.6 the increase starts at 0 %
moisture content.

1.3 Ideas behind our experiment

Some of the ideas behind our attempt to determine the moisture transport coefficients are listed below:

* The dimensions of the specimens (in the flow direction) should be in the same range as those used in ordinary buildings.

* Some of the compositions of the concrete qualities to be used in the study should closely correspond to compositions of concrete qualities commonly used in Sweden.

* Simulation of the customary conditions, e.g. slab on the ground, seal curing and drying from one side with normal relative humidity on that side, should be carried out.

* A check should be conducted to see if there is a big increase in the moisture flow from the specimens in direct contact with water (capillary suction), as compared to specimens in contact with moist air.

2   CHARACTERISATION OF THE MOISTURE FLOW

2.1   Moisture flow coefficients

The density of the moisture flow rate in a material, under
isothermal conditions, is normally given by one of the
following equations;

$$\vec{g} = -\delta_v \; \text{grad} \; v \qquad\qquad\qquad (\; 2.1 \;)$$

$$\vec{g} = -\delta_p \; \text{grad} \; p_v \qquad\qquad\qquad (\; 2.2 \;)$$

$$\vec{g} = -D_w \; \text{grad} \; w \qquad\qquad\qquad (\; 2.3 \;)$$

$$\vec{g} = \lambda_m \; \text{grad} \; s \qquad\qquad\qquad (\; 2.4 \;)$$

$\vec{g}$ = the vector density of moisture flow rate $(kg/(m^2 s))$

v = the humidity by volume in the pores (kg/m^3)

δ_v = the moisture permeability with regard to
humidity by volume (m^2/s)

p_v = the partial vapour pressure in the pores (Pa)

δ_p = the moisture permeability with regard to
partial vapour pressure $(kg/(msPa))$

w = the moisture content mass by volume (kg/m^3)

D_w = the moisture diffusivity (m^2/s)

s = the suction in the pore water, the (Pa)
pressure between the pore water and
the ambient total pressure

λ_m = the moisture conductivity $(kg/(msPa))$

Equations (2.1) and (2.2) are normally used when the relative humidity (RH) in the pores of the material is below about 97 to 98 % (in the hygroscopic range).

Equation (2.3) can be used in the whole range from dry material up to material which is saturated with water. One disadvantage of grad w as the driving force for the moisture flow is that w in the border line of two different materials that are in connection with each other is not the same. With grad w as the driving force, it is impossible to calculate even the stationary case if you does not know the sorption isotherms for the materials.

Equation (2.4) is seldom used, as the suction in the pore water is normally not measured (in Sweden).

The moisture transport coefficients (δ_v, δ_p, D_w and λ_m) for many materials are not constants, but vary with the moisture content in the material and probably with the temperature. They may also be different depending on whether the material is under desorption or absorption.

In a real material there is not one single potential even if Eq.(2.1) to Eq.(2.4) treat the moisture transport as dependent on one potential only. The transport coefficients in Eq. (2.1) to Eq.(2.4) describe the total transport of moisture in the material. Theoretically, you can divide the moisture flow into two parts, one which depends on pure diffusion and one which depends on the capillary suction which acts on the moisture in the liquid phase. FIG 2.1 describes the flow in a material.
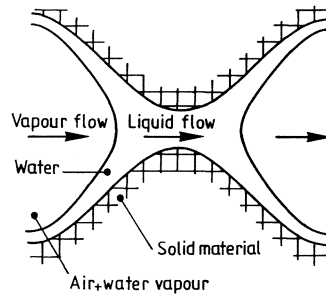
FIG 2.1   Combined moisture transport in a material.
         Andersson (1985).

$$g = g_v + g_1 = \delta_{v1} \text{ grad } v + \lambda_{m1} \text{ grad } s \qquad\qquad (\; 2.5 \;)$$

g_v = the moisture flow which depends on pure diffusion

g_1 = the moisture flow which depends on pure liquid transport

δ_{v1} = the transport coefficient for pure diffusion

λ_{m1} = the transport coefficient for pure capillary suction

There is a relationship between v and s; see below.

In FIG 2.2, Andersson (1985), the principal variation of the moisture transport coefficients δ_{v1} and λ_{m1} is drawn as a function of the moisture content.
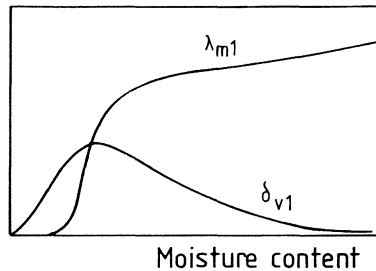
FIG 2.2   Principal variation of the moisture transport
         coefficients δ_{v1} and λ_{m1} with the moisture content
         of the material.
         Andersson (1985).

2.1.1 Relations between different moisture flow coefficients

The moisture flow under isothermal conditions is given by Eq. (2.1) to Eq.(2.4). The equality of the chemical potentials of the liquid and its vapour at equilibrium gives the relation between the partial vapour pressure and the pressure in the liquid, the Kelvin equation; see Andersson (1985).

$$p - p_{vs} = (RT\rho_w/M_w) \ln(p_v/p_{vs}) \qquad\qquad (\ 2.6\ )$$

p_{vs} is normally very small compared to p and the equation (2.6) is written

$$p = (RT\rho_w/M_w) \ln(p_v/p_{vs}) \qquad\qquad (\ 2.7\ )$$

p = the pressure in the liquid $\qquad\qquad$ (Pa)

p_{vs} = the partial vapour pressure at saturation $\quad$ (Pa)

R = general gas constant $\qquad\qquad$ (8.314 J/mol K)

T = temperature $\qquad\qquad$ (K)

ρ_w = the density of the liquid water $\qquad\qquad$ (kg/m^3)

M_w = the molar weight of water $\qquad\qquad$ (0.018 kg/mol)

Derivation in one dimension gives

$$\delta p/\delta x = (RT\rho_w/(M_w p_v))\ \delta p_v/\delta x \qquad\qquad (\ 2.8\ )$$

The gas law gives the relation between the partial vapour pressure and the humidity by volume (v)

$$p_v = vRT/M_w \qquad\qquad (\ 2.9\ )$$

Derivation gives

13

$$\delta p_v/\delta x = (RT/M_w) * \delta v/\delta x \qquad\qquad (2.10)$$

The moisture content in the material is a function of the relative humidity in the pores

$$w = w(\phi) = w(p/p_{vs})$$

Derivation gives

$$\delta w/\delta x = \delta w/\delta\phi * \delta\phi/\delta x = \delta w/\delta\phi * 1/p_{vs} * \delta p_v/\delta x \quad (2.11)$$

Eq.(2.1), (2.2) and (2.10) give

$$\delta_v = (RT/M_w)*\delta_p \qquad\qquad (2.12)$$

Eq. (2.2), (2.3) and (2.11) give

$$\delta_p = \delta w/\delta\phi * 1/p_{vs} * D_w \qquad\qquad (2.13)$$

Eq.(2.2), (2.4) and (2.8) give

$$\delta_p = (RT\rho_w/(M_w p_v)) \; \lambda_m \qquad\qquad (2.14)$$

With Eq. (2.12), (2.13) and (2.14) it is possible to relate all four moisture flow coefficients to each other.

2.2 **The fundamental flow potential**

Arvidsson and Claesson (1989) said "the use of transport coefficients is an unnecessary complication. In the measurements of the moisture flow as function of RH for a material, we actually measure the fundamental flow potential (Ψ), while the moisture flow coefficients are obtained from a numerical derivation of the Ψ-curves that are given at discreet points. In the numerical simulation, we have to integrate the moisture flow coefficients, i.e. return to Ψ, in order to obtain the flow."

14

2.2.1 The definition of the fundamental flow potential

FIG 2.3 shows the principal character of the curve $\delta_v = \delta_v(v)$ for the moisture permeability. The moisture flow density (g) is according to Eq. (2.1)

$$\vec{g} = - \delta_v(v) * grad(v)$$

The humidity by volume is a function of position: $v=v(x,y,z)$.

Consider the following integral of $\delta_v(v)$:

$$\psi(v) = \psi_{ref} + \int_{v_{ref}}^{v} \delta_v(v')dv' \qquad\qquad (\ 2.15\ )$$

The integral is equal to the shaded area in FIG 2.3. The function $\psi(v)$ is, in the same way as $\delta_v(v)$, different for different materials.
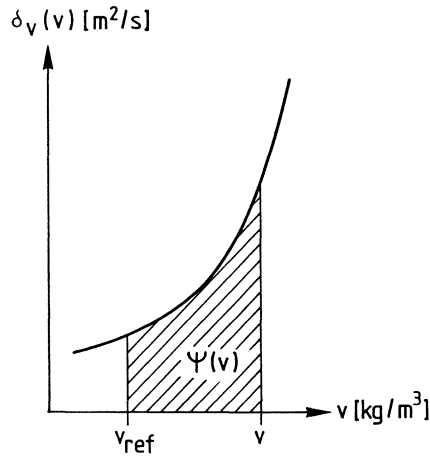
FIG 2.3 Definition of the fundamental flow potential.

The function ψ depends on the moisture state v. Its value is ψ_{ref} for $v=v_{ref}$. The derivative of ψ with respect to v gives $\delta_v(v)$.

15

$$\frac{d\psi}{dv} = \delta_v(v) \qquad\qquad (\ 2.16\ )$$

Now we have from Eq. (2.15) and Eq. (2.16)

$$\vec{g} = -\ \frac{d\psi}{dv} * \text{grad} (v) = -\ \text{grad}\ (\ \psi\ (v)) \qquad\qquad (\ 2.17\ )$$

Here we have used the derivation rule

$$\frac{\partial}{\partial x}\ (\psi(v)) = \frac{d\psi}{dv}\ *\ \frac{\partial v}{\partial x} \qquad\qquad (\ 2.18\ )$$

The moisture flow density is according to Eq. (2.17) given by the gradient of ψ :

$$\vec{g} = -\ \text{grad}\ \psi \qquad \psi = \psi\ (v) \qquad\qquad (\ 2.19\ )$$

The reason to introduce this new function ψ is that the moisture transport coefficient becomes +1. The problem with a variable moisture flow coefficient disappears.

2.2.2   Advantages with the fundamental flow potential

Consider a steady-state measurement of the moisture permeability of the type used in this thesis. A one-dimensional, steady-state flow is established through the specimen.

16
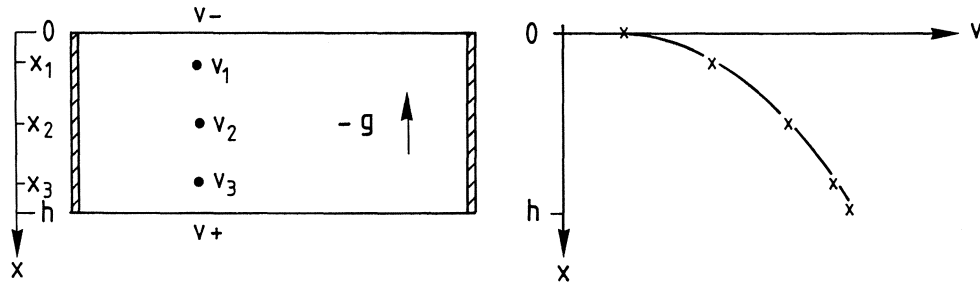
FIG. 2.4 "Measured properties" in a specimen.

The value of v is v_+ one side and v_- on the other. The steady-state moisture flow density is g. The steady-state relative humidity or $v = v_s * \phi$ is measured at different levels. Thus we measure

g, $v_- = v(0)$, $v_1 = v(x_1)$, ..., $v_+ = v(h)$

From this we shall determine the function $\delta_v(v)$. The classical procedure is to use the differences in v to obtain approximative values of $\delta_v(v)$

$$\delta_v \left[\frac{v_i + v_{i+1}}{2} \right] \approx (-g) * \frac{x_{i+1} - x_i}{v_{i+1} - v_i} \qquad (\ 2.20\ )$$

With the fundamental flow potential we proceed as follows;

$$-g = \frac{d\psi}{dx} \rightarrow \int_{x_a}^{x_b} (-g) dx = \int_{x_a}^{x_b} \frac{d\psi}{dx} * dx = \psi(x_b) - \psi(x_a) \qquad (\ 2.21\ )$$

We have since g is a constant the important relation

$$(-g) * (x_b - x_a) = \psi(x_b) - \psi(x_a) \qquad (\ 2.22\ )$$

17

The product of (-g) and thickness $(x_b - x_a)$ gives the difference in ψ .

We now choose
$$v_{ref} = v_- = v(0) \rightarrow \psi(0) = \psi_{ref}$$

Then we have with $x_a = 0$ and $x_b = x_i$
$$\psi_i - \psi_{ref} = \psi(x_i) = (-g) * x_i \qquad\qquad (\ 2.23\ )$$

(In this study we will use $\phi_- = 33\ \%$)

The value of v at x_i is $v_i = v(x_i)$. We have obtained the relation between ψ and v at the points v_i.
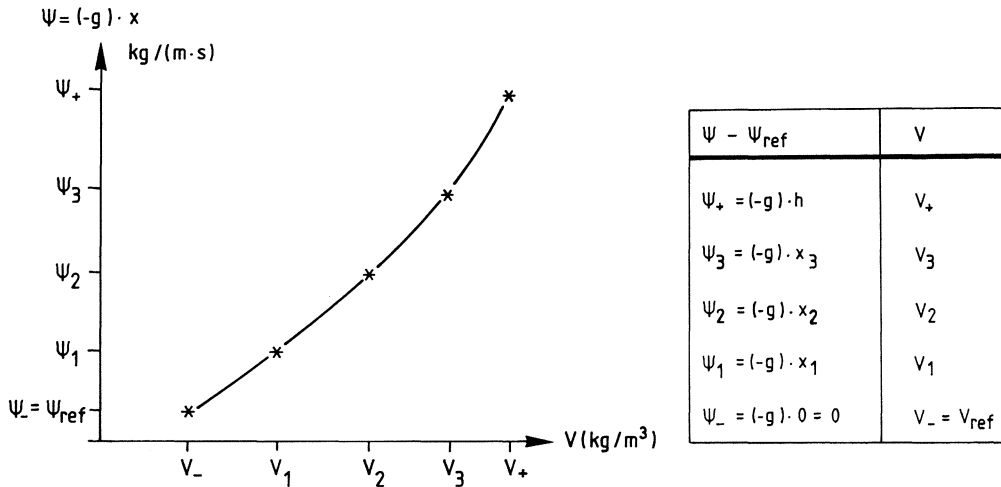
FIG 2.5   Relation between the fundamental flow potential and the humidity by volume in the pores of the specimen.

The moisture permeability is obtained by derivation

$$\delta_v = \frac{d\psi}{dv} \qquad\qquad (\ 2.24\ )$$

It is important to note that the relation between ψ and v is obtained directly from the measurements, while $\delta_v(v)$ involves a numerical or graphical derivation.

Consider next a numerical simulation. The following is mainly from Claesson (1987). The balance equation for moisture in one dimension is

$$\partial w / \partial t = -\partial(g) / \partial x \qquad\qquad (\ 2.25\ )$$

where g is given by Eq. (2.1) to Eq.(2.4) and Eq. (2.19).

In a numerical calculation of Eq. (2.25), the material is divided into nodes; see FIG 2.6.

moisture content $\quad w_i$

humidity by volume $\quad v_i$
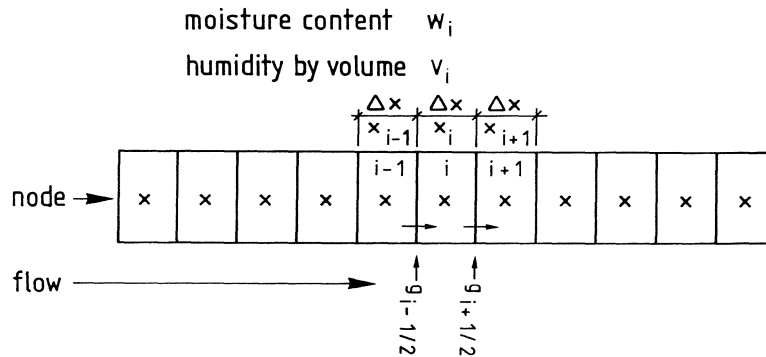
FIG 2.6   Nodes and definitions for numerical simulation.

The following calculations are made for every timestep.

1) $g_{i-0.5}$ and $g_{i+0.5}$ are calculated

2) Δw_i * $\Delta x_i = (g_{i-0.5} - g_{i+0.5})$ * Δt which gives w_i at
   time $t+\Delta t$

3) w_i at time $t+\Delta t$ and the sorption isotherm $w(\phi)$ and the
   humidity by volume at saturation (v_s) yield v_i at time $t+\Delta t$.

In the calculation of the moisture flow, eq. $g_{i-0.5}$, with a conventional potential we have

19

$$g_{i-0.5} \approx \bar{\delta}_v * (v_{i-1} - v_i)/(x_i - x_{i-1}) \qquad\qquad (\ 2.26\ )$$

$\bar{\delta}_v$ = the mean value of δ_v in the interval v_{i-1} to v_i

If δ_v varies strongly, as it may with concrete, one must inter-polate or, what is better, solve Eq. (2.1) between the nodes, Arfvidsson and Claesson (1989).

With the approach using the fundamental flow potential we have; see Eq. (2.22)

$$-g_{i-0.5} * (x_i - x_{i-1}) = \psi_i - \psi_{i-1} \qquad\qquad (\ 2.27\ )$$

The differences in ψ and x give the moisture flux. With ψ it is unnecessary to interpolate, when δ_v varies strongly, to get the correct moisture flow.

2.2.3 The relation between the fundamental flow potential and the moisture flow coefficients

Eq. (2.16) gives

$$\delta_v(v) = \frac{d\psi}{dv} \qquad\qquad (\ 2.16\ )$$

In one dimension we have

$$g = -\delta_p * \frac{dp_v}{dx} = -\delta_p * \frac{dp_v}{dv} * \frac{dv}{dx} \rightarrow \delta_p * \frac{dp_v}{dv} =$$

$$= \delta_v(v) = \frac{d\psi}{dv} \rightarrow \delta_p = \frac{d\psi}{dp_v} \qquad (\ 2.28\ )$$

$$g= -D_w\ *\ \frac{dw}{dx} = -D_w\ *\ \frac{dw}{dv}\ *\ \frac{dv}{dx} \rightarrow D_w\ *\ \frac{dw}{dv} = \delta_v(v) = \frac{d\psi}{dv} \rightarrow$$

$$D_w = \frac{d\psi}{dw} \qquad (\ 2.29\ )$$

$$g = \lambda_m\ *\ \frac{ds}{dx} = \lambda_m\ *\ \frac{ds}{dv}\ *\ \frac{dv}{dx} \rightarrow \lambda_m\ *\ \frac{ds}{dv} = \delta_v(v) = \frac{d\psi}{dv}$$

$$\rightarrow \lambda_m = \frac{d\psi}{ds} \qquad (\ 2.30\ )$$

3 EXPERIMENTS

3.1 Experimental arrangement

By using a method which relies on the measurement of the water
vapour flow from a specimen and the distribution of the
relative humidity in the specimen, under stationary conditions,
the moisture permeability can be calculated, and its dependence
on RH can be determined. The flow of water is unidimensional
and goes from the bottom to the top of the specimen. The
experimental arrangement is shown in principle in FIG 3.1. FIG
3.2 shows a photo of one specimen, and FIG 3.3 shows a photo of
the climate room where the specimens were kept for many years.
There were about 150 specimens in all.

fan — impermeable box — cup with a saturated salt solution, e.g. $MgCl_2$ — 9 mm tube in which RH is measured — specimen — vessel in which the specimen stands in water or in high RH
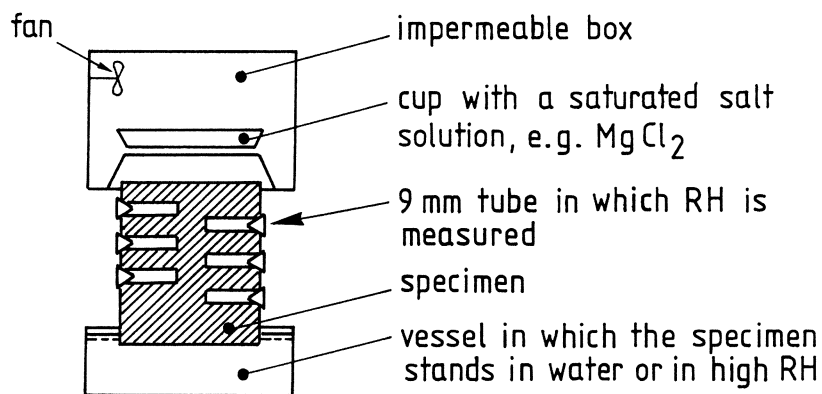
FIG 3.1 The experimental arrangement in principle.
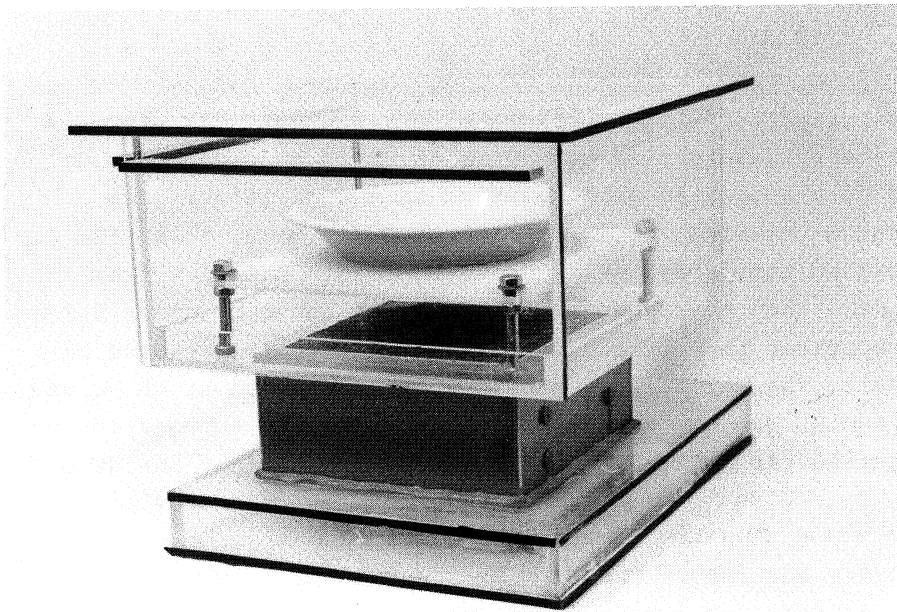
FIG 3.2 Photo of the experimental arrangement.
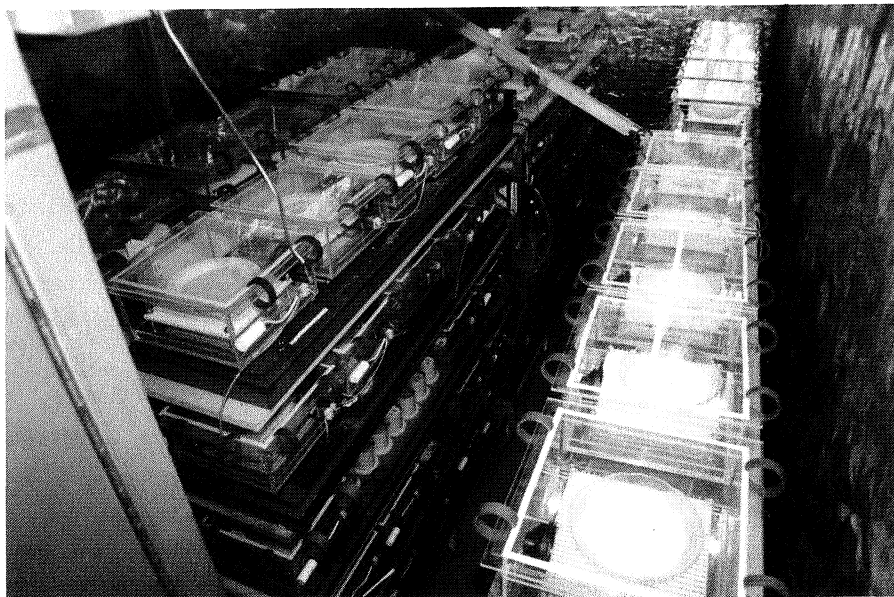
FIG 3.3 Photo of the climate room where the specimens were
         stored.

The upper part of the experimental arrangement consists of a practically impermeable box in which RH is held constant by means of a saturated salt solution in a cup, in our case magnesium chloride, $MgCl_2$, for which RH is about 33 %. The cup is weighed regularly, every week, to obtain the flow from the specimen. When the magnesium chloride in the cup, about 0.2 kg, has increased in weight by about 0.01 kg, it is replaced by new salt. The wet salt is regenerated in an oven at 40 °C and used again. The top surface of the specimen is exposed to the air inside the box. A small fan circulates the air inside the box.

The cross section of the specimen is 0.2*0.2 m. The heights of the specimens are 0.063, 0.100 and 0.150 m.

The surfaces of the specimen exposed to the surrounding air in the room are sealed with 2 mm almost impermeable epoxy resin. The bottom surface of the specimen stands in water or in air with high RH, which is effected by a water surface about 2 to 3 centimetres below the specimen.

Plastic tubes of about 14 mm external and about 9 mm internal diameters are embedded in the sides of the specimen. The length of the tubes is about 80 mm. The external surface of the tubes is grooved to assure good adherence to the cement paste in the specimen. The internal end surface of the tubes is open towards the specimen, and RH in the tubes is in equilibrium with RH in the specimen. Starting with the uppermost tube, with the lowest RH, the relative humidity is measured gradually downwards by means of a small capacitive RH-sensor.

The RH-sensor was made by Vaisala in Finland but rebuilt by our technicians, so the external diameter of the RH-sensor is about 8.5 mm. There is a packing ring, about 30 mm from the end of the RH-sensor, which makes a water vapour tight sealing to the tube. An RH-sensor is shown in FIG 3.4.
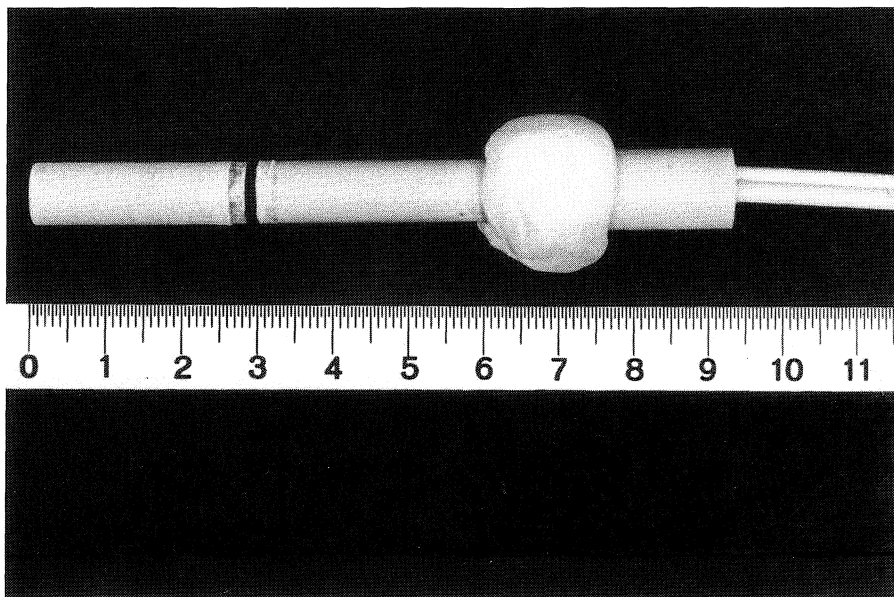
FIG 3.4 Photo of an RH-sensor.

Before the tests were started, the specimens were seal cured
for at least one month and then allowed to suck water for some
weeks, so that they would definitely be on their desorption
isotherm during the tests.

3.2 Tested materials

The tested materials comprise concrete, cement mortar and
cement paste. There are normally 6 specimens of each tested
quality.

3.2.1 Concrete

The following test program concerning different compositions of
concrete was carried out.

Concrete with w_o/C 0.4, 0.5, 0.6, 0.7 and 0.8, all with the same amount of aggregate; see TABLE 3.1.

Concrete with w_o/C 0.7 with different amounts of aggregate; see TABLE 3.2.

Concrete with w_o/C 0.7 with different amounts of air; see TABLE 3.3.

TABLE 3.1   Composition of concrete with different w_o/C.

w_o/C	Cement, C kg/m^3	Water, w_o kg/m^3	Sand/Gravel kg/m^3	Crushed stone 8–18 mm, kg/m^3
0.4	418	167.2	990	810
0.5	368	184.0	990	810
0.6	328	196.8	990	810
0.7	296	207.2	990	810
0.8	270	216.0	990	810

TABLE 3.2   Composition of concrete with w_o/C 0.7 with different amounts of aggregate.

Tot amount aggregate kg/m^3	Cement C kg/m^3	Water w_o kg/m^3	Sand/Gravel kg/m^3	Crushed stone 8–18 mm, kg/m^3
1692	334	233.8	931	761
1730	320	224.1	952	778
1765	307	215.1	971	794
1800	296	207.2	990	810
1827	285	199.2	1005	822
1854	274	192.1	1020	834

TABLE 3.3 Composition of concrete with w_o/C 0.7 with different
amounts of air.

Nominal air content %	Measured air content in fresh concrete %	Cement C kg/m³	Water w_o kg/m³	Total amount of aggregate kg/m³
4	4.4	275	192.2	1800
6	6.1	255	178.5	1800
8	8.0	235	164.8	1800
10	9.2	216	151.1	1800

The gradation curve for sand/gravel is shown in FIG 3.5.

Percentage material passing each sieve
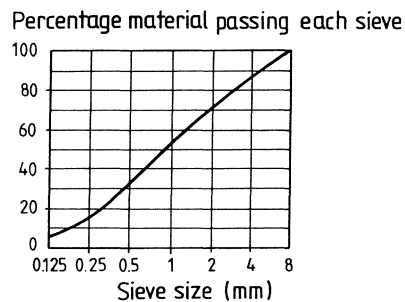
FIG 3.5 Gradation curve for sand/gravel to concrete.

The crushed stone, 8-18 mm, consists of quartzite.

The slump for the different types of concrete was measured,
although not at the same time as the specimens were cast. The
results are shown in TABLE 3.4.

TABLE 3.4 Measured slump.

Different w_o/C		w_o/C 0.7 with different amounts of aggregate	
w_o/C	Slump mm	Aggregate kg/m³	Slump mm
0.4	5	1692	230
0.5	23	1730	200
0.6	70	1765	155
0.7	135	1800	135
0.8	210	1827	105
		1854	75

27

3.2.2 Cement mortar

Compositions of the cement mortars with different w_o/C are shown in TABLE 3.5.

TABLE 3.5 Composition of cement mortar.

w_o/C	Cement, C kg/m^3	Water, w_o kg/m^3	Sand/Gravel kg/m^3
0.4	479	191.7	1600
0.5	421	210.5	1600
0.6	375	225.2	1600
0.7	339	237.0	1600
0.8	308	246.7	1600

The gradation curve for sand/gravel is shown in FIG 3.6.
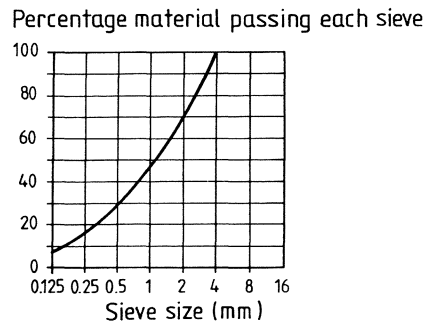
FIG 3.6 Gradation curve for sand/gravel to cement mortar.

3.2.3 Cement paste

For cement paste only 3 different w_o/C were tested, namely 0.4, 0.5 and 0.6. Only 4 specimens were tested for w_o/C 0.4.

There could be some separation in the specimens as no steps were taken to prevent this.

4 ERRORS IN THE MEASURED MOISTURE FLOW

The measured moisture flow is the uptake of the salt per time
unit. The moisture flow through a specimen is not completely
unidimensional, so the measured moisture flow for a specimen is
not the real unidimensional flow at the vertical section were
RH is measured. The measured moisture flow had to be corrected
for
* the flow through the epoxy resin on the sides of the specimen
* the influence of the masked edge at the upper surface of the
  specimen
* the influence of the RH-measurement tubes in the specimen
* the flow through the sealant on the outside of the specimen
* the flow between the upper box and the climate room.

4.1 Moisture flow through the epoxy resin

The influence of the moisture flow through the epoxy resin is
not the same for all the specimens. It depends on the height of
the specimen, on the distribution of the RH in the specimen and
on the moisture permeability of the epoxy resin.

4.1.1 <u>Measurements of the moisture resistance of the epoxy resin</u>

The moisture resistance of 4 different epoxy resins has been
tested with the cup method. The tightest was selected. The cups
were made of glass and had a diameter of 185 mm and a height of
95 mm. The epoxy resins were placed on disks of cellulose fibre
reinforced cement. The disks were placed as lids on the cups;
see FIG 4.1. The gap between the cup and the disk was sealed
with a mixture of beeswax and paraffin. In the cups there was a
saturated salt solution of K_2SO_4, which gives 97.6 % RH. The
cups were placed in a climate room with +20 °C and 50 % RH.

29

Sealing of beeswax
and paraffin wax

V_2

V_1

d

Saturated salt solution
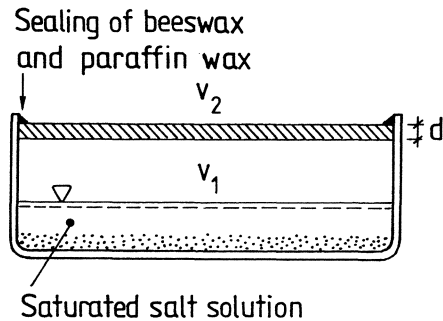
FIG 4.1 Principle of the measurement of the moisture
resistance with the cup method.

When the moisture flow rate for the different cups was
constant, the moisture resistance was calculated. The epoxy
resin named EP 91 had the highest moisture resistance
(Z_V=2200 * 10^3 s/m) and had a thickness of 2 mm. In the
calculation of the moisture resistance of the epoxy resins, the
moisture resistance of the cellulose fibre reinforced cement
has been taken into account.

$$Z_V = \frac{\Delta v}{g}$$

Δv = difference in humidity by volume at the different sides of
the epoxy resin

4.1.2 Influence of the flow through the epoxy resin

With a moisture resistance of 2200 * 10^3 s/m and a thickness of
2 mm for the epoxy resin, a constant moisture permeability is
calculated to 900 * 10^{-12} m^2/s.

For a moisture barrier based on epoxy resin, Nilsson (1977) has
shown that the moisture permeability depends on RH; see FIG
4.2.

k/d(g/m^2 h mmHg)
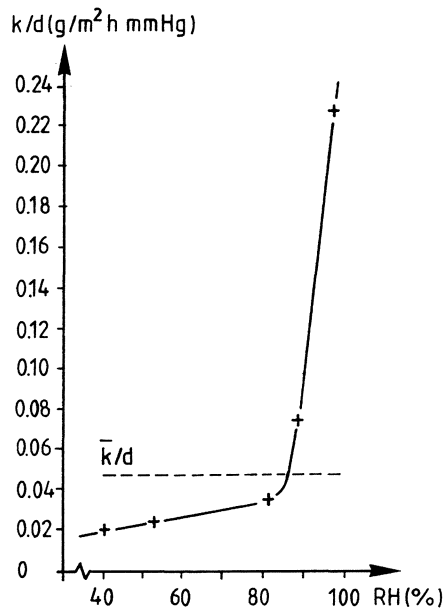
FIG 4.2 "The moisture permeability" of a moisture barrier
        as a function of RH.
        Nilsson (1977).

k/d in FIG 4.2 is defined by the relation $g=-\dfrac{k}{d} * \Delta p_v$

FIG 4.2 shows that the moisture permeability increases strongly
above about 85 % RH.

The moisture permeability of our epoxy resin, EP 91, is assumed
to have the same dependence on RH as shown in FIG 4.2.

The constant moisture permeability, $900 * 10^{-12}$ m^2/s, is
assumed to be proportional to $\bar{k}/d$ in FIG 4.2. It is then easy
to calculate the moisture permeability as a function of RH.

The influence of the epoxy resin is calculated with a
two-dimensional computer program, JAM-2. The model in FIG 4.3
is used. The moisture permeability of the concrete is almost
the same as that in Chapter 7.

31

MF=0   33 % RH

33 %   specimen   Moister flow
RH   (MF) = 0

                                                    h = 0.063, 0.100
                                                        and 0.150

└─Epoxy   Water or high RH   ₵

2 10 10 10 10 10 10 10 10 10 10 mm

2   100   mm
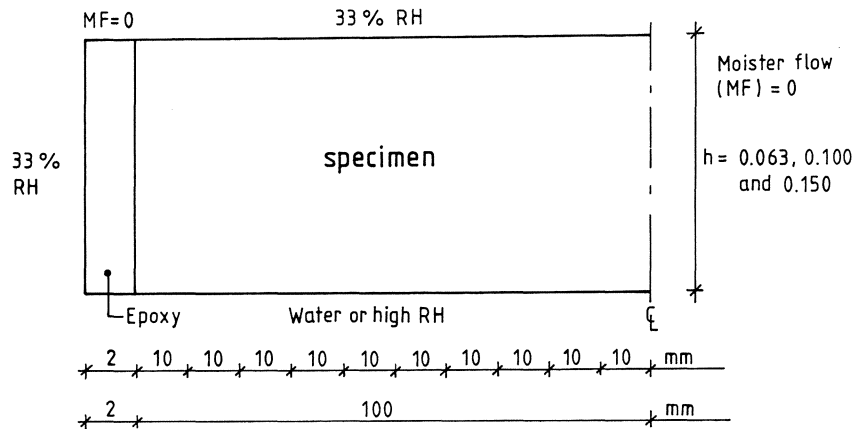
FIG 4.3   Two-dimensional computer model for calculating the
          influence of the moisture flow through the epoxy
          resin.

The moisture flows at the bottom and the top of the specimen
are calculated for every 10th mm. The moisture flows at the
bottom and the top of the specimen have the distribution shown
in FIG 4.4. The distribution in FIG 4.4 has been magnified
considerably, the real distribution being much more even.

$$g_{out}^{mean,1}$$ —1— 2— 3— 4 5 6 7 8 9 10 $$g_{out}^{1-10}$$

1 2 3 4 5 6 7 8 9 10 $$g_{in}^{1-10}$$
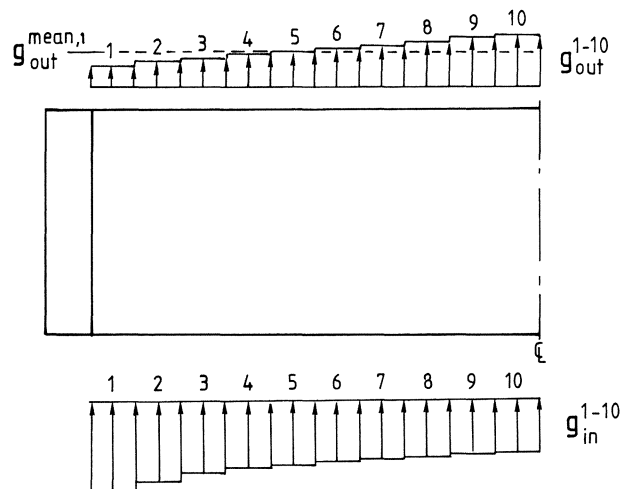
FIG 4.4   Moisture flows at the bottom and the top
          of a specimen.

The moisture flow near the epoxy resin at the bottom is bigger than the moisture flow at the central part of the specimen. This is because there is a moisture flow through the epoxy resin. In the central part, g_{in}^{10} and g_{out}^{10}, the moisture flow is almost unidimensional, and g_{in} almost equals g_{out}

One approximation of the calculated unidimensional flow is

$$g^{10} = (g_{in}^{10} + g_{out}^{10})/2$$

The calculated mean value of the moisture flow that goes from the specimen is

$$g_{out}^{mean,1} = (g_{out}^{1}+\ldots+g_{out}^{10})/10$$

If the calculated unidimensional flow is referred to $g_{out}^{mean,1}$ we have the correction-factor, corr.

$$corr = \left[(g_{in}^{10} + g_{out}^{10})/2\right]/g_{out}^{mean,1}$$

The measured moisture flow for a specimen is a mean value for the whole top surface. An approximation of the unidimensional moisture flow is then

$$g = g(measured) * \left[(g_{int}^{10} + g_{out}^{10})/2\right]/g_{out}^{mean,1} \qquad (4.1)$$

The unidimensional moisture flow calculated above was for a two-dimensional model.

If it is assumed that the moisture flow from the top surface of the specimen has the distribution shown in FIG 4.5, we probably have a more realistic model.
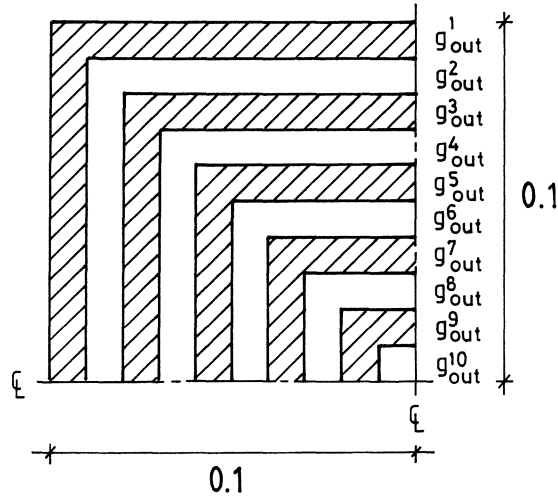
FIG 4.5 Assumed moisture flow from one-fourth of the top
surface of a specimen. "Three"-dimensional model.

The calculated mean value of the moisture flow from the
specimen is

$$g_{out}^{mean,2} = (4g_{out}^{10} + 12g_{out}^9 + 20g_{out}^8 + \ldots + 76g_{out}^1)/400$$

An approximation of the unidimensional flow is then

$$g = g(measured) * \left[(g_{in}^{10} + g_{out}^{10})/2 \right] / g_{out}^{mean,2} \qquad (4.2)$$

In TABLE 4.1 the corrections of the measured moisture flow
according to Eq. (4.1) and (4.2) are shown.

TABLE 4.1 Correction factor to the measured moisture flow,
            depending on moisture flow through the epoxy resin.

Concrete quality	Height of specimen	Accord. to Eq.(4.1)	Accord. to Eq.(4.2)
w_o/C 0.7	0.063	1.005	1.007
	0.100	1.012	1.017
	0.150	1.029	1.035
w_o/C 0.4	0.063	1.006	1.010
	0.100	1.016	1.022
	0.150	1.035	1.042

In TABLE 4.1 it is shown that Eq. (4.1) and (4.2) give
virtually the same result for the same height of the specimen.

There is only a small difference in the results for w_o/C 0.7
and 0.4, so there is only a small influence of the concrete
quality, which shows that the epoxy resin is very dense.

4.2 **Influence of masked edge at the upper surface of the
     specimen**

In all the specimens the sealing between the specimen and the
upper box is by and large the same. The sealing is shown in
FIG 4.6.

FIG 4.6 The sealing between the specimen and the upper box.

The dimensions of the sealants may vary somewhat as they are made by hand, and for many specimens the sealants were improved during the measuring period.

4.2.1 Corrections according to a method by Joy and Wilson

Joy and Wilson (1965) have given a formula for the effects of the masked edge in the cup method. In FIG 4.7 a cup with a masked edge is shown.

FIG 4.7 Masked edge and the moisture flow path in the cup method.

The given formula is

$$\frac{\Delta g}{g} = \frac{4 * d}{\pi * S} * \ln\left(\frac{2}{1+\exp\left(\frac{-2\pi b}{d}\right)}\right)$$

(4.3)

g = moisture flow with no masked edge $(kg/(m^2 s))$

Δg= increased moisture flow caused by the masked edge
   $(kg/(m^2 s))$

d = specimen thickness   (m)

b = width of the masked edge   (m)

S = four times the test area divided by the perimeter (the
   diameter of a circle or the side of a square).

The external width of our specimens, including the masked edge,
is 200 mm. The bottom sides of the specimens have no masked
edge. This can be taken in to account if into Equation (4.3)
d is taken to be 2 times the height of the specimen; see the
moisture flow path in FIG 4.7.

The moisture flow is proportional to the specimen area if there
is no masked edge. The reduction in the flow based on the total
area can be calculated as

$$A_{test} * \left(1 + \frac{\Delta g}{g}\right)/A_{tot}$$

In FIG 4.8 the reduction of the moisture flow is given as a
function of the width of the masked edge. The reduction is
based on the total area, 0.2 * 0.2 m.

Reduction of the moisture flow (%)
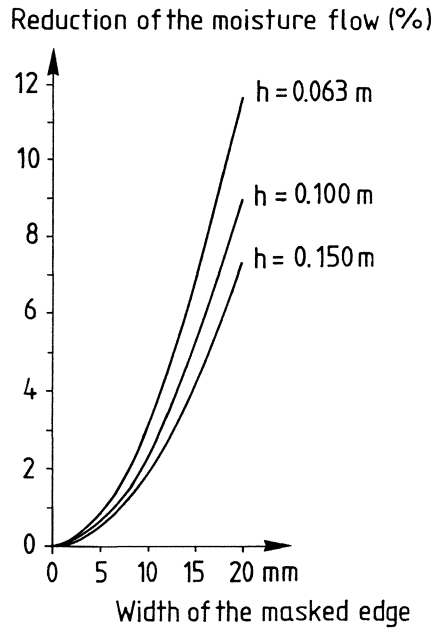
FIG 4.8 Reduction of the moisture flow as a function of
the masked edge. Reduction based on the total area,
0.2 * 0.2 m.

In the calculated reduction in FIG 4.8 it is assumed that the
notch on the top of the specimen has no influence and that the
masked edge is impermeable. In Equation (4.3) diffusion is
assumed, which probably means that the moisture transport
coefficient is constant and does not depend on the moisture
content of the specimen.

4.2.2 Computer calculations

With a two-dimensional computer program, Wallenten (1989) has
calculated the influence of the notch on top of the specimen
compared to a masked edge without a notch. The notch and the
masked edge are assumed to be impermeable. The calculated
results for our specimens are shown in FIG 4.9.

The width in the two-dimensional calculations was 0.2 m. the reduction of the moisture flow is (1-flow with masked edge/flow without masked edge) * 100.

Reduction of the moisture flow (%)
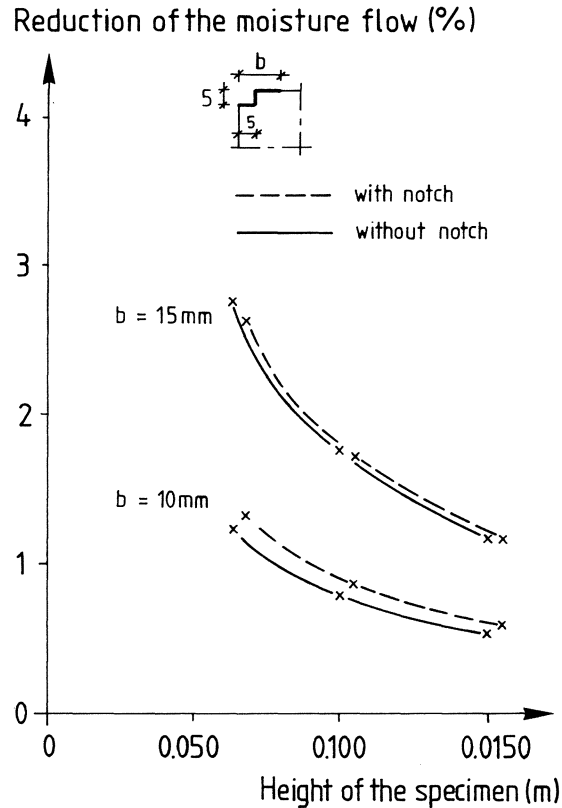
FIG 4.9   The influence of the notch on top of the specimen. Calculated with a two-dimensional computer program.

In FIG 4.9 it is shown that the influence of the notch compared to the width of the masked edge is negligible.

The calculations which Wallenten made have been checked with calculations made with the computer program Jam-2. With Jam-2 the case of a masked edge without notch was calculated. In Jam-2 the calculations were made with variable moisture permeability for the specimen and with measured moisture

39

resistance for the plexiglass and the building sealant at the top of the specimen. In TABLE 4.2 the calculated reduction of the moisture flow is shown for two concrete qualities.

TABLE 4.2 Calculated reduction of the moisture flow depending on the masked edge on top of the specimen. Specimens made of concrete and with the bottom surface in water. Two-dimensional calculations made with Jam-2.

Width of the masked edge. mm	w_o/C	Reduction of the moisture flow. %		
		Height 63 mm	Height 100 mm	Height 150 mm
10	0.8	1.37	0.82	0.53
	0.5	1.19	0.73	–
	–	1.23[1]	0.78[1]	0.53[1]
15	0.8	2.91	1.78	1.13
	0.5	2.37	1.45	–
	–	2.74[1]	1.75[1]	1.18[1]

1) Calculated by Wallenten; see FIG 4.9

The results in TABLE 4.2 show that the reduction of the moisture flows is nearly the same, with the same masked edge, when calculated with different computer programs and under different conditions for the materials.

Hagentoft (1989) has given a theoretical derivation of how the results from two-dimensional calculations of the influence of the masked edge can be transformed into three-dimensions. The basic figure Hagentoft used is shown in FIG 4.10.
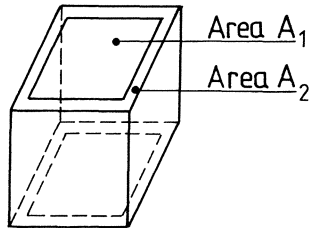
Area A_1
Area A_2

FIG 4.10 Basic figure for the calculation of the influence
of the masked edge on the specimen.

The formula Hagentoft arrived at is

$$\frac{\Delta g}{g} = \frac{A_2}{A_1 + A_2} * (\epsilon_2 + \epsilon_4) \qquad (4.4)$$

g = moisture flow with no masked area $(kg/(m^2 s))$
Δg = the decrease in the moisture flow caused
        by the masked part of the surface area $(kg/(m^2 s))$
A_1 = the unmasked part of the surface area
A_2 = the masked part of the surface area
ϵ_2 = parameter describing the influence of the masked edge
        of the upper surface on the moisture flow
ϵ_4 = Dito for a masked edge of the bottom surface,
        zero in our case

First the reduction of the moisture flow, g/g, in the
two-dimensional case is calculated by the program Jam-2. Areas
A_1 and A_2 are known. Then ϵ_2 is calculated. In the corners of
the masked area the calculated ϵ_2 is not the true value, as it
is the value for a two-dimensional calculation. A calculation
that Hagentoft made with a three-dimensional program showed
that ϵ_2 in the corners of the masked area, for our specimens,
is nearly two times the value of the two-dimensional
calculation if the width of the masked area is 10 mm. If the

41

corners of the masked area are regarded as a square with the same sides as the width of the masked area and the rest of the masked area is treated as the flow is two-dimensional the results that are shown in TABLE 4.3 are obtained for specimens where the width of the masked area is 10 and 15 mm.

TABLE 4.3 Calculated reduction of the moisture flow which depends on the masked area at the top of the specimen. Three-dimensional results derived from two-dimensional calculations.

Width of the masked area mm	Calculated reduction of the moisture flow. %		
	Height 63 mm	Height 100 mm	Height 150 mm
10	2.5	1.6	1.1
15	5.5	3.5	2.4

If the results in TABLE 4.3 are compared with the two-dimensional results in TABLE 4.2, it is seen that the calculated reductions in TABLE 4.3 are about twice the reduction in TABLE 4.2.

When the results in TABLE 4.3 are compared with the three-dimensional results in FIG 4.8, it is seen that the results in TABLE 4.3 are lower. The higher the specimens, the bigger the quotient between the results in FIG 4.8 and TABLE 4.3. For the height 63 mm the quotient is about 1.3, and for the height 150 mm the quotient is about 1.8.

The results in TABLE 4.3 are probably lower than the real reduction of the moisture flow as ϵ_2 is regarded to be the same along the sides of the specimen, but in reality it varies along the sides from the two-dimensional value to the three-dimensional value in the corners of the masked area.

Finally the results in FIG 4.8 and TABLE 4.3 are of the same
magnitude. For the normal width of the sealing between the
upper box and the specimen, 10 - 12 mm, the reduction of the
moisture flows is small, about 2 to 3 %. The coefficients of
correction to the measured flow are shown in APPENDIX A at
comments.

4.3 Influence of the RH-measurement tubes in the specimen

Two opposite sides of the specimen contain tubes in which RH is
measured. The tubes have an internal diameter of about 9 mm and
an external diameter of about 15 mm. The length of the tubes
is about 80 mm. The tubes are made of polypropylene, which is
regarded as impermeable compared to the permeability of the
specimen. These RH-measurement tubes reduce the moisture flow
in the specimens. According to Claesson (1990), the circular
tubes can be replaced by square tubes in the computer
calculations if the perimeter of the tubes is the same. A
section of a specimen which is used in the calculations is
shown in FIG 4.11. The height of the specimen is 63 mm.
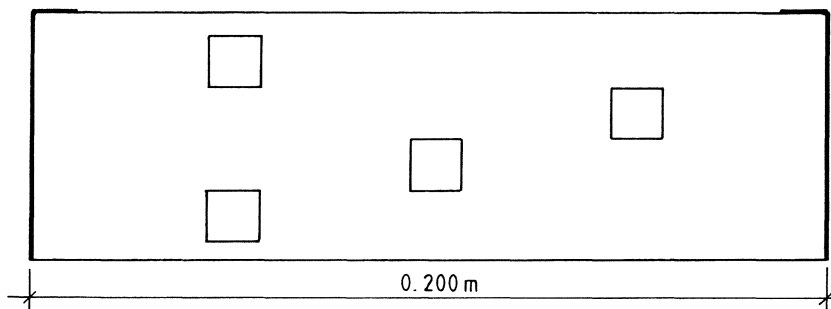

FIG 4.11 One of the configurations used in the
            computer calculations of the influence of the
            RH-measurement tubes on the moisture flow.

For a specimen with a height of 100 mm, calculations have been
made both with constant and with variable moisture permeability
of the specimen, and the reduction of the moisture flow is the
same in the both cases.

The results obtained with the two-dimensional Jam-2 are shown
in TABLE 4.4. For each height, calculations have been made for
both of the sides with RH-measurement tubes, as the sides are
not identical.

TABLE 4.4   Calculated influence of the RH-measurement tubes on
             the moisture flow. Two-dimensional calculations.

Height of the specimen mm	Reduct. of the moisture flow %			Coefficient of Correction Total
	Side 1	Side 2	Total	
63	11.4	13.7	10.0	1.1111
100	11.9	12.4	9.7	1.1074
150	7.7	8.8	6.6	1.0706

The specimens are considered as though they consist of three
parts, the two sides with RH-measurement tubes and the part in
the middle where there is a homogeneous material. The side
parts have a width of 80 mm (the length of the tubes), and the
middle part has a width of 40 mm. The total reduction of the
moisture flow is calculated with the parallel composite
material model. The total reduction is shown in TABLE 4.4. The
coefficients of correction, depending on the RH-tubes, to the
measured flow are also shown in TABLE 4.4.

4.4 **The moisture flow through the sealant between the outside
     of the specimen and the upper box**

Between the upper box and the epoxy resin on the outside of the
specimen there is a building sealant according to FIG 4.6. The
widths along the plexiglass and the epoxy resin are normally 6
mm. There is a small slit between the specimen and the

plexiglass of the upper box in which the moisture can reach the building sealant on the outside of the specimen. The slit is assumed to be 0.5 mm, and the moisture flow through the sealant is calculated with Jam-2. The moisture flows as functions of RH in the slit are shown in TABLE 4.5. RH in the climate room is 35 %. The moisture permeability of the building sealant is measured at $14 * 10^{-9}$ m^2/s.

TABLE 4.5 Calculated moisture flow through the building sealant between the outside of the specimen and the upper box.

RH in the slit %	Moisture flow g/day
50	0.0012
60	0.0020
70	0.0029
80	0.0037
90	0.0045
95	0.0049

RH in the slit is assumed to be the same as the calculated RH in the specimen. RH in the specimen was calculated in 4.1.2 although not related there. For concrete with w_o/C 0.8 and the bottom side in water RH is about 90 %. For concrete with w_o/C 0.5 and the bottom side in water RH is about 60 %. For specimens with high measured moisture flow, the flow through the building sealant is negligible, but for specimens with low flow the leakage through the sealant is about 2 to 4 % of the measured moisture flow.

4.5 **Moisture flow between the upper box and the climate room**

The plexiglass which the upper box is made of is not impermeable, so there could be a moisture flow through it. To avoid this, RH in the climate room is nearly the same (about 35 %) as RH in the upper box (about 33 %).

To control the total moisture flow between the upper box and the climate room, a box which had an impermeable steel plate instead of the specimen was placed in the climate room. The salt in this box was weighed at the same time as the salt for the ordinary specimens. The weight changes of this "dummy" were less than 1 g/year and this flow is quite negligible.

4.6 Summary of corrections of the measured moisture flow

The measured moisture flow for all the specimens is corrected with

a) the moisture flow through the epoxy resin having variable permeability; see TABLE 4.1, column 4 (Eq.4.2)

b) the influence of the sealing between the upper box and the specimen; see FIG 4.8. The sealing is assumed to have a width of 11 mm

c) the influence of the RH-measurement tubes in the specimen; see TABLE 4.4, the column for total correction

d) the moisture flow through the building sealant on the outside of the specimen; see TABLE 4.5.

The corrections used are shown in APPENDIX A.

5 MEASUREMENTS OF THE RELATIVE HUMIDITY

5.1 Calibration of the RH-sensor

It is important to calibrate the RH-sensors very often, because
there could be large drift of the RH-sensors. During the first
year or so of measurement, the drift of the RH-sensors between
two calibrations (about two weeks) could be up to 6 % RH. This
large drift caused great difficulties in evaluating the correct
RH-gradient, since the real difference in RH between two adja-
cent measurement tubes in a specimen could be only a few tenths
of a percent RH. This considerable drift is one of the reasons
why we made calibrations before and after each measurement.
Another reason is that the RH-sensor is unprotected and could
collect dust or other impurities on the polymer sheet during
the measuring period. This would probably add another
characteristic to the RH-sensor. The calibration period for an
RH-sensor normally had a duration of 9 days and was followed by
a measuring period of about 10 days. Then a new calibration
period followed; see FIG 5.1. With a calibration made before
and after a measurement, the magnitude of the drift is known.
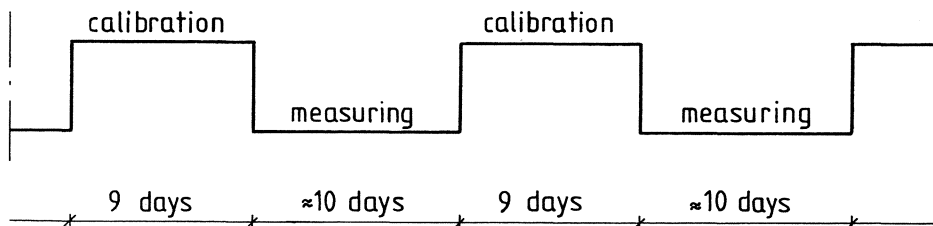
FIG 5.1 Measuring and calibration periods for an RH-sensor.

47

Initially the calibrations were made in the climate room where
the specimens were stored. The calibrations were made by means
of saturated salt solutions. After a check of the influence of
the temperature changes of the climate room on the readings
from the RH-sensor had been made, a temperature-stable
calibration box was built and placed in a separate room. The
calibration box is made of expanded polystyrene with the
external dimensions 1.0 x 0.8 x 0.7 m. The thickness of the
wall is 0.1 m. The box is cooled continuously with a Peltier
cooler. To make the box temperature-stable, it is heated with
two electric heating conductors. The temperature of the
calibration box is measured with a thermocouple. The difference
between the measured temperature and the set-point temperature
controls the input power of the electric heating conductors. In
the first version of the box the variations of the temperature
in the box were about ± 0.5°C(3 x standard deviation, 3 σ), and
in the calibration vessels, which were placed in the
calibration box, about ± 0.05°C (3 σ).

The calibration vessels were placed in a concrete block which
diminishes the temperature variations inside the calibration
vessels. The calibration box and the concrete block are shown
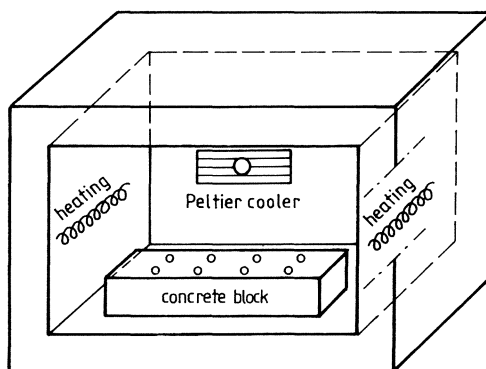in FIG 5.2.

FIG 5.2 The calibration box with its front panel removed.

A calibration vessel consists of a small transparent plastic
bottle, which contains a saturated salt solution. In the
central part of the bottle, there is a water-impermeable but
water-vapour permeable tube in which the RH-sensor is inserted.
The water-vapour permeable wall of the tube prevents liquid
from entering the inside of the tube. A calibration vessel with
an RH-sensor is shown in FIG 5.3.
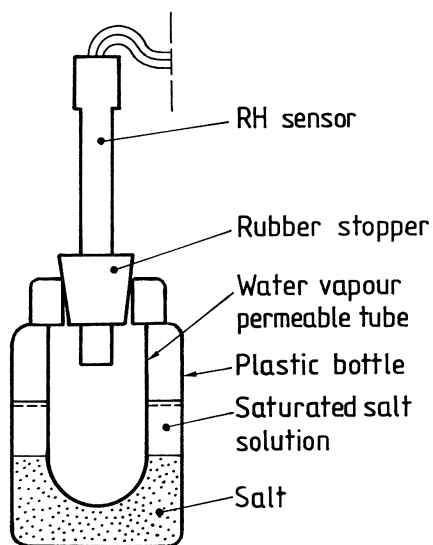
FIG 5.3 Calibration vessel with RH-sensor.

In a second version of the calibration box a better temperature
control unit was used. The variations of the temperature in the
box were reduced to about ± 0.3°C (3σ), and in the calibration
vessels the variations of the temperature were about ± 0.05°C
(3σ).

5.1.1 Calibration procedure

The RH-sensors were calibrated with saturated salt solutions.
The saturated salt solutions used and their relative humidity

at 20°C are listed in TABLE 5.1. All the figures in TABLE 5.1, except for sodium bromide, are taken from ASTM E104-85.

TABLE 5.1 Calibration salts and their RH at 20°C.

Namne		RH %
Lithium chloride	LiCl	11.3 ± 0.3
Magnesium chloride	$MgCl_2$	33.1 ± 0.2
Sodium bromide	NaBr	59.1 ± 0.4
Sodium chloride	NaCl	75.5 ± 0.1
Potassium chloride	KCl	85.1 ± 0.3
Potassium nitrate	KNO_3	94.6 ± 0.7
Potassium sulfate	K_2SO_4	97.6 ± 0.5

The uncertainty figures in TABLE 5.1 are the bias (systematic error) of the saturated salt solutions under ideal conditions. Definitions of the accuracy terms are given in section 5.1.2. The equilibrium relative humidity values in ASTM E104-85 are taken from Greenspan(1977), which contains the results for 28 saturated salt solutions at different temperatures. The values for sodium bromide are taken directly from Greenspan(1977).

The RH-sensors are calibrated before and after each measurement. The measuring periods are about 10 days. For every calibration point, the calibration time is normally 24 ± 2 hours. A typical reading in mV as function of time is shown in FIG 5.4. The time, on the X-axis, is in logarithmic scale. As seen in FIG 5.4, the changes in the measured value are small after 24 h.
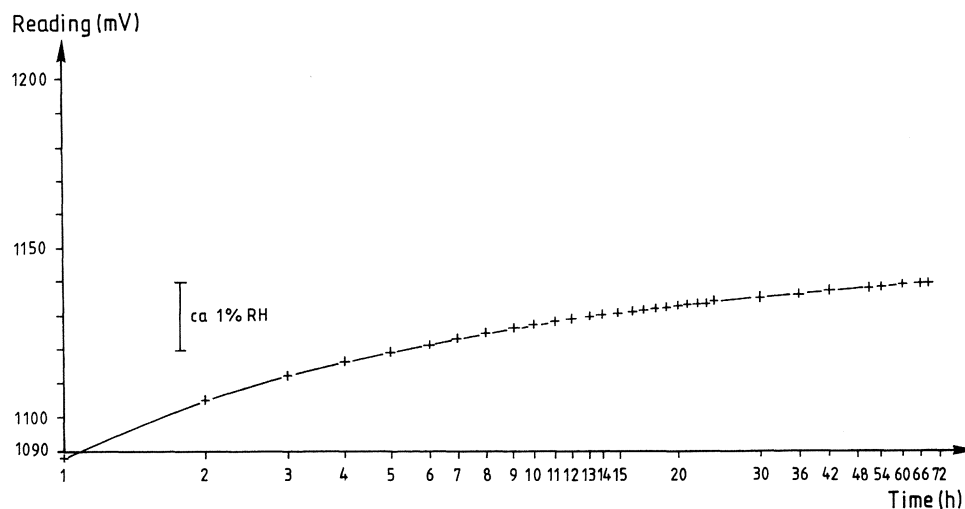
Reading (mV)

FIG 5.4 Reading from RH-sensor as function of time. The
         calibration climate used was 97.6%RH.

The calibration starts with LiCl (11.3 % RH) which has the
lowest RH. After that follow the different salt solutions with
increasing RH. After K_2SO_4 (97.6 % RH) the RH-sensors are
returned to LiCl and $MgCl_2$ (33.1 % RH), so that the RH-sensors
are on their absorption isotherm both during the calibration
and before the measuring starts. Between two calibration
periods the whole calibration curve may have changed somewhat.
FIG 5.5 shows the upper part of a typical calibration curve.
Curve 1 is from the calibration before measurement, and curve 2
is from calibration after measurement. The middle curve in FIG
5.5 is the curve used on which the RH-readings are based.

RH (%)

100 —

95 —

curve 1 —   — curve 2
90 —

85 —

80 —

75 —
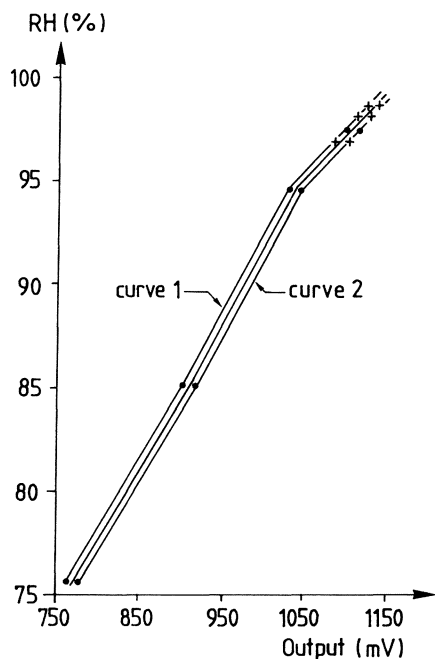   750   850   950   1050   1150
              Output (mV)

FIG 5.5 The upper part of a typical calibration curve.

FIG 5.5 also contains calibration points at 97.0, 98.2, 98.8 %
RH, marked by + . These calibration points are made with
unsaturated salt solutions of potassium chloride (KCL). The
lowest point, 97.0 % RH, is made with a molality (moles of
solute per kg solvent) of 1.0. This point is read on the
calibration curves for the saturated salt solutions. The mean
value (96.9) for several readings with different RH-sensors is
adjusted to 97.0 % RH. The adjustment is made because the
molalities for the KCL solutions used are 1.0, 0.8, 0.6, 0.4
and 0.2 and with these low concentrations, (100-RH) is
proportional to the molality. With 97.0 % RH for the 1.0
molality KCL and 100% RH for pure water, RH for the other
molalities will get one figure after the decimal point. This
small adjustment of 0.1 % RH is probably lower than the
uncertainty of the calibration curves for the saturated salt
solutions. Robinson and Stokes (1955) have given a formula
which gives the theoretical RH as 96.8 % at 25 °C for the 1.0

52

molality KCL-solution. In Hägg (1963) there is an approximative
formula which gives 96.6 % RH for 1.0 molality KCL-solution.
The influence of unsaturated salt solutions is described
in greater detail in Hedenblad (1988).

5.1.2 Errors in the calibration process

In the ASTM standard E 177 the terms precision, bias and
accuracy are defined. The following is taken directly from ASTM
E 177. The precision of a measurement process refers to the
degree of mutual agreement between the individual measurements
from the process. The usual basis of indexes of precision is
the standard deviation, σ, of the statistical distribution of
the measurements involved. Bias, or systematic error, is a
consistent deviation from the accepted reference level.
Accuracy refers to the degree of agreement of measurements with
an accepted reference level. Accuracy is therefore used as a
term that includes precision and bias. The terms bias and
precision are shown in FIG 5.6. Accepted reference level refers
to an authorized and accepted value of the property concerned,
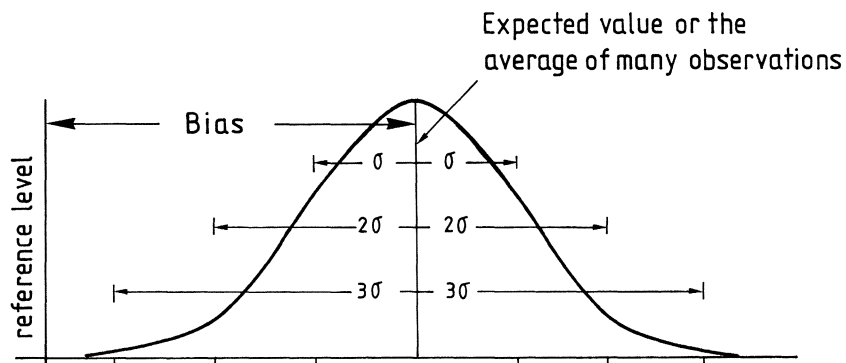a standard.

FIG 5.6 Frequency distribution of a measurement. The figure
         is based on the normal distribution. ASTM E 177.

According to ASTM E104-85, lack of temperature equilibrium (± 0.5°C) during the calibration can increase the bias statement to ± 2.5% RH. A theoretical calculation at 20 °C and 95 % RH reveals that the RH can change ± 2.8 % for a rapid temperature change of 0.5 °C. In the calculation it is assumed that the water vapour concentration in the calibration vessel is the same all the time. According to ASTM E 104-85, the precision of the saturated salt solutions is ± 0.5 % RH, when the temperature instability of the salt solutions is ± 0.1 °C.

Greaves (1986) claims that the repeatability of the saturated salt solutions that a certain manufacturer of RH-measuring devices, uses (e.g. LiCl, $MgCl_2$, NaCl, KNO_3) is better than 0.1 % RH when the temperature stability is better than ± 0.05°C. Repeatability normally refers to the precision achieved in one laboratory with the same operator making the measurements.

Lafarie (1988) has classified the errors that can arise in a measurement of the relative humidity. As examples of bias, or systematic errors, he mentions nonlinearity of the instrument and temperature effects (when measuring is carried out at a temperature different from the calibration temperature). As examples of random errors he mentions sensor hysteresis and calibration errors. One error that Lafarie did not mention is drift of the sensors, which is a systematic error.

In the following an analysis is made of errors in our tests.

Systematic errors: There are no corrections made by the electronic circuits to make the readings from the sensor linear. The sensors are calibrated at 7 points with saturated salt solutions. The sensors are almost linear between 33.1 and 94.6 % RH, and the calibration curves are drawn as straight lines from one calibration point to the next. As seen in FIG 5.5, there is a breaking-point at 94.6 % RH. It cannot be determined if this breaking-point is exactly at 94.6 % RH or at a higher value, as there is no saturated salt solution with a relative humidity between 94.6 and 97.6 % RH. But if the breaking-point

is higher than 94.6 % RH, the RH read will be too low in this region. The measurements are made at almost the same temperature as the calibration. In conclusion, there will be no systematic errors or very small errors between 33.1 and 94.6 % RH caused by nonlinearity of the instrument and temperature effects.

The drift of the RH-sensors varies from time to time. But if the drift is greater than about 1 % RH between two calibrations, the measured values are not used and a new measurement with a newly calibrated RH-sensor is made. The mean value of the calibration curves for the two calibrations (before and after measurement) is used when defining the real RH-value. For most of the calibrations, the calibration curves are nearly parallel over about 75 % RH. That means that all three curves give about the same $\delta RH/\delta x$ for a specimen, but not exactly the same absolute value of RH. The bias for the drift of the RH-sensor is the distance from the mean value calibration curve and the two calibration curves (before and after measurement).

The bias figures in TABLE 5.1 could be interpreted to mean that the correct RH for a given salt is not known, but lies between the given value and ± the bias. The bias for the drift of the RH-sensor and the bias for the correct RH-value should be combined.

Eisenhart (1963) has provided some ways to combine allowances for systematic errors. The following is directly from Eisenhart. When
1) the numbers of systematic errors that shall be combined are small
2) the systematic errors are approximately in the same range
3) one is nearly sure that the individual systematic errors do not exceed their range
it is then probably safe to use the approch of a uniform distribution of error and take the bias for each individual range as the average of the individual ranges.

In TABLE 5.2 the limits of error of a sum of n items are listed for a bias of ± 0.5 for each individual range and with uniform distribution.

TABLE 5.2   Limits of error of a sum of n items with the same
            bias of ± 0.5 with uniform distribution.
            Eisenhart (1963).

n	probability	
	0.95	0.99
1	±0.48	±0.50
2	±0.78	±0.90
3	±0.97	±1.19

Greenspan (1977) claims that the bias figures in TABLE 5.1 are 3 times the standard deviation for the predicted value, which means that the probability is 0.99 that the correct value lies between the bias limits.

If we assume that the probability is 0.99 that the correct RH-value lies between the calibration curves before and after measurement, then it is easy to calculate the total bias for n=2.

Total bias = 0.9 x the average of the indivual ranges / 0.5
or
Total bias = 0.9 x the sum of the individual ranges

0.9 comes from TABLE 5.2 column 3 and 0.5 results from the fact that the figures in TABLE 5.2 are for a bias of ±0.5.

Random errors: A small investigation on two RH-sensors gave the result that hysteresis between absorption and desorption is about 1% RH. As the measurements are made from the top of the specimen and downwards, RH should normally increase between two

adjacent measurement tubes and the RH-sensor should "always" be on its absorption isotherm. If there is a measurement tube which has a lower measured RH-value than the measurement tube above it, its RH-value is not used.

If the RH-sensor is on its absorption isotherm and is then placed in a lower RH and after that is placed in the original RH, the sensor returns to its absorption isotherm on nearly the same reading (mV); see FIG 5.7.
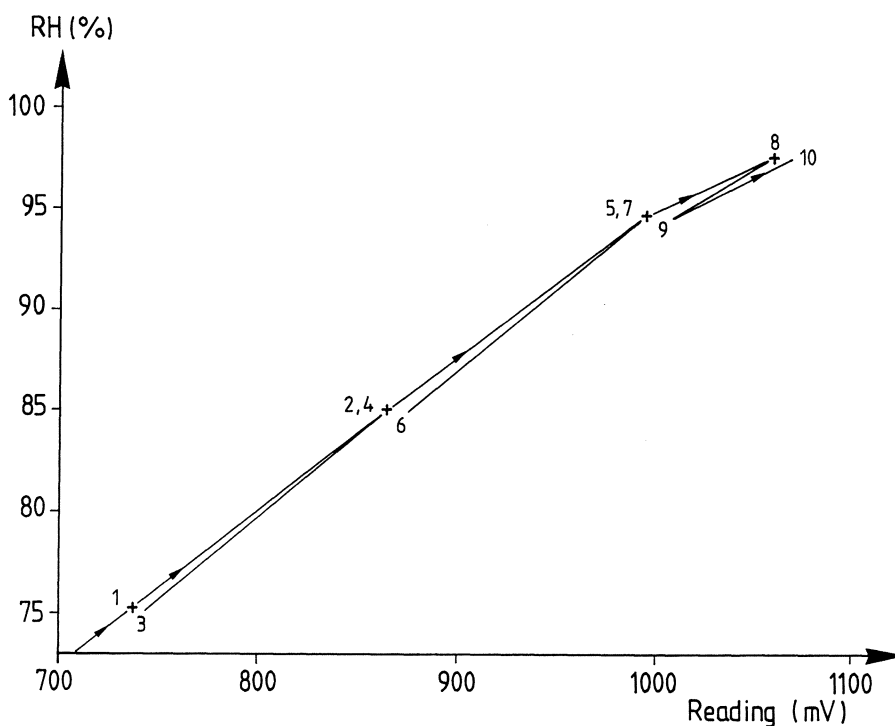

FIG 5.7 Scanning curves for an RH-sensor.

If Greaves' statement is correct, namely that the sensor repeatability is 0.1 % RH when the temperature stability is better than ± 0.05 °C, the precision of the saturated salt solutions should be in the same range in our calibrations.

A small investigation (30 calibrations) of the calibration error for RH-sensors that had been calibrated from 11.3 % up to 97.6 % RH and then returned to 11.3 % and then 33.1 % RH gave the result that the precision was about 0.18 % RH (1σ) at 33.1 % RH.

Accuracy: According to Eisenhart (1963 and 1969) the bias and the precision should both be mentioned in an accuracy statement. An overall **uncertainty** can be calculated and should include the total systematic error and at least 3 times the standard error. This approach has been used in section 5.3

5.2 Measurements of RH in the specimen

After calibration, the RH-sensor is protected against dust and water vapour with a plastic cap during the transport to the climate room where the specimens are stored. After removal of the plastic cap the RH-sensor is immediately inserted in the uppermost measurement tube in the specimen, which has the lowest RH. The RH-sensor is placed in the same measurement tube for about 24 h before the reading of the RH-sensor is made. After that the RH-sensor is removed and placed in the adjacent measurement tube. The measurement period is 9 to 11 days, depending on the numbers of measurement tubes (9,10 or 11) in the specimen.

5.2.1 Error in the measurement of RH in the specimen

The greatest error in the RH-measurement is when there has been a leakage between the measurement tube and the rubber stopper, but the measured RH is then normally much lower than it should be. This error is normally revealed when the RH-profile in the specimen is drawn during the analysis of the moisture flow coefficient.

Another error in the RH-measurement is the temperature
instability in the specimen during the measurement. The
temperature instability in the measurement tubes in a specimen
has been recorded during 24 h. For the recorded period the
temperature instability was about ± 0.2 °C (3 x σ). At the same
time were the temperature changes in the climate-room about ±
0.4 °C.

If the water vapour concentration in the air in the measurement
tube is assumed to be the same all the time, it is possible to
calculate a upper limit to the change in the RH. When RH is
about 100 % the change in RH will be ± 1.2 % for a change of
the temperature of ± 0.2 °C at + 20 °C. Nilsson (1987) has
measured effects on RH in concrete, of a certain change in
temperature. FIG 5.8 shows the preliminary results for
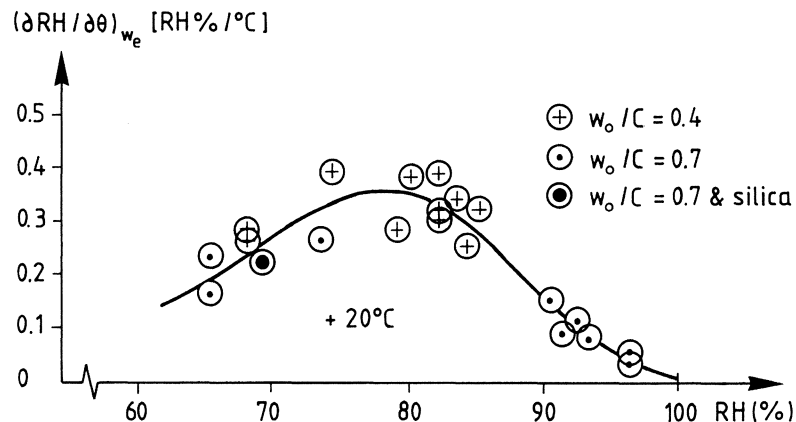different concrete qualities.

FIG 5.8   The temperature effect on the equilibrium RH in
          concrete. Mean temperature +20°C.
          Nilsson (1987).

In FIG 5.8 it is shown that the maximum change in the RH is for
RH about 75 to 80 %. The change is about 0.35 % RH per °C. With
a temperature change of ± 0.2 °C, the change in RH will be 0.07

%. The changes in FIG 5.8 are changes in RH when the moisture content in the concrete is constant.

An analysis of the measured RH as function of time and of the temperature changes in the climate room for some specimens gives the result that the maximum change in RH due to changes in temperature is about ± 0.1 %, and this value is close to the values of Nilsson, when the temperature change is ±0.2 °C.

5.3 The total error in the RH-measurement

The drift of the RH-sensors is determined for each measurement and 0.9 times the drift is added to the total uncertainty of the RH-measurement. The maximum change in RH (± 0.1 %) due to changes in temperature during the measurement is supposed to be 3 times the standard error, and regarded as a random error. The random errors in the calibration process and the measurement are combined into one figure ($\sigma=\sqrt{(\sigma^2 + \sigma^2)}$). The total random error is then 0.55 % RH (3σ). The total uncertainty for the different RH-levels determined by the different saturated salt solutions is listed in TABLE 5.3.

TABLE 5.3 The overall uncertainty in RH at different RH-levels.
Drift of the sensors is excluded.

RH %	Tot uncertainty %
33.1	0.71
59.1	0.95
75.5	0.68
85.1	0.81
94.6	1.14
97.6	1.03

Linear interpolation between these points is used.

6 EVALUATION OF THE MOISTURE PERMEABILITY

The moisture permeability, δ_v, is not evaluated for every specimen. Instead the fundamental flow potential, ψ, (see section 2.2) is evaluated. The mean, maximum and minimum ψ specimens of the same quality are calculated and then δ_v is calculated for these three ψ:s. In our stationary case it is simple to calculate ψ as function of RH, see FIG 6.1. With $\psi_{ref}=0$ at the top of the specimen, we have $\psi(x_i)=(-g) * x_i$; se Eq. (2.23).
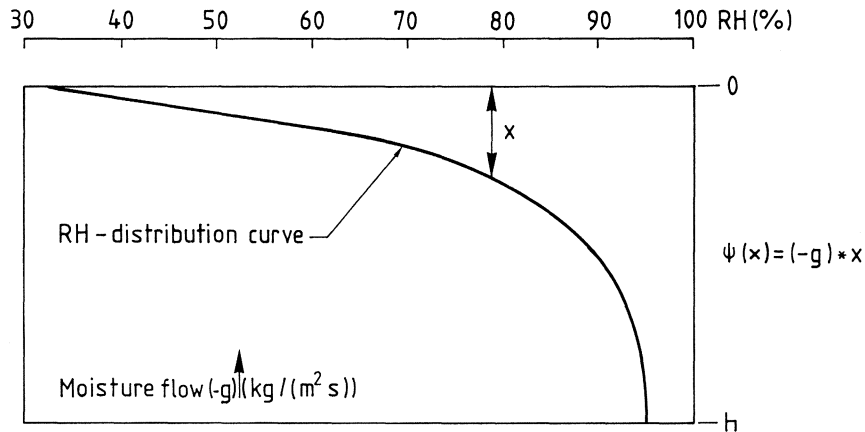

FIG 6.1 Evaluation of the fundamental flow potential (ψ).

The moisture flow, g, is measured and given in APPENDIX A for the different specimens. The moisture flow is corrected for the influence of the boundary conditions, see Chapter 4 and APPENDIX A.

The distance from the top of the specimen to the RH-distribution curve at a given RH is x. Then we have from Eq. (2.15) when $\psi_{ref}=0$

$$\psi = -g * x = \int_{v_{ref}}^{v} \delta_v(v') * dv' \qquad\qquad (\ 6.1 \ )$$

61

Eq. (6.1) says that for different RH:s in the specimen, ψ is calculated as g * x. For increasing RH in the specimen, ψ increases as x increases. At the top of the specimen ψ is 0 because x is 0.

The distances from the top of a specimen to the minimum, mean and maximum RH-curve are given for different RH in APPENDIX B, see also APPENDIX C. The mean ψs are calculated for different RHs in APPENDIX C and graphically shown in APPENDIX D, where also the minimum and maximum ψs are shown.

In the evaluation of the mean ψ for a given quality of material, considerations have been accorded to the measured mean RH-curves for the specimens of that quality. Take for instance concrete with w_o/C 0.7. Between 33 % and 84 % RH account has only been made of the specimens that stand with their bottom side in moist air (C7A2, C7B2 and C7C2), as these specimens have measured RH between these two RH. Between 86 % and 89 % RH account has also been made of a specimen with its bottom side in water (C7B1). The first RH measured in C7B1 is 85.3 %. Between 90 % and 94 % RH considerations have been given to 5 specimens (the four above plus C7A1), see APPENDIX B. The first RH measured in C7A1 is 90.5 %.

From Chapter 2 Eq. (2.16) we have

$$\delta_V = \delta\psi/\delta v \qquad\qquad (2.21)$$

Which is the same as

$$\delta_V = \delta\psi/(\delta\phi * v_s) \qquad\qquad (6.2)$$

Then δ_V is the slope of the ψ-curves in APPENDIX D divided by the humidity by volume at saturation. The slopes of the ψ-curves have been evaluated graphically.

62

7 RESULTS FOR CONCRETE

The results presented in this chapter show the moisture
permeability with regard to humidity by volume in the pores of
the specimens (δ_V) as function of RH or as the mean moisture
permeability for specimens with defined moisture conditions at
the boundaries.

7.1 Effect of the water-cement ratio

The concrete qualities shown in FIG 7.1 to FIG 7.4 have water-
cement ratio 0.5, 0.6, 0.7 and 0.8. The amount of aggregate is
the same in the different concrete qualities. The mean measured
δ_V for up to 6 specimens of each concrete quality is shown in
FIG 7.1 to FIG 7.4. The measured maximum and minimum δ_V are
also shown in the same figures. The maximum and minimum
δ_V-curves are from the specimens, with the same w_o/C, with the
highest and lowest fundamental potential, when allowance
has been made for the total uncertainty in the RH-measurement;
see section 5.3. For the definition of the fundamental flow
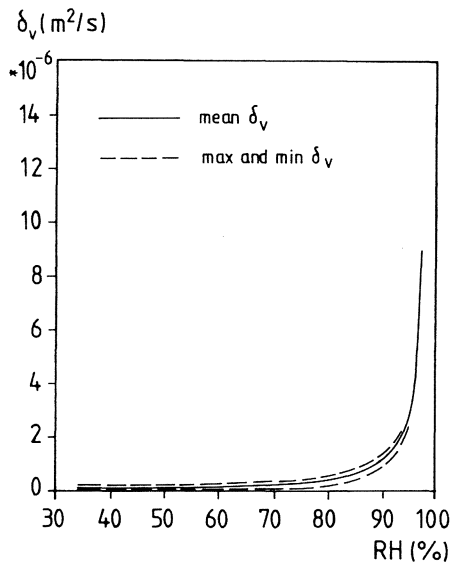potential see section 2.2.1.

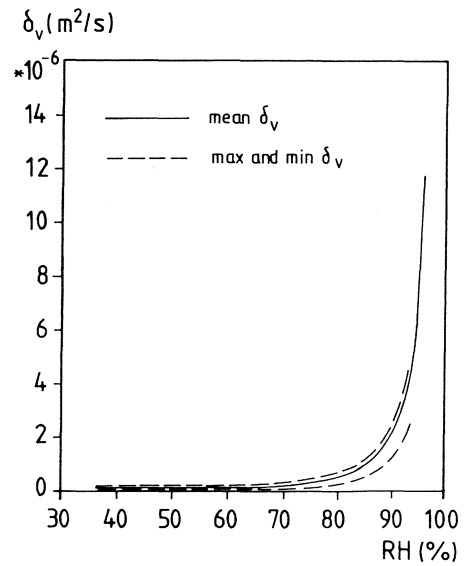FIG 7.1 Measured moisture permeability for concrete with w_o/C 0.5.

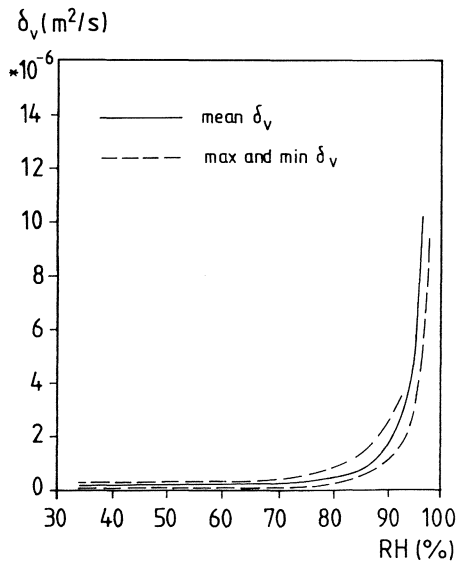FIG 7.2 Measured moisture permeability for concrete with w_o/C 0.6.

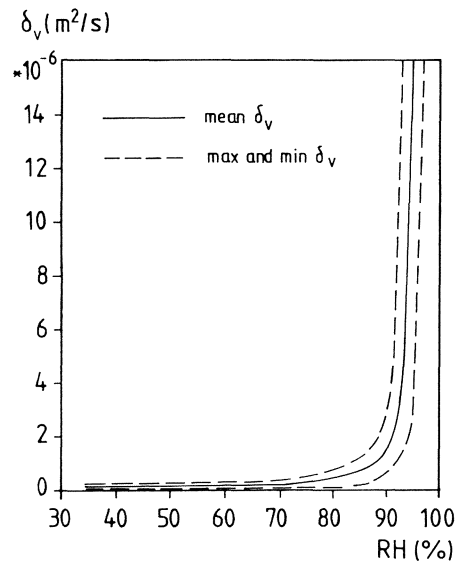FIG 7.3 Measured moisture permeability for concrete with w_o/C 0.7.

FIG 7.4 Measured moisture permeability for concrete with w_o/C 0.8.

64

In FIG 7.1 to FIG 7.4 it is shown that the moisture permeability depends on RH. For lower RH, up to about 70 %, δ_V is nearly constant. Between about 70 % and 90 % RH there is an increase in δ_V with RH. Above about 90 % RH, δ_V increases strongly with increasing RH. δ_V is not determined the whole way up to the moisture saturation point. The saturation point probably lies around 100 % RH; see section 11.1.1.

The measured maximum and mimimum δ_V-curves have the same shape as the mean δ_V-curves.

The results for different w_O/C and RH are shown in TABLE 7.1. The averages of the mean moisture permeability for w_O/C 0.6 to 0.8 at the different RH-levels are shown in the seventh column. The eighth column shows the coefficients of variation for w_O/C 0.6-0.8.

TABLE 7.1 Moisture permeability for concrete with different w_O/C.

RH	$\delta_V * 10^6$ (m^2/s)					Average	Coef.
%	w_O/C .4	w_O/C .5	w_O/C .6	w_O/C .7	w_O/C .8	.6 −.8	of var
33−65	0.13	0.14	0.15	0.18	0.18	0.17	0.11
70	0.19	0.20	0.19	0.19	0.18	0.19	0.02
75	0.22	0.25	0.26	0.26	0.30	0.27	0.08
80	0.28	0.33	0.38	0.40	0.37	0.38	0.04
84	0.35	0.45	0.64	0.58	0.48	0.57	0.14
86	0.39	0.59	0.83	0.77	0.60	0.73	0.16
88	0.46	0.82	1.18	0.99	0.76	0.98	0.21
90	(0.53)	1.02	1.74	1.44	1.34	1.51	0.14
91		1.20	2.2	1.90	1.67	1.91	0.13
92	(0.57)	1.48	2.6	2.3	2.4	2.4	0.07
93		1.68	3.5	2.7	3.3	3.2	0.14
94		2.2	4.3	3.4	6.8	4.8	0.36
95	(0.70)	2.8	5.4	4.4	12.7	7.5	0.61
96		4.3	7.8	6.4	19	11.1	0.62
97		9.0	11.7	10.0	28	16.7	0.61
98					53		
	1	4	5	5	6	Number of specimens	

The moisture permeability is not evaluated for higher RH than
96 to 98 %, because it is very difficult to evaluate the steep
slopes of the RH-curves. The results in TABLE 7.1 clearly show
that w_o/C in the range 0.6 to 0.8, has no, or little, influence
on δ_v up to about 95 % RH. This is a surprising result and <u>one</u>
explanation can be that the interface between the aggregates
and the cement paste is much more permeable than the cement
paste; see section 12.2 and APPENDIX E.

δ_v depends strongly on w_o/C over about 95 % RH. Maximum δ_v is
about $130 * 10^{-6}$ m^2/s for w_o/C 0.8 and about $20 * 10^{-6}$ m^2/s for
w_o/C 0.6; see TABLE 7.2. This is probably one of the reasons
why "watertight" concrete works.

7.1.1 <u>Specimens with the bottom side in water</u>

The mean moisture permeability ($\delta_v^{mean,1}$) has been calculated
for the specimens that stand in water.

$$\delta_v^{mean,1} = g * h / (v_s * (1 - 0.33)) \hspace{2cm} (7.1)$$

g   = density of moisture flow rate $(kg/(m^2s))$
h   = height of the specimen   (m)
v_s = humidity by volume at saturation (kg/m^3)
0.33 = RH at the top of the specimen   (1)

It is questionable whether $\delta_v^{mean,1}$ is a correct measure, as
most of the differences in the moisture flow depend on what
occurs above 95 % RH. But it is used since it is comparable
with the results obtained by Nilsson (1980). For different w_o/C
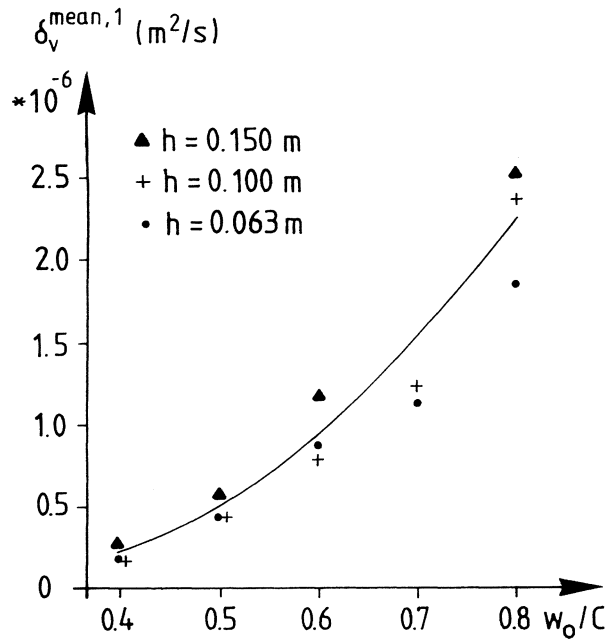$\delta_v^{mean,1}$ is shown in FIG 7.5.

$\delta_v^{mean,1}$ (m^2/s)

FIG 7.5   Effect of water-cement ratio on the mean moisture
permeability within the range 33 % ≤ RH ≤ liquid
water, $\delta_v^{mean,1}$.

FIG 7.5 shows that the ratio between w_o/C 0.8 and 0.5 is about
4 to 5. Nilsson (1980) has found about the same ratio for the
diffusivity for cement mortars with w_o/C 0.8 and 0.5. The
results in FIG 7.5 and the results obtain by Nilsson are not
directly comparable, as Nilsson's results have the moisture
content mass by volume as potential and they are for cement
mortar, whereas the results in FIG 7.5 have the humidity by
volume in the pores of the specimen as potential and are for
concrete. But in both cases the curve shapes are nearly the
same and the ratios for $\delta_v^{mean,1}$ and for the diffusivity between
w_o/C 0.8 and 0.5 have the same magnitude.

In FIG 7.5 it is shown that for nearly all w_o/C that the higher
the specimen, the higher is $\delta_v^{mean,1}$. One explanation can be
that carbonation has occurred at the top surface of the

specimen, giving lower δ_V at the surface. If the carbonation depth for specimens with the same w_o/C is the same, the carbonation depth should have greater influence for lower specimens. Another explanation can be that the moisture flow has not reached equilibrium for the highest specimens. This explanation is supported by the fact that for w_o/C 0.7 and 0.8 the specimens with a height of 0.150 m. have not reached equilibrium of the moisture flow (after 120 weeks), and $\delta^{mean,1}$ for the two heights 0.063 and 0.100 m are nearly the same at w_o/C 0.4, 0.5 and 0.6. A third explanation can be that the sealing between the upper box and the specimen has been improved for specimens with heights 63 and 100 mm. This has not been done for the specimens with height 150 mm, which are shown in FIG 7.5. The sealing has later been improved and the influence on $\delta_V^{mean,1}$ is shown in FIG 7.6. In Chapter 10 there is a fuller discussion of the subject mentioned above.
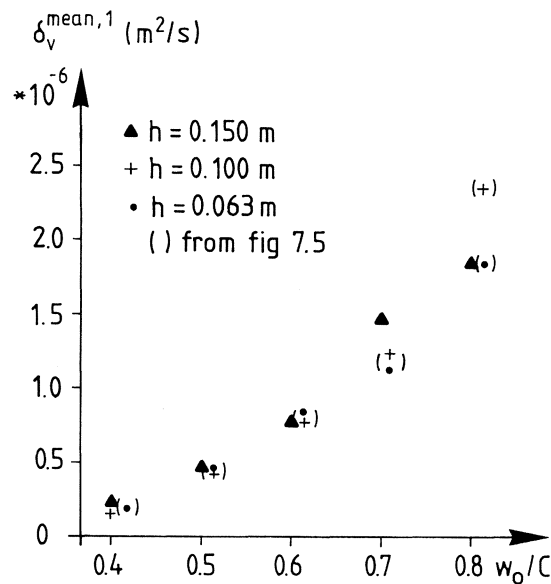

FIG 7.6 Effect of water-cement ratio on the mean moisture permeability within the range 33 % $\leq$ RH $\leq$ liquid water, $\delta_V^{mean,1}$. The sealing between the upper box and the specimen has been improved.

FIG 7.6 shows results for the same specimens but determined at two instances, the second (without parenthesis) 2 years after the first (with parenthesis). For most of the specimens with a height of 0.150 m the results are not lower than for the other heights, even though the specimens are much older.

7.1.2   Specimens with the bottom side in moist air

The mean moisture permeability ($\delta_{v}^{mean,2}$) has been calculated for the specimens that stand in moist air, which is brought about with a water surface some centimetres below the specimen. It is assumed that the RH at the bottom of the specimen is 95 %. This is probably somewhat low, see section 11.2.1, but the error in $\delta_{v}^{mean,2}$ is small.

$$\delta_{v}^{mean,2} = g * h / (v_{s} * (0.95 - 0.33)) \qquad\qquad (7.2)$$

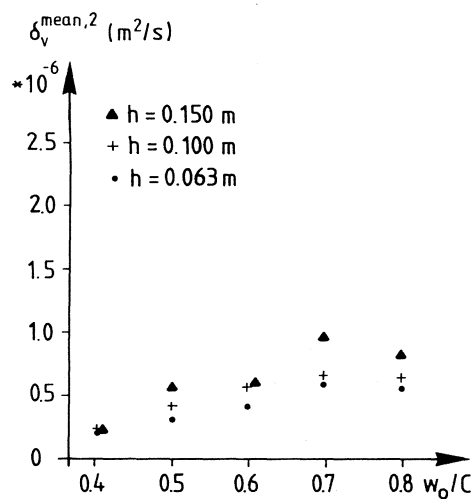The effect of the water cement ratio on $\delta_{v}^{mean,2}$ is shown in FIG 7.7.

FIG 7.7   Effect of water-cement ratio on the mean moisture permeability within the range 33 % $\leq$ RH $\leq$ moist air, $\delta_{v}^{mean,2}$.

In FIG 7.7 it is shown that $\delta_V^{mean,2}$ are almost the same for w_o/C 0.6, 0.7 and 0.8. There is no, or little, influence of w_o/C on $\delta_V^{mean,2}$ and on the moisture flow, specially for the heights 0.063 and 0.100 m.

For w_o/C 0.4 and 0.5, $\delta_V^{mean,2}$ is nearly the same as $\delta_V^{mean,1}$ in FIG 7.5. For these w_o/C there is only a small difference in the moisture flow if the specimens stand in water or in high RH. The influence of the height of the specimen is the same in FIG 7.7 as in FIG 7.5. For a discussion see section 7.1.1.

The influence of the heights of the specimens on the ratio $\delta_V^{mean,2}/\bar{\delta}_V^{mean,2}$ where $\bar{\delta}_V^{mean,2}$ is the average value for all concretes with the same w_o/C, is shown in FIG 7.8.
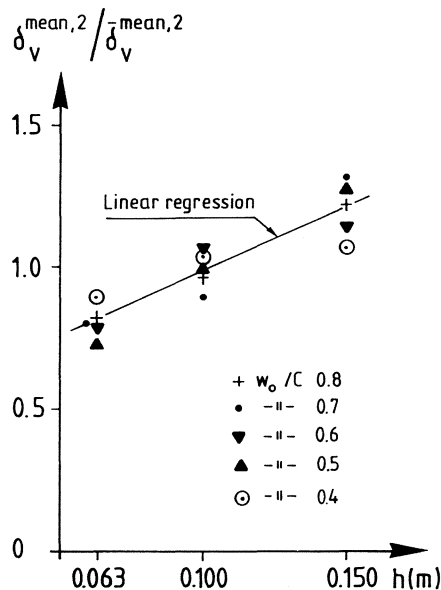

FIG 7.8 The influence of the heights of the specimens on the ratio $\delta_V^{mean,2}/\bar{\delta}_V^{mean,2}$ ($\bar{\delta}_V^{mean,2}$ is defined in the text).

In FIG 7.8 it is shown that there is an influence of the height on $\delta_V^{mean,2}$. The higher the specimen the higher is $\delta_V^{mean,2}$. For a discussion of these results see Chapter 10.

70

7.1.3 Estimated moisture permeabilities above 95 % RH

If the concretes have not leaked alkalies to the bottom vessel, the maximum RH in the specimens should be lower than 100 % due to the fact that the pore water contains solved alkalies; see Hedenblad (1988). The maximum RH is different for different w_o/C. The following values are used; see also TABLE 11.2 column 3.

w_o/C	max RH
0.8	98.5
0.7	98.0
0.6	97.6
0.5	97.0
0.4	96.0

For w_o/C 0.6, 0.7 and 0.8 the average values of the measured moisture permeabilities (TABLE 7.1) are used up to 95 % RH. Over 95 % RH the moisture permeabilities are estimated. The estimated values and the measured values in calculations of the stationary case should give about the same RH-distribution as the measured RH-distribution in the specimens with their bottom sides in water. The calculated moisture flow should also be nearly the same as the measured moisture flow.

Many different combinations of the estimated moisture permeabilities can of course give about the same RH-distribution and the same moisture flow as for the measured specimens. Several different combinations have been investigated, before the final combinations were chosen.

One idea behind the choice of moisture permeabilities, for concrete with w_o/C 0.6, 0.7 and 0.8, has been that the moisture flow in the largest pores and above all in the boundary zone between aggregate and cement paste is dependent on the moisture content in the concrete and not directly on RH.

71

In section 13.1.3 and 13.2 a relation between the "surface
flow" and the surface concentration is given. "Surface flow" is
the adsorbed layer flow rate. The surface concentration is in
principle the "moisture content" in the isotherm. In the
calculations the "apparent surface flow" is put at zero at 95 %
RH. This will correspond to that there is not any liquid flow
in the boundary zone between aggregate and cement paste.
There is probably liquid flow below 95 % RH, see APPENDIX
E, this is the reason why the liquid flow is given the name
apparent. Liquid flow is assumed to occur in the boundary zone
above 95 % RH. The isotherms for different w_o/C are shown in
FIG 14.1. Considerations for the fact that the cement contains
alkali have been taken in FIG 14.1. The surface concentration
(in the boundary zone) is put at zero at 95 % RH.

The relation between the apparent surface flow and the
(surface concentration)^2/RH for concrete with w_o/C 0.8 is shown
in FIG 7.9. The relation is derived in Chapter 13.
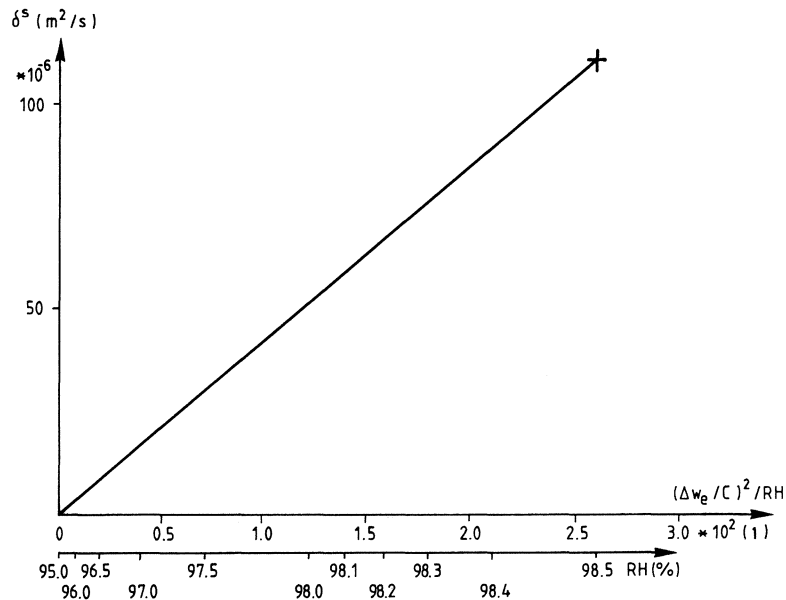

FIG 7.9   The relation between the "apparent surface flow" and
          the ("surface concentration")^2/RH above 95 % RH for
          concrete with w_o/C 0.8.

The apparent surface flow (δ^s, m^2/s) is added to the moisture permeability at 95 % RH (7.5 $*$ 10^{-6}, m^2/s) to get the total moisture permeability. The apparent surface flow at the maximum value of the sorption isotherm has been estimated on basis of a computer simulation in which the measured RH-profile has been reproduced. The other apparent surface flows, at lower RH, have been read from the curve (FIG 7.9 for w_o/C 0.8).

The above method has not been applied to concrete with w_o/C 0.5. Instead the measured moisture permeabilities according to TABLE 7.1 column 3 have been used up to 95 % RH. Over 95 % RH the moisture permeability has been estimated and adjusted until the calculated RH-distribution and the calculated moisture flow are nearly the measured values. The estimated δ_v:s are nearly the same as the measured δ_v:s. The estimated moisture permeabilities over 95 % RH are shown in TABLE 7.2.

TABLE 7.2 Estimated moisture permeability, from 95 % RH, for concrete with w_o/C 0.4, 0.5, 0.6, 0.7 and 0.8.

RH	$\delta_v * 10^6$ (m^2/s)				
%	w_o/C 0.4	w_o/C 0.5	w_o/C 0.6	w_o/C 0.7	w_o/C 0.8
95	$(0.695)^{1)}$	2.78	7.5	7.5	7.5
95.5	–	3.3	8.0	–	–
96.0	$(0.71)^{1)}$	4.2	8.5	9.5	11
96.2		4.7	–	–	–
96.4		5.4	–	–	–
96.5		–	10.5	13.5	17
96.6		6.3	–	–	–
96.8		7.5	–	–	–
97.0		9.0	14	17.5	26
97.2			16.5	21.5	–
97.4			19	25	–
97.5			20.5	–	40
97.6			22.5	28.5	–
97.8				32.5	–
98.0				37.5	63
98.1					72
98.2					80
98.3					90
98.4					105
98.5					128

1) One specimen only

With the moisture permeabilities according to TABLE 7.1 column
2,3 and 7 and according to TABLE 7.2 the RH-distribution curves
have been calculated for the specimens with a height of 0.1 m.
In FIG 7.10 and FIG 7.11 the calculated and the measured
RH-distribution are shown for concrete with w_o/C 0.5, 0.6, 0.7
and 0.8. FIG 7.10 shows the results for specimens with their
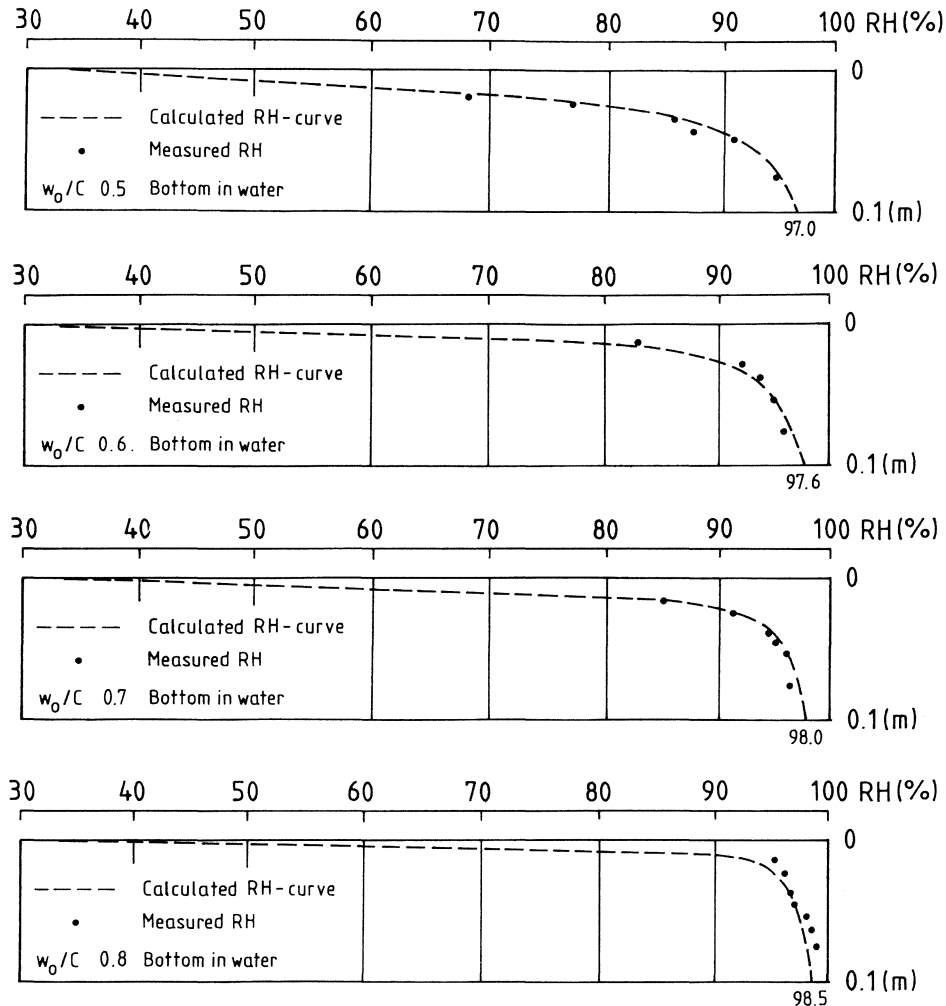bottom surface in water.

FIG 7.10   Calculated and measured RH-distribution of specimens
with a height of 0.1 m. Concrete with w_o/C 0.5, 0.6,
0.7 and 0.8. The bottom surfaces are in water.

74

FIG 7.11 shows the results for specimens with their bottom
surface in moist air. The calculated moisture flows are the
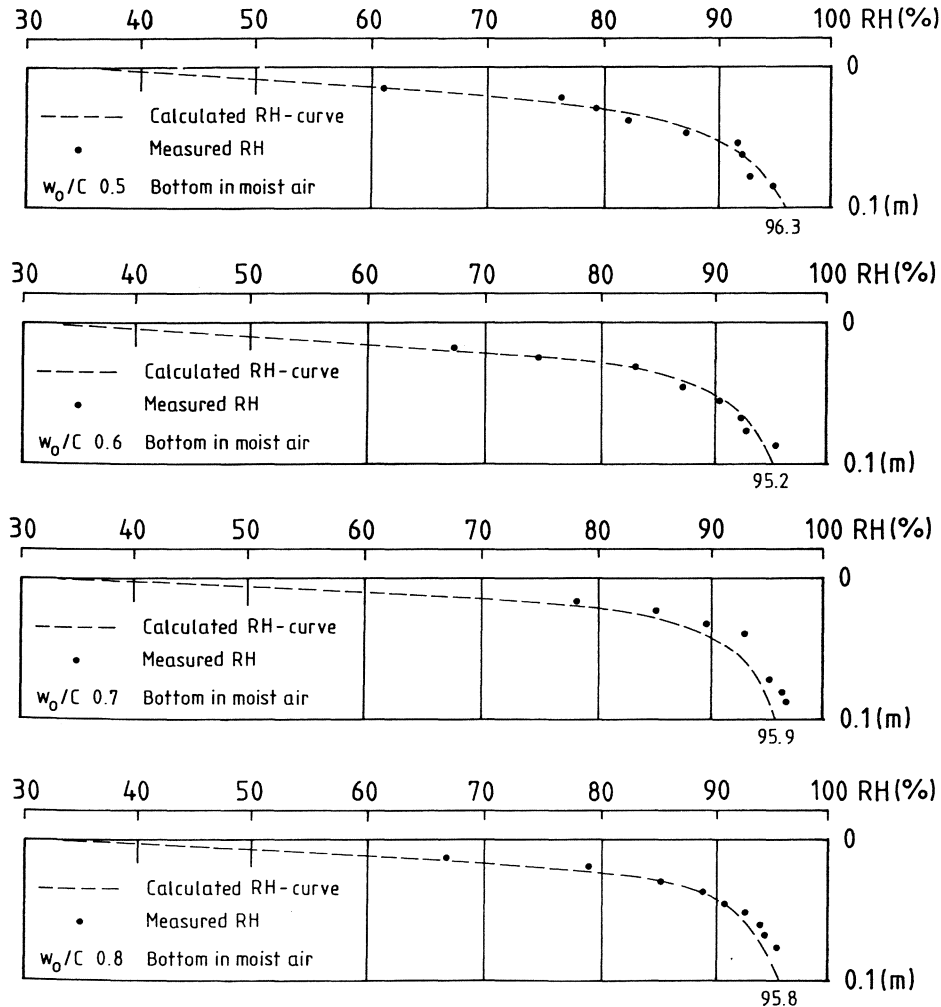same as the measured moisture flows, see APPENDIX A, column 3.

FIG 7.11 Calculated and measured RH-distribution of specimens
          with the height 0,1 m. Concrete with w_o/C 0.5, 0.6,
          0,7 and 0,8. The bottom surface is in moist air.

When comparing FIG 7.10 and FIG 7.11 it is seen that the
difference in RH at the bottom sides of the specimens with the
same w_o/C is about 1 to 3 %. This discrepancy is further
discussed in Chapter 11.

7.2 **Effect of different amounts of air**

In FIG 7.12 $\delta_v^{mean,1}$ according to Eq.(7.1) is shown as a function of the air content of the concrete. The concretes have w_o/C 0.7. The bottoms of the specimens are in water.
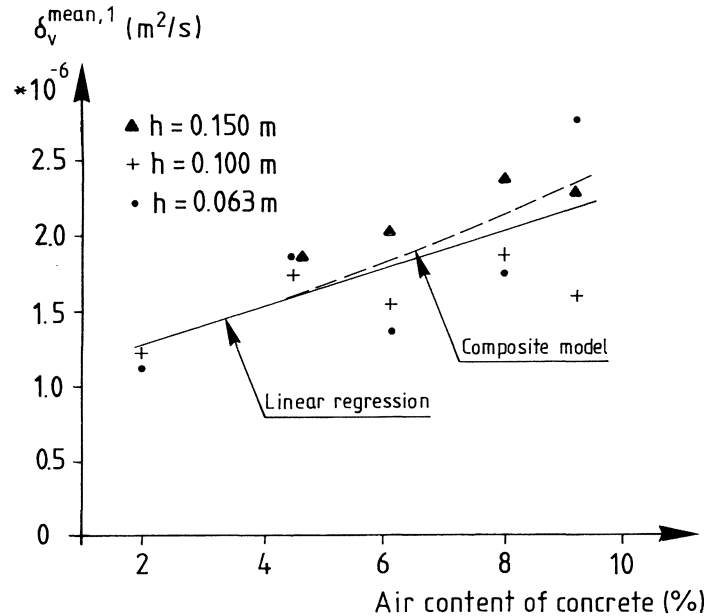

FIG 7.12   Effect of the air content of concrete on mean
            moisture permeability in the range 33 % ≤ RH ≤
            liquid water, $\delta_v^{mean,1}$. Concrete with w_o/C 0.7.

The concrete without additional air is supposed to have an air content of 2 %. The scatter is great in FIG 7.12, but it seems that higher air content gives higher $\delta_v^{mean,1}$. Linear regression for the measured results shows that $\delta_v^{mean,1}$ has increased about 70 % when the air content is increased from 2 % to 9.2 %. The calculated results of a composite model are shown in FIG 7.12. The result of the model is adjusted so that it coincides with the linear regression line at 2 % air content. For more information about the composite model see APPENDIX E.

In FIG 7.13 $\delta_V^{mean,2}$ according to Eq. (7.2) is shown as a function of the air content of the concrete. The concrete has w_o/C 0.7. The bottoms of the specimens are in moist air.
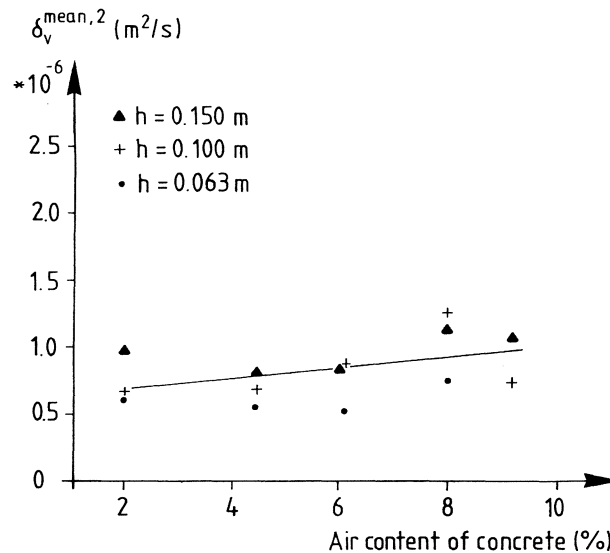

FIG 7.13 Effect of the air content of concrete on mean moisture permeability in the range 33 % ≤ RH ≤ moist air, $\delta_V^{mean,2}$. Concrete with w_o/C 0.7.

As in FIG 7.12 the scatter is great in FIG 7.13. Linear regression in FIG 7.13 shows that $\delta_V^{mean,2}$ has increased about 40 % when the air content has inceased from 2 % to 9.2 %. It is a considerably lower value than that valid when the bottom surface is placed in water. This difference is difficult to explain.

7.3 Effect of aggregate content

The effect of the aggregate content on $\delta_V^{mean,1}$ is shown in FIG 7.14. The concrete has w_o/C 0.7. $\delta_V^{mean,1}$ is defined in 7.1.1.

77

FIG 7.14 Effect of the aggregate content on the mean moisture permeability in the range 33 % ≤ RH ≤ liquid water, $\delta_V^{mean,1}$. Concrete with w_o/C 0.7.

The linear regression curve for $\delta_V^{mean,1}$ in FIG 7.14 shows that $\delta_V^{mean,1}$ increases when the aggregate content is increased. Between aggregate content 1692 and 1854 kg/m^3, $\delta_V^{mean,1}$ for the linear regression has increased about 60 %. In FIG 7.14 there are results from two heights of the specimens, 0.063 and 0.100 m.

In FIG 7.15 $\delta_V^{mean,1}$ is shown for the same specimens as in FIG 7.14 but about two years later. In FIG 7.15 there are also results from specimens with a height of 0.150 m. The specimens in FIG 7.15 have been kept in the same experimental set-up for about 5 years. The sealing between the upper box and the specimen has been improved for all the specimens in FIG 7.15.
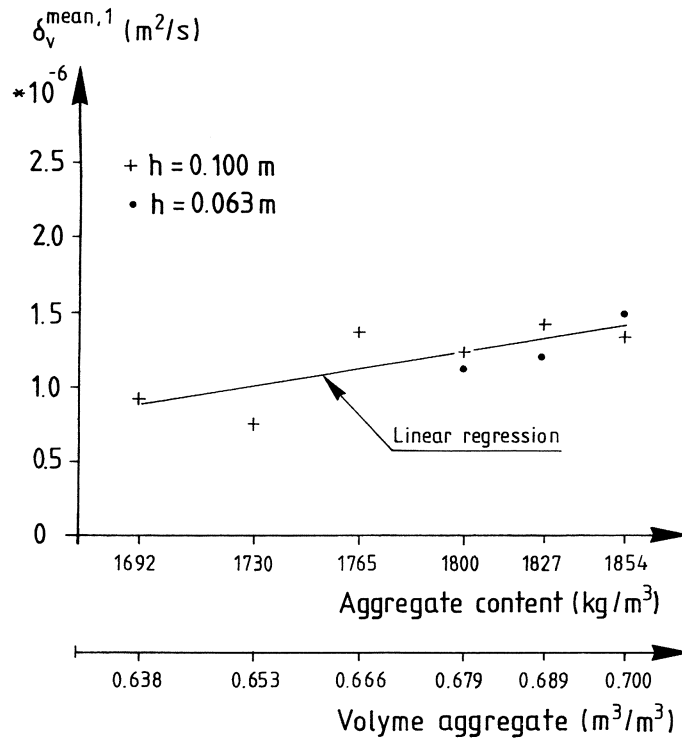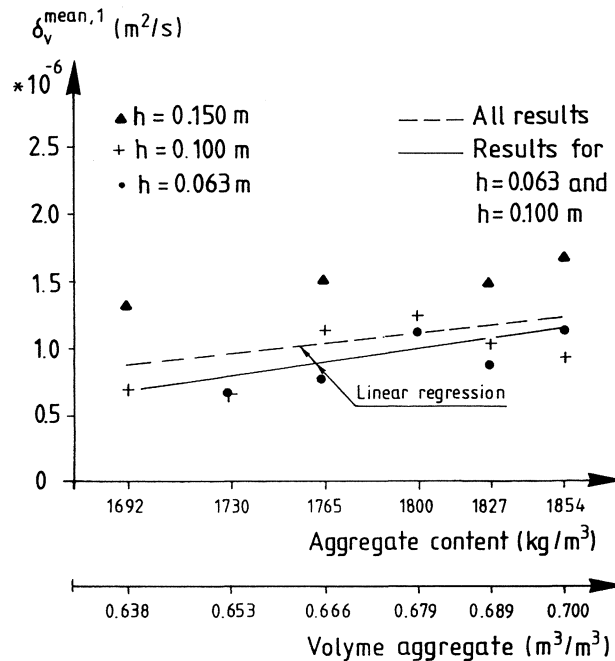
FIG 7.15 Effect of the aggregate content on the mean moisture permeability in the range 33 % $\leq$ RH $\leq$ liquid water, $\delta_V^{mean,1}$. Concrete with w_o/C 0.7. The specimens have dried about 5 years.

For most of the specimens in FIG 7.15 $\delta_V^{mean,1}$, is lower than in FIG 7.14. If this is a result of the improvement of the sealing between the upper box and the specimen or if it is a result of the longer time of exposure is not clear. One can not exclude that the concretes continue to hydrate. This probably means that the moisture permeability is reduced.

Linear regression shows that $\delta_V^{mean,1}$ probably increases with increasing aggregate content. The full line is the linear regression line for specimens with the heights 0.063 and 0.100 m. The broken line is linear regression for all the specimens in FIG 7.15. In both cases the lines increase with increasing aggregate content. The slope of the line for the specimens with the heights 0.063 and 0.100 m is nearly the same as the slope of the linear regression line in FIG 7.14.

79

In FIG 7.15 it is shown that $\delta_V^{mean,1}$ is higher for higher specimens of the same quality. In FIG 7.16 the ratio $\delta_V^{mean,1}/\bar{\delta}_V^{mean,1}$, where $\bar{\delta}_V^{mean,1}$ is the average value of $\delta_V^{mean,1}$ for concretes with the same aggregate content, is shown as function of the heights of the specimens.

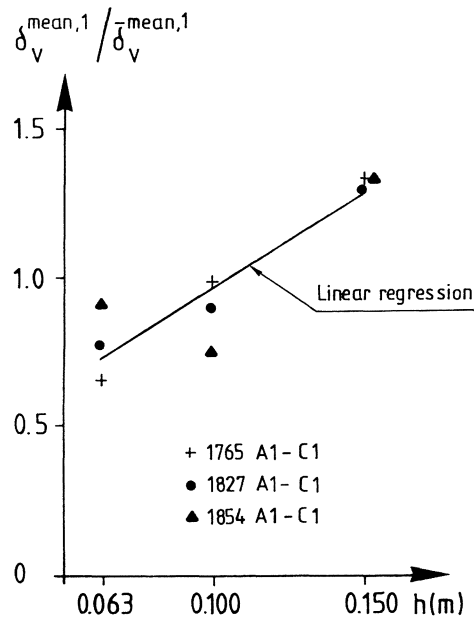FIG 7.16 The influence of the heights of the specimens on the ratio $\delta_V^{mean,1}/\bar{\delta}_V^{mean,1}$; $\bar{\delta}_V^{mean,1}$ is defined in the text. The specimens have dried about 5 years.

In FIG 7.16 it is shown that the higher the specimen, the higher is the quotient, even if the spread for the heights 0.063 and 0.100 m is big.

The effect of the aggregate content on $\delta_V^{mean,2}$ is shown in FIG 7.17. The concrete has w_o/C 0.7. $\delta_V^{mean,2}$ is defined in section 7.1.2.
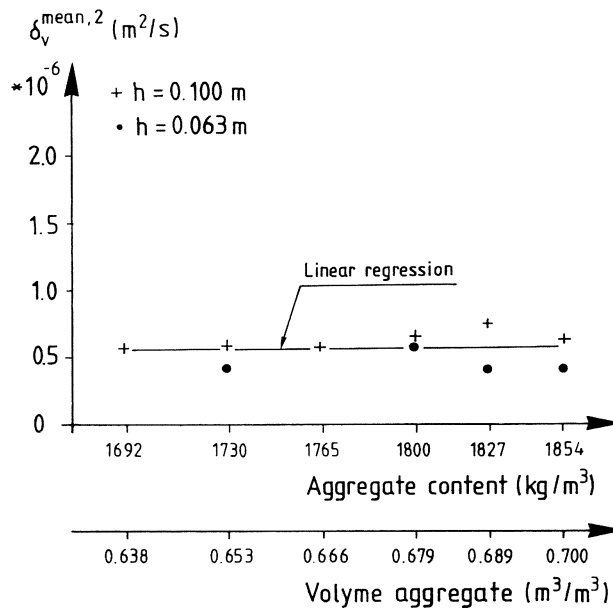
FIG 7.17   Effect of the aggregate content on the mean moisture permeability in the range 33 % ≤ RH ≤ moist air, $\delta_V^{mean,2}$. Concrete with w_o/C 0.7.

The linear regession line for $\delta_V^{mean,2}$ in FIG 7.17 shows that $\delta_V^{mean,2}$ is about the same for all the different aggregate contents.

One explanation for the result for $\delta_V^{mean,2}$ and $\delta_V^{mean,1}$ is that the boundary zones between paste and aggregate increase when the aggregate content increases. In this boundary zone the resistance to water flow is low. In the measure $\delta_V^{mean,1}$ there is more water flow, in the specimen, than in the measure $\delta_V^{mean,2}$. Consequently $\delta_V^{mean,1}$ should increase more with the aggregate content than $\delta_V^{mean,2}$.

In TABLE 3.4 it is shown that the slump of the concrete decreases when the aggregate content increases. The "boundary zone" and the air content of the concrete with low slump are probably bigger than with high slump. This will give a more permeable concrete, and a second explanation is given.

81

8 RESULTS FOR CEMENT MORTAR

The results which are presented in this chapter show the
moisture permeability with regard to humidity by volume in the
pores of the specimens (δ_V) as function of RH or as the mean
moisture permeability for the specimens with defined moisture
conditions at the boundaries.

8.1 Effect of water-cement ratio

The cement mortar qualities that are shown in FIG 8.1 have
water-cement ratio 0.4, 0.5, 0.6, 0.7 and 0.8. The composition
of the cement mortars is shown in Chapter 3.2.2. The amount of
sand/gravel is the same for the different water-cement ratios.
The moisture permeability (δ_V) as function of RH is shown in
FIG 8.1.

$\delta_V(m^2/s)$

$*10^{-6}$

w$_O$/C
——— 0.8
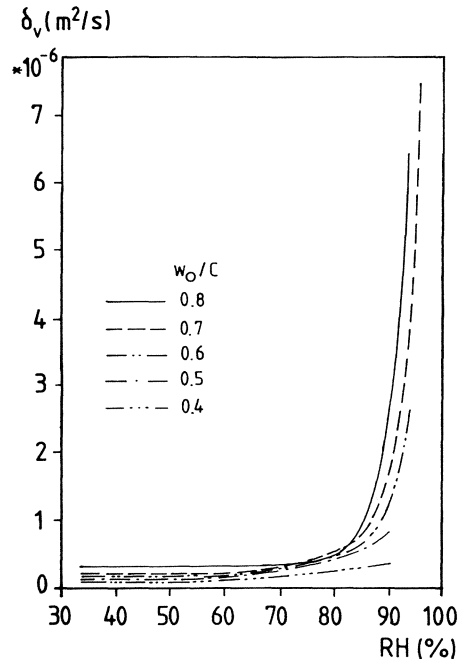— — — 0.7
—··— 0.6
—·— 0.5
—···— 0.4

RH (%)

FIG 8.1 Measured moisture permeability for cement mortar as
function of RH. w$_O$/C 0.4, 0.5, 0.6, 0.7 and 0.8.

In FIG 8.1 it is shown that the moisture permeability up to
about 60 % RH depends on the water-cement ratio and hardly at
all on the RH. Between about 60 and 80 % RH there is a small
increase of δ_v with RH. Over about 80 % RH there is a strong
increase of δ_v with RH for w_o/C 0.6, 0.7 and 0.8. For w_o/C 0.4
and 0.5 the increase with RH is not so pronounced as for the
other qualities. The moisture permeability as function of RH is
also shown in TABLE 8.1. The maximum RH in the table is the
really measured value.

TABLE   8.1   Moisture permeability for cement mortar with
different w_o/C.

RH	$\delta_v * 10^6$ (m^2/s)				
%	w_o/C 0.4	w_o/C 0.5	w_o/C 0.6	w_o/C 0.7	w_o/C 0.8
33-65	0.10	0.13	0.18	0.20	0.30
70	0.20	0.23	0.30	0.31	0.30
75	0.24	0.33	0.37	0.41	0.30
80	0.28	0.43	0.46	0.56	0.46
84	0.30	0.51	0.58	0.71	0.70
86	0.32	0.55	0.67	0.86	1.11
88		0.65	0.85	1.15	1.62
90		0.77	1.10	1.52	2.40
91		0.88	1.23	1.81	3.06
92			1.53	2.26	3.87
93			1.95	2.85	5.22
94			2.68	3.79	6.44
95				4.86	
96				7.78	
**	6	6	6	6	3

** Number of specimens.

8.1.1 Specimens with the bottom side in water

For the definition of $\delta_v^{mean,1}$ see Chapter 7.1.1. In FIG 8.2
$\delta_v^{mean,1}$ is shown as function of w_o/C. For nearly all w_o/C there
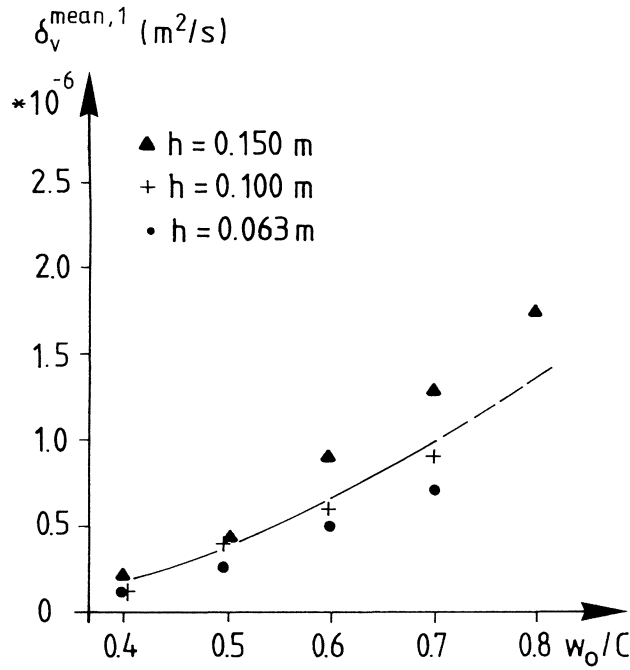are specimens with the heights 0.063, 0.100 and 0.150 m.

$$\delta_v^{mean,1} \ (m^2/s)$$

$*10^{-6}$

▲ h = 0.150 m
+ h = 0.100 m
• h = 0.063 m

FIG 8.2   Effect of water-cement ratio on the mean moisture
         permeability within the range 33 % ≤ RH ≤ liquid
         water, $\delta_v^{mean,1}$. Cement mortar.

FIG 8.2 shows that the ratio between w_o/C 0.8 and 0.5 is about
4. This is nearly the same as for concrete even though $\delta_v^{mean,1}$
is lower for cement mortar than for concrete with the same
w_o/C. This is more pronounced for higher w_o/C.

In FIG 8.2 it is seen that $\delta_v^{mean,1}$ depends on the heights of
the specimens. This is more clearly shown in FIG 8.3, which
shows the quotient $\delta_v^{mean,1}/\bar{\delta}_v^{mean,1}$ as function of the heights
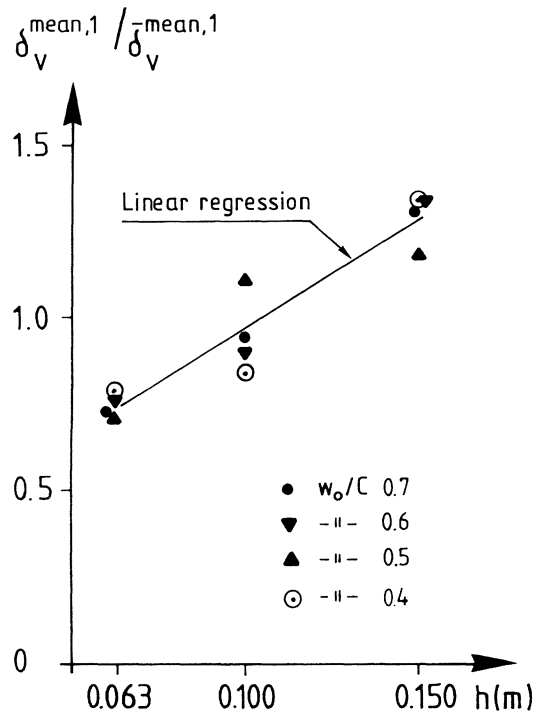of the specimens.

FIG 8.3 Effect of the heights of the specimens on the ratio $\delta_V^{mean,1}/\bar{\delta}_V^{mean,1}$. Cement mortar.

For w_O/C 0.4, 0.6 and 0.7 there is nearly a linear dependence with the heights of the specimens. For w_O/C 0.5 there is an irregular dependence.

The sealing between the upper box and the specimen has been improved for the specimens with w_O/C 0.4 and 0.8. The results of the completion of the sealing are shown in FIG 8.4. The results for the completed specimens are about 2 years "older" than the results in FIG 8.3.
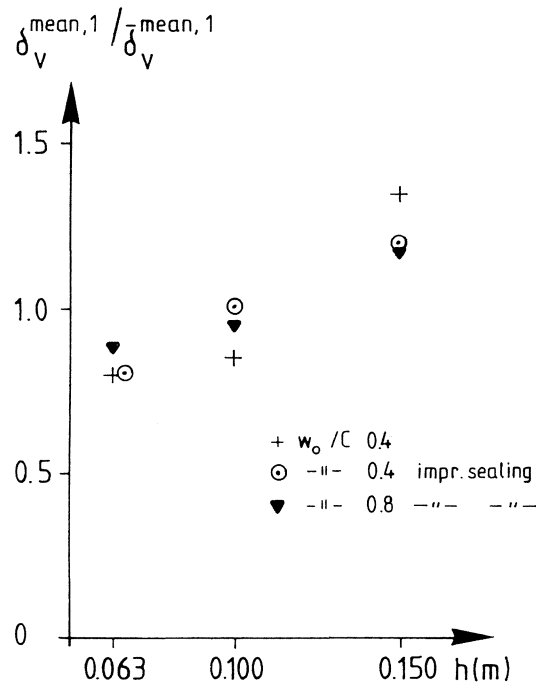
$$\delta_V^{mean,1} / \bar{\delta}_V^{mean,1}$$

1.5

1.0

0.5

0

+ w_o /C   0.4
⊙ $-\parallel-$ 0.4   impr. sealing
▼ $-\parallel-$ 0.8 $-\parallel-$ $-\parallel-$

0.063   0.100   0.150   h(m)

FIG 8.4   Effect of the heights of the specimens on the
ratio $\delta_V^{mean,1}/\bar{\delta}_V^{mean,1}$. The sealing between the
upper box and the specimen has been improved.
Cement mortar.

It is shown in FIG 8.4 that the improvement of the sealing has
small influence on the quotient $\delta_V^{mean,1}/\bar{\delta}_V^{mean,1}$ and that the
influence of the heights still exists after about 5 years of
drying.

8.1.2   <u>Specimens with the bottom side in moist air</u>

For the definition of $\delta_V^{mean,2}$, see Chapter 7.1.2. In FIG 8.5
$\delta_V^{mean,2}$ is shown as function of w_o/C. For each w_o/C there are
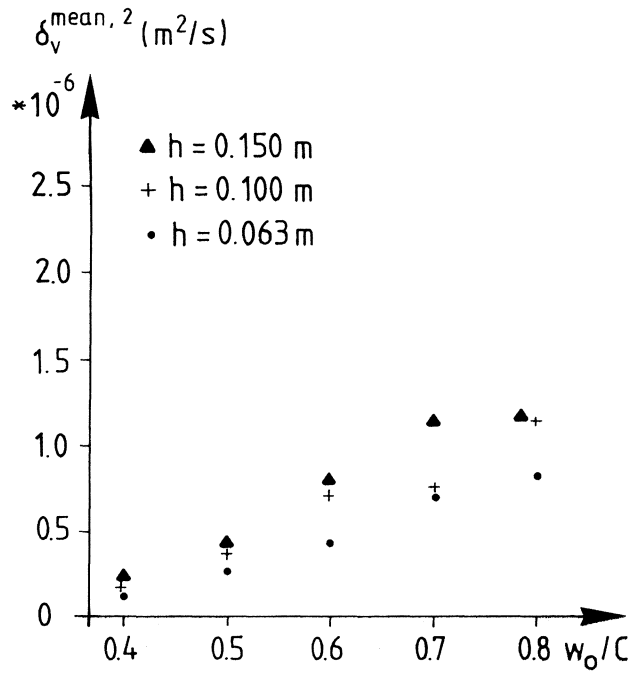specimens with the heights 0.063, 0.100 and 0.150 m.

FIG 8.5   Effect of the water-cement ratio on the mean
           moisture permeability within the range
           33 % ≤ RH ≤ liquid water, $\delta_v^{mean,2}$. Cement mortar.

In FIG 8.5 $\delta_v^{mean,2}$ seems to depend on the heights of the
specimens. This is more clearly shown in FIG 8.6 where the
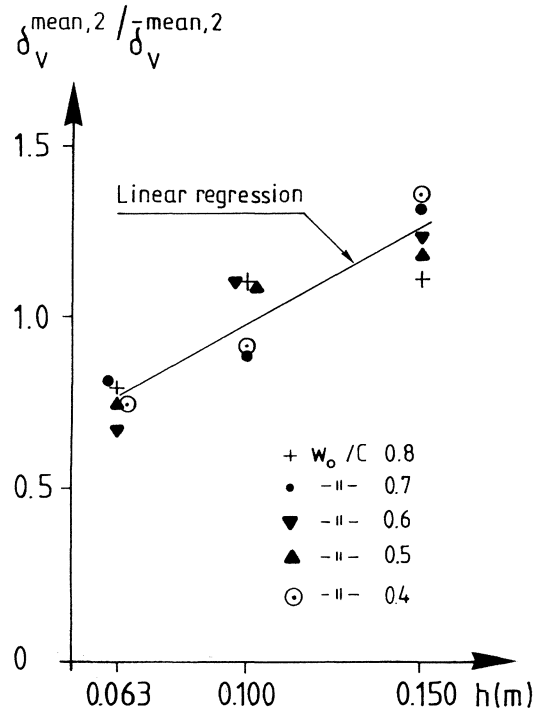ratio $\delta_v^{mean,2}/\overline{\delta}_v^{mean,2}$ is shown as function of the height.

FIG 8.6 Effect of the heights of the specimens on the ratio $\delta_V^{mean,2}/\bar{\delta}_V^{mean,2}$. Cement mortar.

Linear regression for the results in FIG 8.6 shows that the coefficient of correlation is 0.91. At the height 0.063 the linear regression line has the value 0.77 and at the height 0.150 m it has the value 1.25.

The sealing between the upper box and the specimen has been improved for specimens with w_o/C 0.5. The results of the completion are shown in FIG 8.7. The results for the specimens with improved sealing are after about 5 years of drying, and the other results are after about 3 years of drying.

$$\delta_V^{mean,2} / \overline{\delta}_V^{mean,2}$$

1.5

1.0

0.5

0

+ w_o /C 0.5
* –"– 0.5 impr. sealing
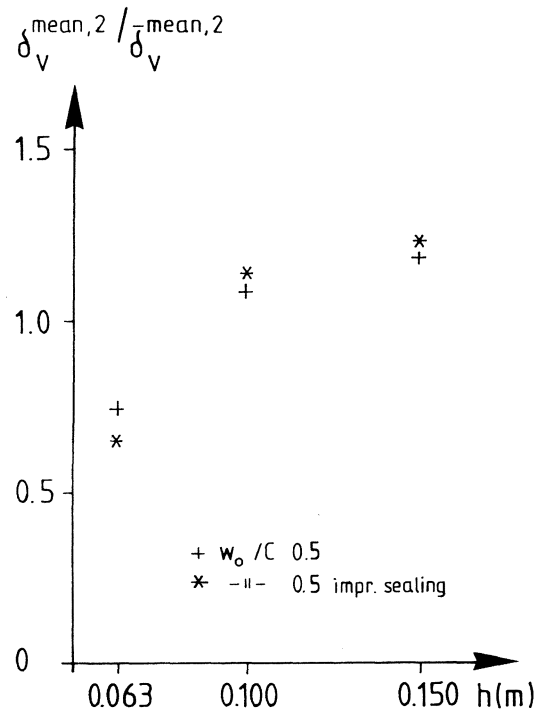
0.063   0.100   0.150 h(m)

FIG 8.7 Effect of the heights of the specimens on the
ratio $\delta_V^{mean,2} / \overline{\delta}_V^{mean,2}$. The sealing between the
upper box and the specimen has been improved.
Cement mortar.

The effect of the improvement of the sealing, shown in FIG 8.7,
is small and the influence of the heights still remains after
the sealing has been improved.

9 RESULTS FOR CEMENT PASTE

The results which are presented in this chapter show the moisture permeability with regard to humidity by volume in the pores of the specimens (δ_v) as function of RH or as the mean moisture permeability for the specimens with defined moisture conditions at the boundaries. Three w_o/C are investigated, but the RH-distributions have only been determined for w_o/C 0.5 and 0.6.

9.1 Effect of the water–cement ratio

The cement pastes that are shown in FIG 9.1 and FIG 9.2 have w_o/C 0.5 and 0.6. The mean measured δ_v for the results in FIG 9.1 is from 2 specimens. The mean measured δ_v in FIG 9.2 is from up to 6 specimens. The measured maximum and minimum δ_v are also shown in the same figures. Note different scales.
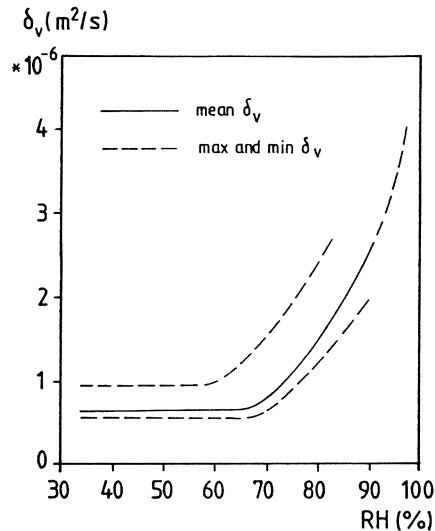

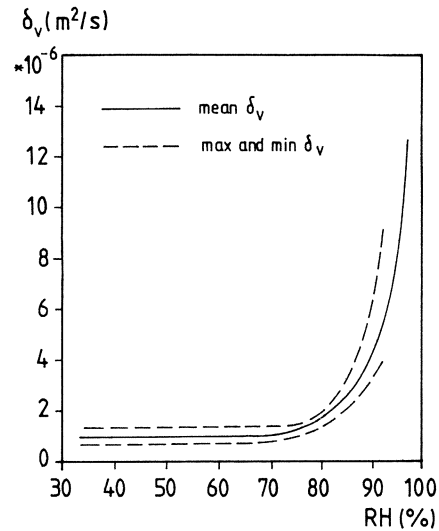FIG 9.1 Measured moisture permeability for cement paste with w_o/C 0.5.

FIG 9.2 Measured moisture permeability for cement paste with w_o/C 0.6.

δ_{V} in FIG 9.1 is only determined up to 91 % RH. The distribu-
tion of RH in the specimens are estimated over 91 %; see
specimen P5A1 and P5B1 in APPENDIX B. The estimated RH-distri-
bution curve gradually and continuously follows the measured
mean RH-distribution curve. For most specimens with the bottom
in water it ends at the maximum RH given in section 7.1.3.

In FIG 9.3 the surface moisture permeability, δ^S, is plotted
against the quotient $(\Delta w_e/C)^2/RH$. $\Delta w_e/C$ is the distance from
the "zero- level" at 65 % RH to the actual moisture content in
the isotherm; see FIG 14.1. The zero-level is set at 65 % RH as
δ_{V} is constant up to this RH.

FIG 9.3   The surface moisture permeability dependence on
           surface flow as function of $(\Delta w_e/C)^2/RH$.
           Cement paste w_o/C 0.5.

As said before, the results over 91 % RH are from estimated RH-
distributions. δ^S over 91 % RH are marked with * in FIG 9.3.
Linear regression is used up to 93 % RH. The coefficient of
correlation is 0.99. If the linear regression line is
extrapolated to 97 % RH, then δ^S at 97 % RH is about $6 * 10^{-6}$
m^2/s. The saturation point in the cement paste is calculated at
97 % RH; see TABLE 11.2.

91

In a given material the gas-phase flow will decrease as the pore system is filled with liquid. When the pore system is completly filled with liquid there is no gas-phase flow at all. In the calculations this is handled so that at the "zero-level" all flow is said to be gas-phase flow, and at saturation the flow is considered as surface flow. Between these two extremes the gas-phase flow is reduced with the quotient $(\Delta w_e/C)/(\Delta w_e/C)_{tot}$.

The average δ_v for w_o/C 0.6 in FIG 9.2 is determined for 6 specimens up to 89 % RH. At higher RH the average RH-distribution in some specimens is estimated (see for instance specimen P6A1 or P6A2 in APPENDIX B) and in other specimens it is measured. Between 94 and 96 % RH the RH-distribution is measured for 2 specimens and estimated for 3 specimens. At 97 % RH is estimated for 5 specimens.

When the surface moisture permeability, δ^S, is plotted against the quotient $(\Delta w_e/C)^2/RH$ the points in FIG 9.4 are obtained. For the surface moisture permeability, see section 13.2. For the isotherm see FIG 14.1. At 70 % RH δ^S is zero as δ_v is constant up to this RH.
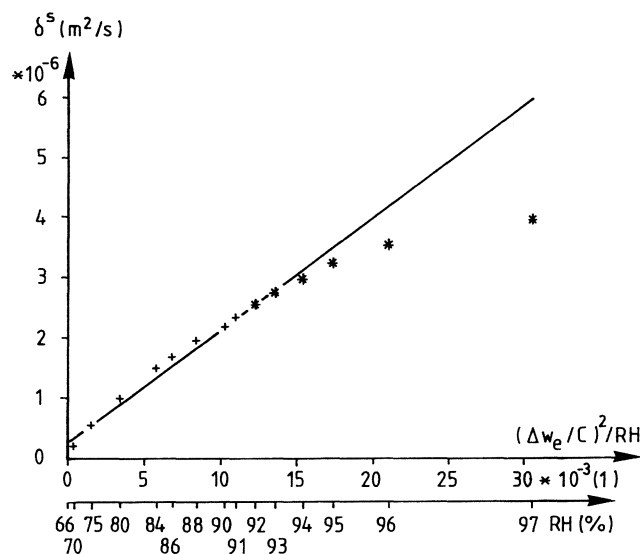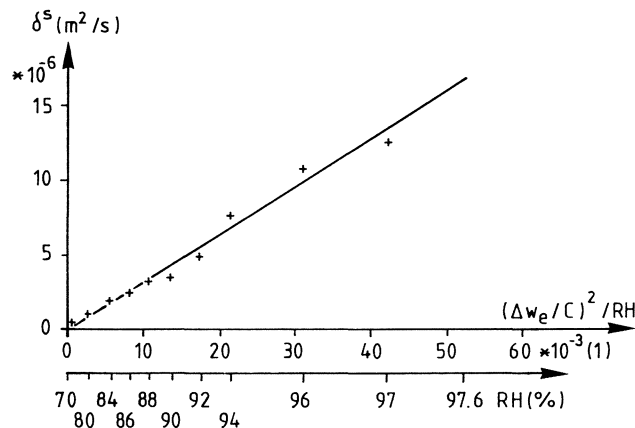

FIG 9.4 The surface moisture permeability dependence on surface flow as function of $(\Delta w_e/C)^2/RH$. Cement paste w_o/C 0.6.

The points over 94 % RH are with more specimens with estimated RH-distribution than with measured RH-distribution. The correlation coefficient for the linear regression is 0.99. The linear regression line is extrapolated to the calculated saturation point of the cement paste (97.6 % RH). At this RH δ^S is $16.8 * 10^{-6}$ m^2/s, which gives the moisture permeability, δ_v, the same value. FIG 9.4 is not a proof, it is only an indication that the estimated RH-distributions are correct.

9.1.1 Specimens with the bottom side in water

For the definition of $\delta_v^{mean,1}$ see section 7.1.1. In FIG 9.5 $\delta_v^{mean,1}$ is shown as function of w_o/C. For w_o/C 0.5 and 0.6 there are specimens with the heights 0.063, 0.100 and 0.150 m. For w_o/C 0.4 there are 2 specimens with the heights 0.063 and 0.150m.
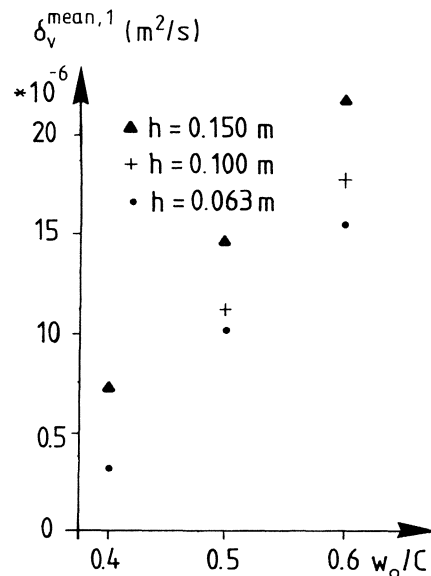

FIG 9.5 Effect of w_o/C on the mean moisture permeability within the range 33 % ≤ RH ≤ liquid water, $\delta_v^{mean,1}$. Cement paste.

93

In FIG 9.5 it is shown that $\delta_V^{mean,1}$ depends on w_o/C. The ratio for $\delta_V^{mean,1}$ between w_o/C 0.6 and 0.4 is about 4. It is also seen that $\delta_V^{mean,1}$ depends on the heights of the specimens. The lower the specimens are, the lower are $\delta_V^{mean,1}$. This is also shown in FIG 9.6, which shows the quotient $\delta_V^{mean,1}/\bar{\delta}_V^{mean,1}$ as function of the heights of the specimens.
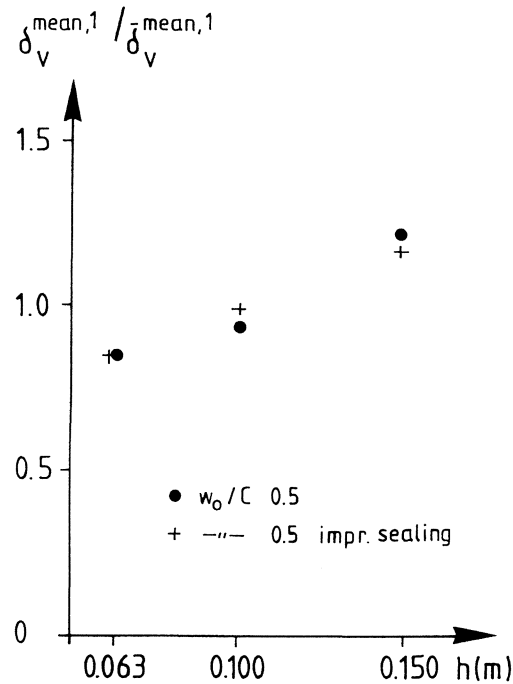
FIG 9.6 Effect of the heights of the specimens on the ratio $\delta_V^{mean,1}/\bar{\delta}_V^{mean,1}$. Cement paste w_o/C 0.5.

In FIG 9.6 there are results from 2 different times. One of the times is before the sealing between the upper box and the specimen has been improved (1989) and the other time is when the sealing has been improved (1992). In both cases we see that there is a dependence on the heights of the specimens.
The oldest results are from specimens that have dried about 5 years.

9.1.2 Specimens with the bottom side in moist air

For the definition of $\delta_V^{mean,2}$ see section 7.1.2. In FIG 9.7 $\delta_V^{mean,2}$ is shown as function of w_o/C. For w_o/C 0.5 and 0.6 there are specimens with the heights 0.063, 0.100 and 0.150 m. For w_o/C 0.4 there are results from 2 specimens with the heights 0.063 and 0.100 m.
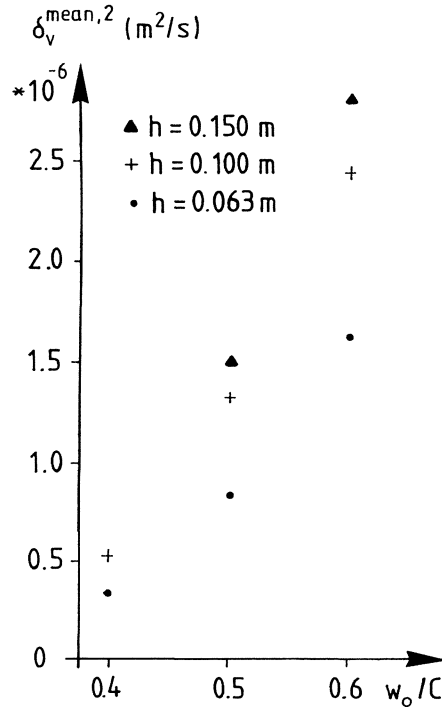
FIG 9.7 Effect of w_o/C on the mean moisture permeability within the range 33 % $\leq$ RH $\leq$ moist air, $\delta_V^{mean,2}$. Cement paste.

In FIG 9.7 it is shown that $\delta_V^{mean,2}$ depends on w_o/C. If FIG 9.7 is compared with FIG 9.5 it is seen that $\delta_V^{mean,2}$ has the same magnitude as $\delta_V^{mean,1}$ for the same w_o/C. This means that there is no, or little difference in the moisture flow if the specimens stand in water or in moist air. In FIG 9.7 there is a dependence of the heights of the specimens on $\delta_V^{mean,2}$. This is

also shown in FIG 9.8, which shows $\delta_V^{mean,2}/\bar{\delta}_V^{mean,2}$ as function of the heights of the specimens.

$$\delta_V^{mean,2}\Big/\bar{\delta}_V^{mean,2}$$

```
1.5 -


1.0 -



0.5 -
            • w_o/C 0.5
            +  "   0.5   impr. sealing
            ▲  "   0.6
            ▼  "   0.6   impr. sealing
0 -
    ┼──────┼──────────────┼──────────
    0.063  0.100          0.150  h(m)
```
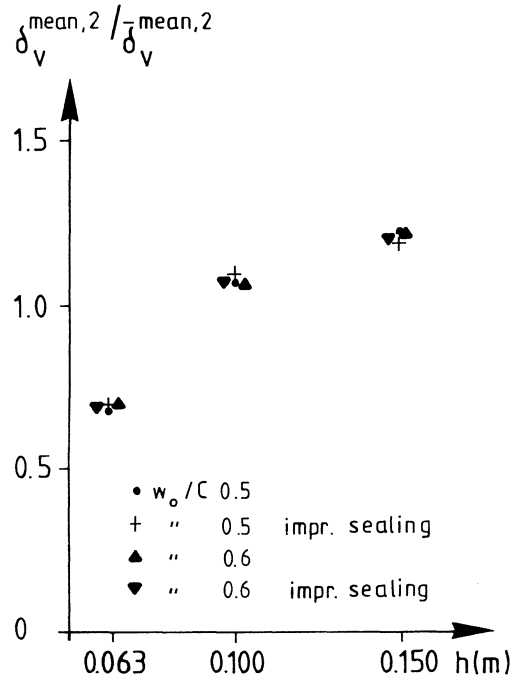
FIG 9.8 Effect of the heights of the specimens on the ratio $\delta_V^{mean,2}/\bar{\delta}_V^{mean,2}$. Cement paste.

In FIG 9.8 there are results from w_o/C 0.5 and 0.6. The results are from before and after the sealing between the upper box and the specimen has been improved. In FIG 9.8 it is shown that there is a dependence on the heights of the specimens. The quotient $\delta_V^{mean,2}/\bar{\delta}_V^{mean,2}$ is nearly independent of the completion of the sealing. There are about 2 years between the different times (before and after improvement).

10 DISCUSSION OF THE SIZE DEPENDENCE

When you look at the results for concrete, cement mortar and
cement paste, one of the most striking results is that there is
a dependence on the height of the specimen. The higher the
specimen the higher are $\delta_V^{mean,1}$, $\delta_V^{mean,2}$ and the fundamental
flow potential (ψ) for specimens of the same quality. This is
somewhat surprising and therefore requires an exposition.
Possible explanations for the result can be
* the moisture flow is not in equlibrium
* errors in the measurements
* carbonation of the top surface
* different materials or curing in the specimens of different
  heights
* correct measurements, but Fick's law in its simple form is
  not valid ("Non-Fickian behaviour")

10.1 Possible errors in the measurements

In many cases the RH-profiles according to scale are the same
for specimens of the same quality and boundary conditions but
with different heights (see specimens C6A2, C6B2 and C6C2 in
APPENDIX B). This implies that the RH-profiles have no
influence on ψ, when the heights of the specimens are diffe-
rent. In $\delta_V^{mean,1}$ and $\delta_V^{mean,2}$ there are no considerations made
for the RH-profiles, but only for the moisture flow and the
boundary conditions. The boundary conditions are equal for
$\delta_V^{mean,1}$ and $\delta_V^{mean,2}$, so for $\delta_V^{mean,1}$ and $\delta_V^{mean,2}$ it is only the
moisture flow which might be incorrectly measured or
inadequately corrected (see Chapter 4).

10.1.1 Possible errors in the measurement of the moisture flow

If there are any errors in the measurements or in the corrections of the moisture flow (see APPENDIX A and Chapter 4), first you can notice that even without any corrections there is an increasing ψ with the heights of the specimens for specimens of the same material quality (see column 5/column 3 in APPENDIX A). A possible explanation can be that the moisture flow is not in equlibrium for the highest specimens in spite of the experiments having lasted about 5 years. A calculation for concrete with w_o/C 0.7 shows that after one year the moisture flow is about 8 % larger and after two years the moisture flow is about 2 % larger than the stationary moisture flow for a specimen with the height 0.15 m. The calculation presumes that the material properties do not change with time or the height of the specimen. The calculation probably shows the magnitude of the required time and that the specimens should be fairly in equlibrium.

One other point in the experiments which can have an influence on the moisture flow is the sealing between the specimen and the upper box. If there is any leakage through this sealing the moisture flow could be affected. If a possible leakage is supposed to be in the same magnitude for all heights of specimens, it should have a larger influence on the higher specimens, which should have a lesser moisture flow through out.

The sealing between the upper box and the specimen has been improved for many specimens. In FIG 7.16, FIG 8.4 and FIG 9.8 it is shown that the influence of the heights remains in spite of a careful sealing.

10.2 Carbonation of the top surface of the specimen

A carbonation of the top surface of the specimens should have
occurred to the same depths, independent of the heights of the
specimens, if the specimens have been exposed to carbon dioxide
during the same time and with the same RH in the air. This
should give a greater influence for the lowest specimens if δ_v
for carbonated material is different from δ_v for non-
carbonated material. At the top surface of the specimens RH is
about 30-40 %. According to FIG 11.6 and FIG 11.7, δ_v for
non-carbonated material should be multiplied with about 0.8 to
get δ_v for carbonated material. This is a rather small
influence. FIG 11.6 and FIG 11.7 are for cement mortar with
w_o/C 0.5.

Another factor which can have an influence on the moisture flow
is that nearly all specimens with the height 0.150 m have been
without the upper box for a year or so. This means that these
specimens' carbonation should have occurred to a greater depth
than in the other specimens. When the specimens had the upper
box in place, it was opened once a week. Only at these
occasions could carbon dioxide get into the upper box. All in
all it does not seem probable that carbonation of the top
surface should have any special influence on the moisture flow.

10.3 Different material in specimens with different heights

The specimens with the same composition were poured and treated
at the same time. At the pouring all material came from the
same making. The treatment was with a vibrating table. During
vibration and the following solidification there is a
separation so that there is more aggregate in the lower part of
the specimens. According to FIG 7.15 and FIG 7.17 the aggregate
content has some influence on $\delta_v^{mean,1}$ and nearly no influence
on $\delta_v^{mean,2}$ for concrete. Besides, the size-effect is equally
marked for cement paste, FIG 9.5 and FIG 9.7, as for concrete.

99

Another factor which can influence the results is the curing of
the specimens. According to Wierig (1965) the curing time
influences the moisture permeability. In FIG 10.1, Wierig's
reults are shown. On the x-axis is the curing time in water (in
months) and on the y-axis is the moisture permeability with
vapour pressure (kp/m^2) as potential. The moisture permeability
is the mean moisture permeability for specimens that on one
side have 95 % RH and on the other side have about 0 % RH.
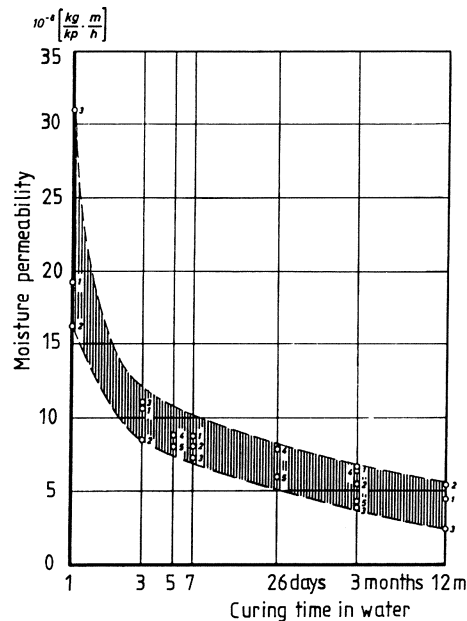
FIG   10.1   The dependence of the curing time in water on the
moisture permeability. Cement mortar with w_o/C 0.6.
Wierig (1965).

In FIG 10.1 it is shown that the longer the curing time the
lower is the moisture permeability. After 12 months of curing
time in water, the moisture permeability has not reached an
asymptotical (lowest) value.

The precuring of our specimens was membrane curing for at least
two months followed by one or more months of capillary suction

100

of water. The precuring of specimens of the same quality has
not been systematically made so that the higher specimens have
had shorter curing time. Even though the conretes were fairly
old when the test started a certain hydration cannot be
excluded. This should cause a gradual change in the δ_v-RH-curve
and thus gradually change the RH-profile. There is, however, no
reason to believe that the effect should be different for
different specimens. Therefore, the shape of the RH-curves
should be the same after the same time irrespectively of the
specimen height.

10.4 Non-Fickian behaviour

From the above discussions it seems as though the measurements
are correct and there is a dependence of the height of the
specimens on the moisture permeability. Of course there is a
spread in our results, but after all it seems that the higher
the specimen, the higher are the moisture permeabilities. This
it not a new finding; this was shown in 1965 by both Wierig and
Pihlajavaara.

Wierig (1965) measured the moisture permeability, at stationary
conditions, for specimens with different thicknesses. The
smallest sample was 0.01 m and the biggest sample was 0.04 m
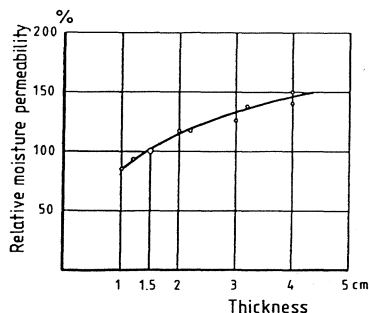thick.

FIG 10.2   Influence of the specimen size on the relative
            moisture permeability. The moisture permeability of
            the 0.015 m thick specimen is put at 100 %.
            Wierig (1965).

In FIG 10.2 it is shown that the relative moisture permeability increases with increasing specimen size. The moisture permeability is 50 % bigger for a sample that is 3 times larger than the reference sample. The curve in FIG 10.2 can be described by

$$\delta_v/\delta_{vo} = (x/x_o)^{0.41} * 100 \qquad\qquad (10.1)$$

Pihlajavaara (1965) presented results from uniaxial drying of "old" specimens made of cement mortar with w_o/C 0.56. The specimens were dried in narrow humidity ranges, about 15 % RH. The start was with specimens stored in water followed by drying in 85 % RH until equlibrium was attained. After that followed drying in 70, 55 and 40 % RH. Pihlajavaara's results are shown in FIG 10.3. The specimens were 0.012 m thick. Some specimens dried from two sides while other dried from one side (the other side was sealed with glued metal sheets).
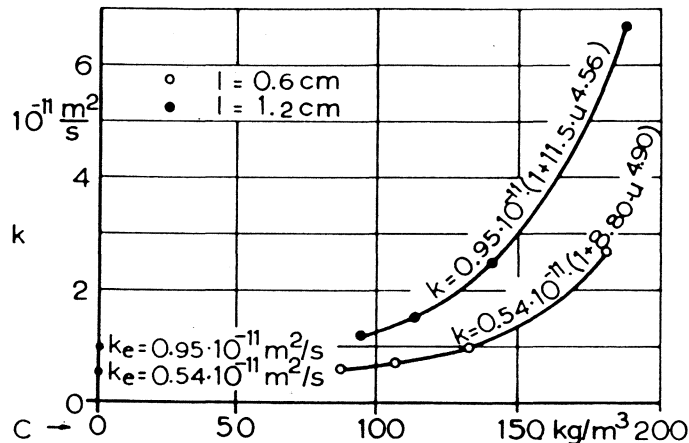

FIG 10.3   The moisture dependence of the diffusivity of cement mortar with w_o/C 0.56. Specimens with the thickness 0.012 m dried from one (l=1.2 cm) side and two (l=0.6 cm) sides. Pihlajavaara (1965).
k is the moisture diffusivity.
C is the moisture content mass by volume.

In FIG 10.3 it is shown that the diffusivity depends both on
the moisture content of the sample and on the thickness of the
sample. The bigger the sample, the higher is the diffusivity.

If Eq.(10.1) is used on the results in FIG 7.8, which is for
concrete with different w_o/C, FIG 10.4 is obtained.

$$\delta_V^{mean,2} \Big/ \bar{\delta}_V^{mean,2}$$

Linear regression

1.0

$(h/\bar{h})^{0.41}$

+ w_o/C 0.8
• –"– 0.7
▼ –"– 0.6
▲ –"– 0.5
⊙ –"– 0.4

0.5

0

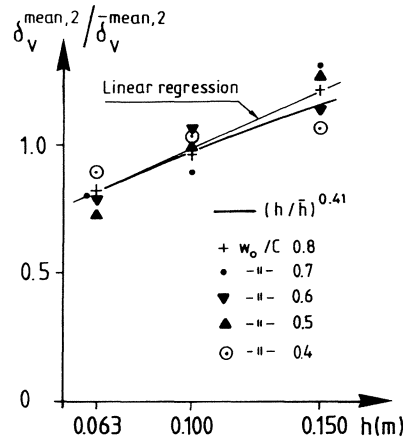0.063   0.100   0.150 h(m)

FIG 10.4   Eq. (10.1) put into the results in FIG 7.8. The
            influence of the heights of the specimens on the
            ratio $\delta_V^{mean,2} / \bar{\delta}_V^{mean,2}$

In FIG 10.4 it is shown that Eq. (10.1), in this particu-
lar case, nearly matches our experimental results.

It is important, if our measurements are correct, to have
specimens with the same dimensions as those which are used in
calculations or to be able to make allowances in the calcula-
tions for the influence of size on moisture permeability.

The results which are described in this thesis can be used for
"old" concrete and particularly for slab on the ground, which
the tests partly should imitate. The moisture permeabilities in
TABLE 7.1, TABLE 7.2 and TABLE 8.1 are for specimens with a
height about 0.1 m and drying from one side. Non-Fickian
behaviour has also been found for other materials. A literature
summary is made by Wadsö (1992). Non-Fickian behaviour is also
discussed in Crank (1975).

11 RELATIVE HUMIDITY IN THE BOTTOM OF THE SPECIMEN

11.1 With the bottom side in water

Half of the number of the specimens stand with their bottom-sides in water. The vessel which contains the water is common to five specimens.

11.1.1 Effect of alkalies in the cement

11.1.1.1 Introduction

When a given material contains different kinds of salts, e.g. sodium chloride (NaCl), or sodium hydroxide (NaOH), the isothermal equilibrium is affected. Garrecht et al (1990) have measured the influence of salts on the sorption isotherm of sandstone for different salts, see FIG 11.1 and FIG 11.2.
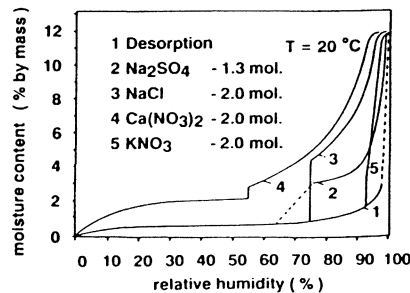
FIG 11.1   Influence of salts   FIG 11.2   Influence of the con-
           on the sorption   centration of NaCl on
           isotherm.   the sorption isotherm.
           Garrecht et al (1990).   Garrecht et al (1990).

Curve 1 in FIG 11.1 is the desorption isotherm without any salt, and it is clearly noticeable that salt in the pores of the sandstone influences the sorption isotherm. It is also shown that the sandstone is saturated with water for a RH-value below 100 %.

In FIG 11.2 curve 1 is the desorption isotherm without any salt. Curve 2 is the desorption isotherm with a concentration of 0.4 mole NaCl and curve 3 is the desorption isotherm with a concentration of 2.0 mole NaCl. The more salt there is in the sandstone, the more the sorption isotherm is affected. A theoretical explanation for non-hygroscopic material is given in Hedenblad (1988). The theoretical explanation gives the same type of curves shown in FIG 11.1 and FIG 11.2.

11.1.1.2 Concrete, cement mortar and cement paste

In the case of cement products, it is above all the contents of alkali metal compounds, chiefly as potassimum hydroxide (KOH) and sodium hydroxide (NaOH), that can affect the humidity equilibrium curve. Peterson (1987) has calculated, for Slite Standard cement (Slite Std) which is used in this study, that the content of alkali metal hydroxides is about 0.34 moles per kg cement, mainly as KOH.

If it is assumed that no alkali metals are bound in the hydration products, it is possible to calculate the maximum RH at complete hydration and water saturation. Raoult's law, see Hägg (1963) gives

$$RH = p_l/p_w = n_w \ / \ (n_w + n_s) * 100 \ (\%) \qquad\qquad (\ 11.1 \ )$$

p_l = partial pressure over a salt solution (Pa)
p_w = partial pressure over pure water (Pa)
n_w = number of moles of water
n_s = number of moles of dissolved salt ions

The number of moles of salt ions can be calculated as

$$n_s = f_i * \text{mole of the salt} \qquad\qquad (\ 11.2 \ )$$

f_i = number of ions per salt molecule

The amount of evaporable water in a saturated cement product can be calculated, see Powers (1960), as

$$w_{es} = (w_o/C - 0.19 \, \alpha) * C \qquad\qquad (11.3)$$

w_{es} = amount of evaporable water at saturation (kg)
α = degree of hydration, assumed to be 1
C = cement content, assumed to be 1 kg

The concentration of KOH and NaOH will be $0.34/w_{es}$ (mole/(kg of water)). The following TABLE 11.1 is achieved.

TABLE 11.1 Maximum RH in cement products according to Raoult's law, Eq. (11.1). No alkalies are supposed to be bound in the hydration products.

w_o/C kg/kg	w_{es}/C kg/kg	n_w mole	n_s mole	maximum RH %
1.0	0.81	45.0	0.84	98.2
0.8	0.61	33.9	1.12	96.8
0.7	0.51	28.3	1.34	95.5
0.6	0.41	22.8	1.66	93.2
0.5	0.31	17.2	2.20	88.7

Example: $w_o/C = 1.0$

$\phantom{w_{es}/C}$ 18 = molecular weight of water
$w_{es}/C = (1-0.19 * 1) = 0.81$ $n_w = 0.81 * 1000/18 = 45.0$
$n_s = 2 * 0.34/0.81 = 0.84$ RH $= 100 * 45/(45+0.84) = 98.2$ %

Some more detailed calculations according to Robinson and Stokes (1955) are made in Hedenblad (1988). One calculation is made under the assumption that no alkali metals are bound in the hydration products and the other calculation is made under the assumption that about 10 to 30 % of the alkali metals are bound. The lower the w_o/C the more alkali metals are bound. Slite Std normally contains 0.28 mole K^+ and 0.06 mole Na^+, Peterson (1987). TABLE 11.2 is taken from Hedenblad (1988).

TABLE 11.2 The relation between w_o/C and max. RH in
cement products. Degree of hydration = 1.

w_o / C kg/kg	Max RH when no alkali metals are assumed to be bound in hydr. prod. %	Max RH when about 10 to 30 % alkali metals are assumed to be bound in hydr. prod. %
1.0	98.6	98.8
0.8	98.1	98.4
0.7	97.7	98.0
0.6	97.1	97.6
0.5	96.1	97.0
0.4	93.9	95.9

As seen in TABLE 11.1 and TABLE 11.2 there is a difference in
the maximum RH between the two tables even when no alkali
metals are assumed to be bound in the hydration products. The
purely theoretical Raoult's law, Eq. (11.1), is probably not so
precise in this case as the formula given by Robinson and
Stokes (1955).

A concrete specimen with w_o/C 0.6 was allowed to suck water
until it was completely saturated. RH was then measured in the
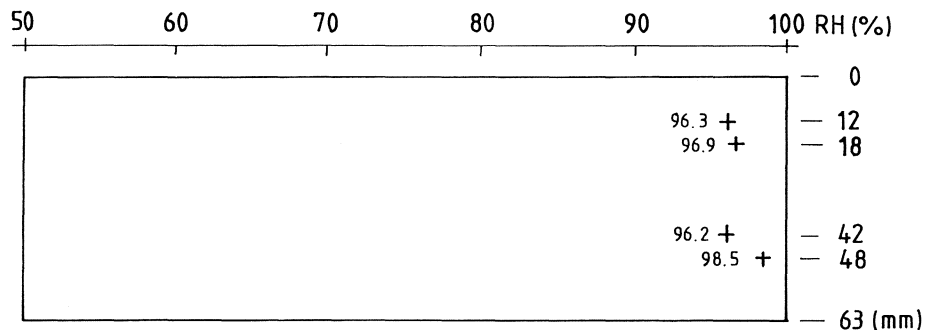specimen at different heights, see FIG 11.3.

FIG 11.3 Measured RH in a water saturated specimen. w_o/C 0.6.

107

The mean value of the three uppermost RH measurements is 96.5 %. This value is somewhat lower than the values in TABLE 11.2 for w_o/C 0.6. The measured value (98.5) at the bottom side of the specimen is higher than the other measured values. This can be a correct measurement of the RH. The bottomside of the specimen has stood in water for about 4 years and Na^+ and K^+ in the bottom part of the specimen could be emitted to the water.

Two specimens made of cement mortar with w_o/C 0.6 were analysed by Euroc Research (Cemlab) in Slite with Atom Absorption Specrometer (AAS) to get the content of K_2O and Na_2O. The results are given as percent of the weight including cement, aggregate and water. The results are shown in FIG 11.4 and FIG 11.5.
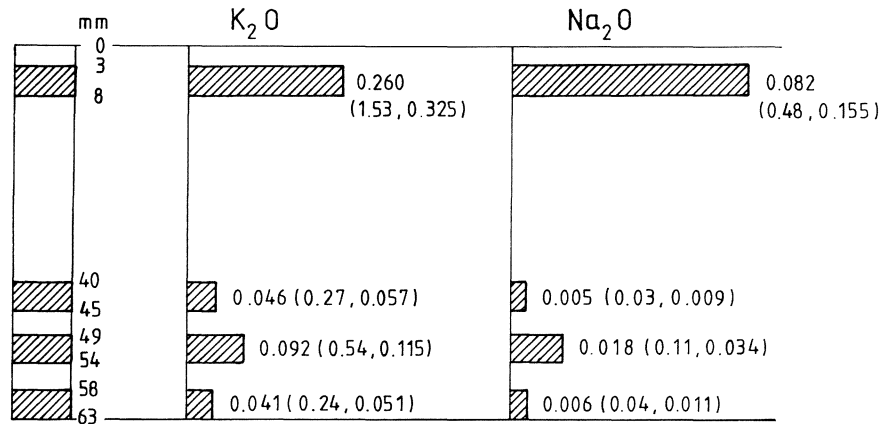

FIG 11.4 Content of K_2O and Na_2O for a specimen with w_o/C 0.6. The bottomside has been in water for about 4 years.
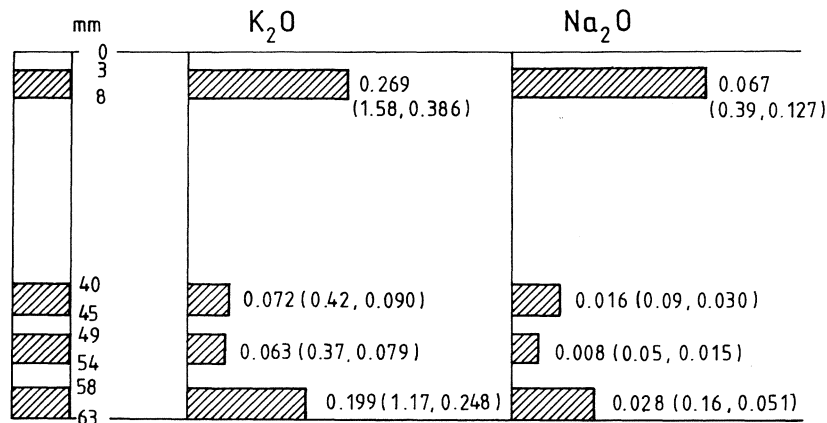
```
      mm           K₂O                    Na₂O
       0
       3
       8       ▨▨▨▨▨ 0.269          ▨▨▨▨▨ 0.067
                     (1.58,0.386)           (0.39,0.127)




      40
      45       ▨▨ 0.072(0.42,0.090)   ▨▨ 0.016 (0.09,0.030)
      49
      54       ▨▨ 0.063(0.37,0.079)   ▨ 0.008 (0.05,0.015)
      58
      63       ▨▨▨ 0.199(1.17,0.248)  ▨▨▨ 0.028 (0.16,0.051)
```

FIG 11.5 Content of K_2O and Na_2O for a specimen with w_o/C
           0.6. The bottom side has been in moist air for about
           4 years.

The first value in the parentheses in FIG 11.4 and FIG 11.5 is
percent of the weight of K_2O or Na_2O per kg cement. The second
value is the content of K^+ or Na^+ in mole per kg cement. In FIG
11.4 and FIG 11.5 it is shown that the contents of K_2O and Na_2O
are much higher at the top of the specimens. The density of the
cement mortar is about 2200 kg/m^3 and the cement content is 375
kg/m^3.

If the cement is supposed to contain 0.28 mole K^+ and 0.06 mole
Na^+ per kg cement, then the contents of K^+ and Na^+ at the top
of the specimens are higher. For the specimen M6A1, FIG 11.4,
the value at the bottom is much lower; this is probably because
K^+ and Na^+ have "leaked" to the water in the bottom vessel.
With a content of about 0.05 mole K^+ and 0.01 mole Na^+ maximum
RH in a water saturated specimen (M6A1) should be about 99.5 %.
The relative humidity at the exact bottom of the specimen is
probably 100, % as most of the alkalies here are released to
the water in the bottom vessel. FIG 11.5 shows that the
alkalies have moved towards the two surfaces.

11.1.2 <u>Effect of carbonation at the bottom surface</u>

Some carbonation at the bottom surface could have occurred
during the preparation of the specimens. Kropp (1983) has
measured the moisture permeability for cement mortar with
w_o/C 0.5. One part of the test was not carbonated while the
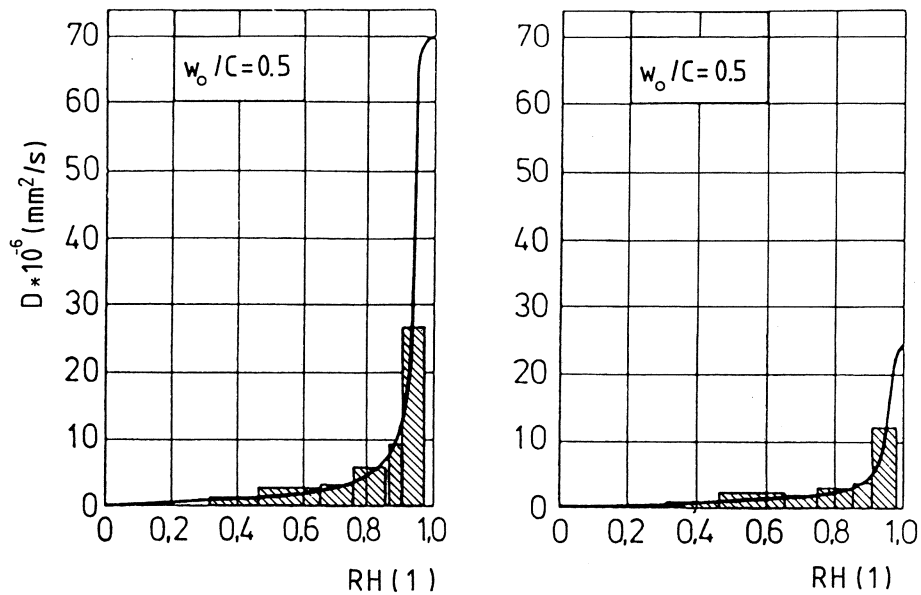other part was. Kropp's results are shown in FIG 11.6 and FIG
11.7.

FIG 11.6 Moisture permeability   FIG 11.7 Moisture permeability
for non-carbonated   for carbonated
cement mortar.   cement mortar.
Kropp (1983).   Kropp (1983).

In FIG 11.6 and FIG 11.7 it is clearly shown that the carbona-
tion of cement mortar influences the moisture permeability. At

110

high RH a reduction to about 1/3 of the value for non-carbonated cement mortar is achieved.

In TABLE 11.3 the calculated reduction of RH, just above the carbonation zone at the bottom of a specimen, is shown. The specimen is made of concrete with w_o/C 0.6. In the calculations it is supposed that the the ratio between cabonated and non-carbonated concrete is the same as for the cement mortar in FIG 11.6 and FIG 11.7.

TABLE 11.3 Calculated reduction of RH just above the carbonation zone. Concrete with w_o/C 0.6. The bottom side is in water. Height 0.100 m.

Carbonation thickness mm.	Reduction of RH %
0.5	0.02
1.0	0.03
2.5	0.07

TABLE 11.3 shows that carbonation to some mm:s depth at the bottom surface has very little influence on RH just above the carbonated zone.

11.2 Effect of the bottom side in moist air instead of water

Half of the number of the specimens stand with their bottom-sides in moist air. This is brought about by a water surface 2 to 3 cm below the bottom surface of the specimens. A PVC-lid is placed about 3 cm from the water surface to get high RH at the top of the bottom vessel. FIG 11.8 shows the arrangement.
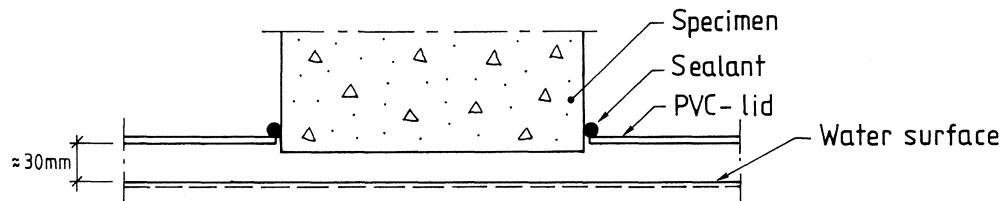
Figure labels: Specimen, Sealant, PVC-lid, Water surface, ≈30mm

FIG 11.8 The arrangement at the bottom of specimens
with their bottomsides in moist air.

11.2.1 Calculated RH just below the specimens

The moisture resistance for the PVC-lid to the bottom vessel
has been measured with the cup method. Two cups were used. The
cups were made of aluminium. The cup method is described in
Chapter 4.1.1. The moisture resistances of the PVC-lids were
$195 * 10^3$ and $540 * 10^3$ s/m. This big difference in moisture
resistance could of course be explained by there probably
having been a leakage in the cup with the lowest moisture
resistance. If the lowest value is used to calculate RH just
below the PVC-lid in FIG 11.8, we get 99.4 %. With the highest
value we get 99.8 % RH. In the calculations it is assumed that
there is no leakage between the specimens and the PVC-lid.

The moisture resistance of the specimens with the height
0.100 m is about $150 * 10^3$ s/m. This value gives a RH just
below the bottom surface of the specimens of about 99 %.

If there is no leakage between the building sealant and the specimen or the PVC-lid, this joint is as tight as the PVC-lid. The calculated differences, in section 7.1.3, between concrete specimens with the bottom surface in water and in moist air are about 1 to 3 % RH. This difference is in the same magnitude as the difference calculated in this section, 100-99=1 % RH. The concretes in section 7.1.3 are supposed to contain alkalies even at the bottom surface and these alkalies lower the maximal RH to a value below 100 %. In FIG 11.5, for the specimen with the bottom in moist air, it is shown that the alkalies have moved towards the two surfaces of the specimen, but it is not clear if they had moved out to the surfaces. At the bottom surface of the specimens water vapour may condense due to the temperature-changes in the climate room. If the water vapour condense and form drops, which can fall down, then alkalies just at the bottom surface can be washed away. The relative humidity at the bottom surface is then about 99 %.

12   PORE STRUCTURE OF HARDENED CEMENT PASTE, CEMENT MORTAR AND CONCRETE

12.1   Portland cement paste

This description is mainly based on Power's work as it was developed during the years 1947 to 1962.

When the cement grains react with water, a cement gel is formed around each cement grain. The cement gel is composed of a system of very thin needle-like, sheet-like and crumbled crystals formed by the reaction between the cement and the mixing water. In addition a considerable number of coarser hexagonal crystals of calcium hydroxide are formed and are intermingled with the cement gel particles. The pore space located between the individual cement gel particles is called the gel porosity. The diameter of the gel pores is about some nm if they are considered as cylindrical, see Fagerlund (1982). The gel pores are filled with water during normal conditions, called gel water, that is physically adsorbed on the surfaces of the gel particles.

For w_o/C ratios larger than about 0.4 the cement gel volume is not large enough to fill all the space between the cement grains. Therefore larger, so - called capillary pores are formed in such cement pastes. The total volume of the capillary pores is called the capillary porosity. The diameters of the capillary pores are in the range 5 to 1000 nm.

In FIG 12.1 the principal structure of the hydrated cement paste is shown.
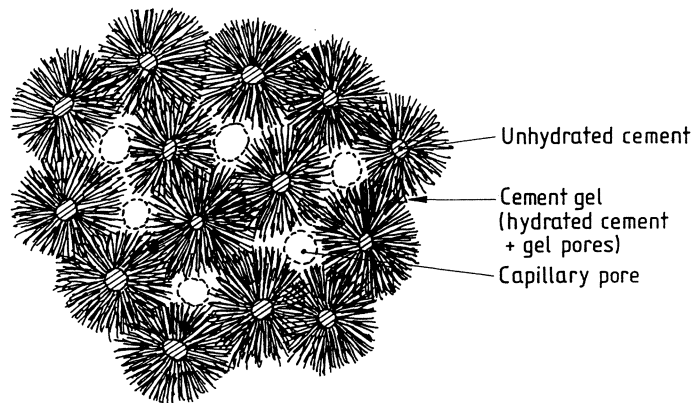
FIG 12.1 The principal structure of hydrated cement paste.
           Hillerborg (1986).

FIG 12.2 shows a scanning electron microscope (SEM) picture of
a well-cured Portland cement paste. w_o/C is 0.8. The individual
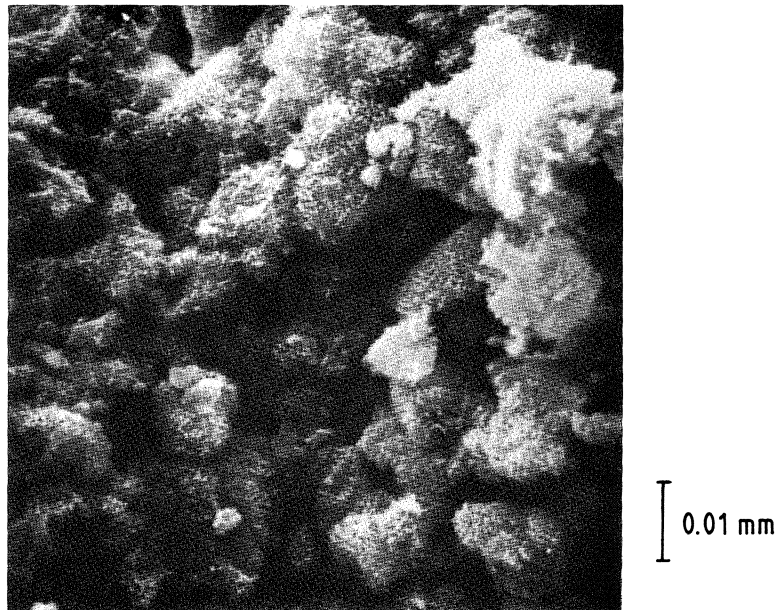gel balls are clearly shown.

FIG 12.2 Photo of a well-cured cement paste. w_o/C 0.8.
           Fagerlund (1982).
           Photo: Inst. of Zoology, Lund University.

12.2 The interface between aggregate and Portland cement paste

The aggregate – matrix interface is normally a weak zone in
concrete. According to Zimbelmann (1985) the interface is
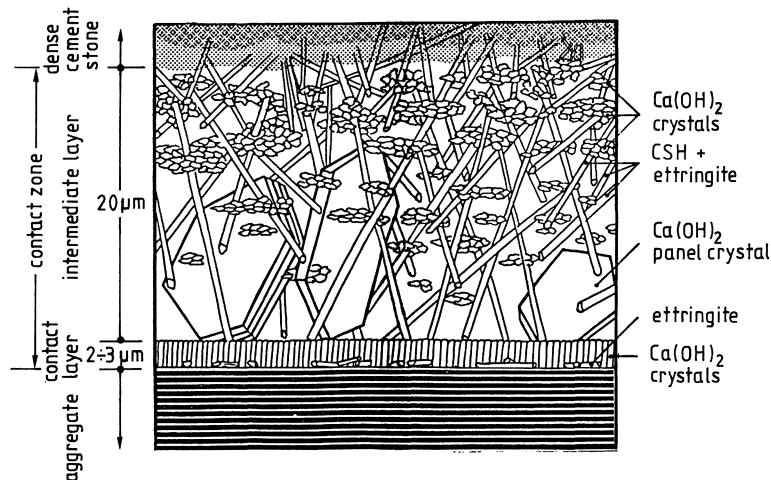composed of different layers as shown in FIG 12.3.

dense cement stone

contact zone

intermediate layer

20μm

contact layer

2÷3 μm

aggregate

$Ca(OH)_2$ crystals

CSH + ettringite

$Ca(OH)_2$ panel crystal

ettringite

$Ca(OH)_2$ crystals

FIG 12.3 The contact zone between aggregate and cement paste.
Zimbelmann (1985).

Around the aggregate there is normally a zone with higher w_o/C
ratio than in the bulk cement paste. Ettringite needles appear
in the interface zone a few minutes after the cement is mixed
with water. Thereafter a contact layer composed of calcium
hydroxide crystals is precipitated on the aggregate surface.
After about 16 hours the growth of this layer is terminated. In
the highly porous intermediate layer located between the
contact zone and the bulk cement paste (see FIG 12.3)
panel-shaped hexagonal calcium hydroxide crystals begin to
grow. They can have an edge length from 10 to 30 μm. Needle-
and rod-shaped hydrates from the reaction between the cement
and the water grow into the intermediate layer. The more the
hydration progresses, the denser the intermediate layer will
be. With increasing w_o/C ratio an increase in the thickness of
the intermediate layer occurs.

According to Monteiro et al (1985) the thickness of the contact zone is larger for larger aggregates. This might depend on the fact that the risk of water separation creating water pockets around the aggregate increases with increasing aggregate size.

In the contact zone around the aggregates there are also microcracks present. According to Metha (1986) such microcracks increase the permeability of concrete.

Scrivener (1989) shows how the porosity in the interfacial region between aggregate and bulk cement varies with the distance from the aggregate. Scrivener shows the results for a 10-week-old specimen with w_o/C 0.5 and the results for a 28-day-old specimen with w_o/C 0.4; see FIG 12.4 and FIG 12.5.
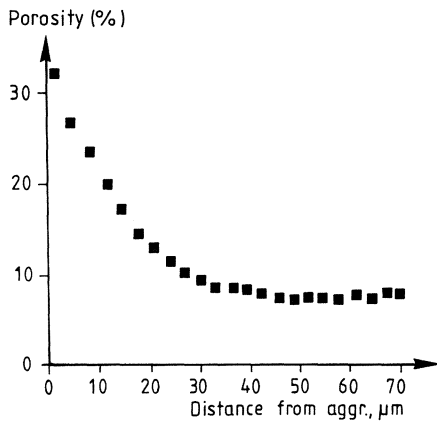
Porosity (%)

Porosity (%)

Distance from aggr., μm

Distance from aggr., μm

FIG 12.4 Porosity for a 10-
    week-old specimen.
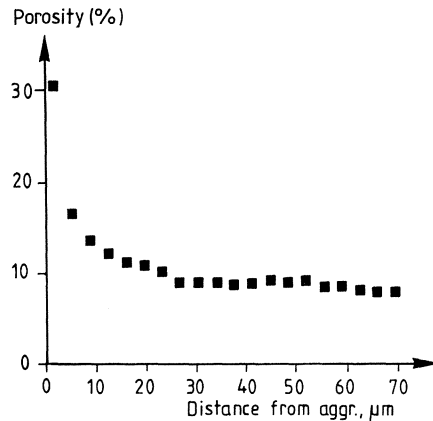 w_o/C 0.5.
    Scrivener (1989).

FIG 12.5 Porosity for a 28-
    day-old specimen.
    w_o/C 0.4.
    Scrivener (1989).

In FIG 12.4 and FIG 12.5 it is seen that the porosity in the interfacial zone is bigger for w_o/C 0.5 than for w_o/C 0.4. Consequently the moisture transport around the aggregate is easier for w_o/C 0.5 than for 0.4.

117

13 SOME THEORETICAL MODELS FOR MOISTURE TRANSPORT

13.1 Basic flow types

The moisture flow through porous material is a complicated process. It has been described by many scientists, eg. Flood et al (1952), Radjy (1974) and Quenard (1989). A physical model is shown in FIG 13.1; the figure is taken from Kohonen (1984).
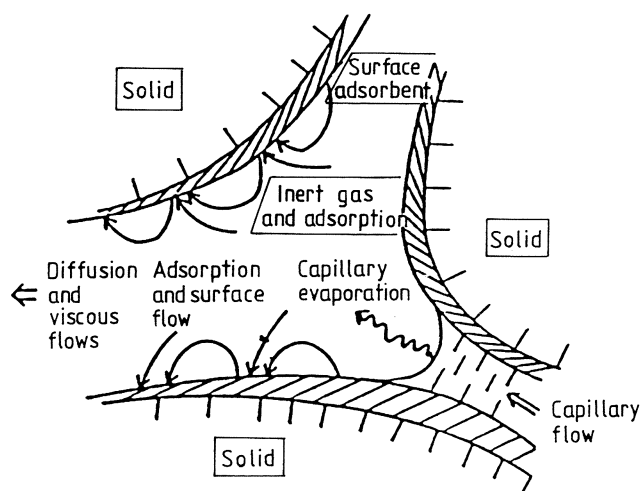

FIG 13.1   A model for moisture transport in
            porous material.
            Kohonen (1984).

There are three different kinds of flows in FIG 13.1, namely diffusion, capillary flow and surface flow, which interact to the total moisture flow in a complicated manner. The description of the pore structure in which flow takes place is often not realistic. Normally it is described as cylindrical pores, and this is a too simplified model.

13.1.1 Diffusion

The moisture flow in air at steady state conditions is governed by Fick's first law.

$$g = -D\ \delta v/\delta x \hspace{4cm} (\ 13.1\ )$$

D = Diffusion coefficient in air (m^2/s)

D is not a constant but depends on the total pressure and the temperature. Andersson (1985) has put together four different expressions of the temperature dependence of D. In the normal temperature range, there is only a slight difference between these expressions. One equation is by Vos et al (1966),
Eq. (13.2).

$$D = (22.2+0.14(T-273.15))\ *\ 10^{-6}\ (m^2/s) \hspace{1.5cm} (\ 13.2\ )$$

T = Absolute temperature   (K)

If the temperature is raised from 0°C to 30°C, D increases 19 %.

Eq.(13.1) is not valid in narrow pores of a given material as there are collisions with the pore walls, and there are not so many collisions between molecules. For a long cylindrical tube this case is given a mathematical solution by Knudsen, the flow is known as Knudsen flow; see Grove (1967). Eq. (13.3) is the Knudsen formula.

$$G=-(4/3)r^3(2\pi RT/M)^{0.5}((2-f)/f)\ *\ \delta v/\delta x \hspace{1.5cm} (\ 13.3\ )$$

G = the flow rate   (kg/s)
r = the radius of the tube   (m)
R = the general gas constant   (8314 J/(kmole s))
M = the molar weight   (kg/kmole)
f = the fraction of molecules, which have diffuse reflections
    at the walls. Normally f is taken to be 1.

Eq.(13.3) is valid when the mean free path of the molecules in the air is much bigger than the diameter of the tube. For molecules in air the mean free path is given by Eq. (13.4); see Grove (1967).

$$\lambda = 2\eta/(\rho\nu) \qquad\qquad (13.4)$$

λ = the mean free path (m)
η = the viscosity (Ns/m^2)
ρ = the density of air (kg/m^3)
ν = the mean velocity $(8RT/(\pi M))^{0.5}$ (m/s)

The mean free path for molecules in air is in the order 10 to 100 nm at room temperature and pressure. The flow in pores less than 10 nm diameter is often considered as Knudsen flow, see Dullien (1979), so water vapour flow in gel pores and the finest capillary pores of cement paste is of the Knudsen type.

Eq.(13.3) is also restricted to a long straight tube. When the tube becomes shorter, Eq. (13.3) must be multiplied with a factor given in TABLE 13.1; see Carman (1956).

TABLE   13.1   Reduction factor for Eq. (13.3)
for short tubes.

L/r	factor
∞	1
10	0.74
8	0.69
6	0.63
4	0.54
2	0.38

13.1.2   Capillary flow or liquid flow

Liquid flow of water in unsaturated material is normally treated as viscous flow. For a single capillary, the flow is given by the Poiseuille equation, Eq. (13.5).

$$G = -(\rho_w \pi r^4/(8\eta)) \ * \ \delta p/\delta x \qquad\qquad (\ 13.5 \ )$$

p = the pressure in the liquid

The equality of the chemical potentials of the liquid
and its vapour at equilibrium, eq.(2.6), gives the relation
between the partial vapour pressure and the pressure in the
liquid. Eq.(2.7, 2.8, 2.10 and 13.5) gives

$$G = -(\rho_w^2 \pi r^4 RT/(8\eta M\phi v_s)) \ * \ \delta v/\delta x \qquad\qquad (\ 13.6 \ )$$

ϕ = the relative humidity (1)
v_s = the vapour pressure at saturation (Pa)

13.1.3 Surface flow

Dacey (1965) says "in the intermediate region between capillary
condensation and partial monolayer coverage the hydrodynamic
treatment of surface transport has yielded the most satisfacto-
tory agreement between theory and experiment". Gilliland et al
(1958) has given a theoretical formula for the surface flow.
When the remaining conditions are constant the formula of
Gilliland et al can be written

$$G_s =- k(X^2/p_v) \ * \ \delta p_v/\delta x \qquad\qquad (\ 13.7 \ )$$

G_s = the adsorbed layer flow rate
k = a constant
X = the surface concentration (the sorption isotherm in
     principle)
p_v = the gas-phase pressure

Gilliland et al have the difference in surface tension between
the covered surface and the bare surface as driving force when
the formula was derived. The formula also takes in account the
sorption isotherm, as X is determined from this. X is raised to
the second power.

Flood et al (1952) proposed an equation that describes the total flow through micropores. The equation for the case when the fluid is considerably below its crititical temperature has a simple appearance. The flow rate in a single circular capillary is

$$G = -(\pi r^4/(8\eta_1)) * (\rho_a/v) * \delta p_v/\delta x \qquad\qquad (13.8)$$

ρ_a = the actual mean density of the adsorbate
v = the equilibrium vapour density of the adsorbable gas
η_1 = the dynamic viscosity of the liquid

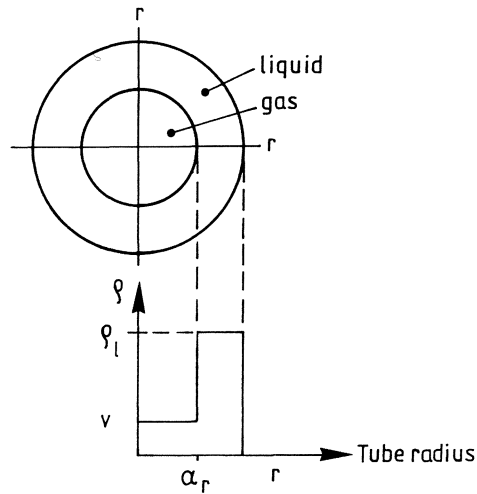The actual mean density can be calculated according to Eq. (13.9) and FIG 13.2.

FIG 13.2 The densities of a adsorbate in a capillary tube when some condensation has occured on the tube wall.

$$\rho_a = v\alpha^2 + \rho_1(1-\alpha^2) \approx \rho_1(1-\alpha^2) \qquad\qquad (13.9)$$

All the variables are defined in FIG 13.2. One condition for
Eq.(13.9) is that ρ_a is going to ρ_1. The density of moisture
flow rate (g) is $g = G/(\pi r^2)$, which together with Eq. (13.9)
gives

$$g \approx -(r^2/(8\eta_1))*((\rho_1(1-\alpha^2))^2/v) * \delta p_v/\delta x \qquad (13.10)$$

The moisture content mass by volume (w_e) for a material with a
given pore radius is

$$w_e = \rho_1(\pi r^2-\pi\alpha^2 r^2)/(\pi r^2) = \rho_1(1-\alpha^2) \qquad (13.11)$$

For a material with pores of equal radius, Eq. (13.10) and
Eq. (13.11) give

$$g \approx -(r^2/(8\eta_1))*(w_e^2/v) * \delta p_v/\delta x \qquad (13.12)$$

It can also be shown that Eq. (13.8) becomes the Poiseuille
equation for viscous liquid flow in a capillary, see 13.1.2,
when the pore is filled with liquid.

13.2 A relation between the moisture transport (permeability) and the sorption isotherm

Eq.(13.7) and in principle even Eq. (13.12) give the relation
between the surface flow and the surface concentration. The
surface flow is dependent on the (surface conc.)^2/gas-phase
pressure , Eq. (13.7), or the (moisture content mass by
volume)^2/vapour density, Eq. (13.12).

Gilliland et al (1958) have shown, for isobutane at 0°C, that
the plot of the surface flow vs the (surface conc.)^2/gas
pressure gives a straight line; see FIG 13.3, FIG 13.4 and FIG
13.5.

$\sqrt{MT}P_T (10^6)$, $\dfrac{MGM.MOLES}{SEC. MM.Hg CM}$ $\sqrt{\dfrac{GM-{}^\circ K}{GM.MOLE}}$

i-C_4H_{10} FLOW THROUGH VYCOR

1200 MM.Hg

PREDICTED $\sqrt{MT}$ P

p, MM.Hg

X, MGM.MOLES/GM

$T_P = 0\,{}^\circ C.$

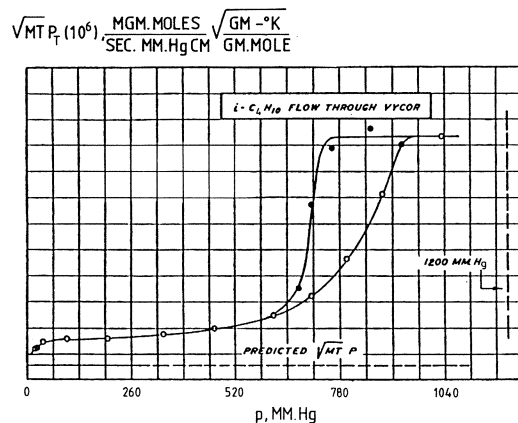| ADS.	DES.
O	●
△	▲

i - C_2H_{10} ISOTHERM ON VYCOR

p, MM Hg

FIG 13.3 Isobutane flow through Vycor glass. Gilliland et al (1958).
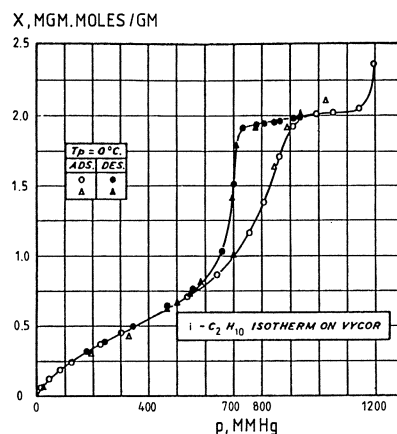
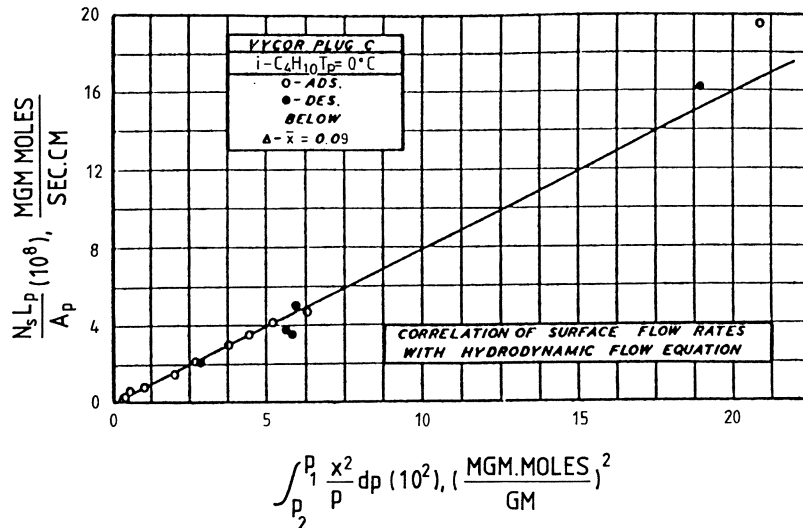FIG 13.4 Sorption isotherme for isobutene on Vycor glass. Gilliland et al (1958).

$\dfrac{N_s L_p}{A_p} (10^8)$, $\dfrac{MGM MOLES}{SEC.CM}$

VYCOR PLUG C
i-C_4H_{10} T_p= 0°C
O - ADS.
● - DES.
BELOW
△ - $\bar{x}$ = 0.09

CORRELATION OF SURFACE FLOW RATES WITH HYDRODYNAMIC FLOW EQUATION

$\displaystyle\int_{p_2}^{p_1} \dfrac{x^2}{p}\,dp\,(10^2)$, $\left(\dfrac{MGM.MOLES}{GM}\right)^2$

FIG 13.5 Correlation of surface flow and (surface conc.)^2/gas-phase pressure. Gilliland et al (1958).

124

The surface flow in FIG 13.5 is evaluated, in FIG 13.3, as the total flow minus the gas-phase flow (marked with line of short dashes). Both adsorption and desorption are considered in FIG 13.5.

Gilliland's treatment might perhaps also be applied to water flow in building materials. Some examples are investigated, namely wood, cellular concrete and cement paste.

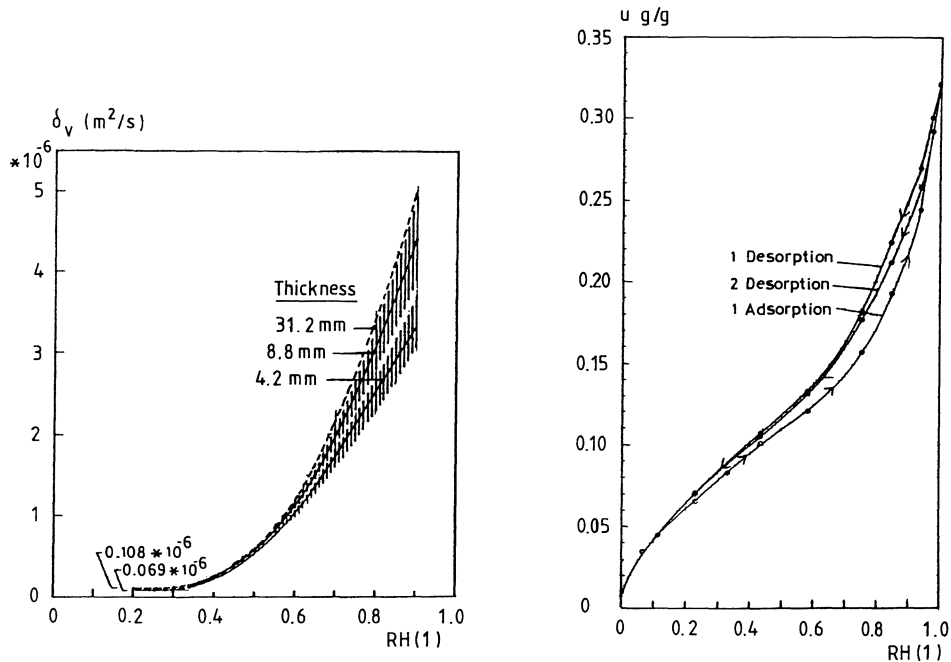Bertelsen (1983) has measured the moisture permeability and the sorption isotherm for spruce; see FIG 13.6 and FIG 13.7.

FIG 13.6 Moisture permeability for spruce as a function of RH. Bertelsen (1983).

FIG 13.7 Sorption isotherms for water in spruce. Bertelsen (1983).

The moisture permeability in FIG 13.6 seems to depend somewhat on the thickness of the samples (4.2, 8.8 and 31.2 mm). Whether this is correct or whether it is an error in the measurements, is not known; see also section 10.4.

In FIG 13.8 the moisture permeability for the sample with a
thickness of 8.8 mm is used. The moisture permeability at 20 %
RH is taken as the gas-phase flow, as below this value the
moisture permeability is nearly constant. The difference in the
measured moisture permeability and the moisture permeability at
20 % RH is taken as dependent on the surface flow. The moisture
content (u) up to 20 % RH is supposed not to influence the
surface flow. The moisture content at 20 % RH is therefore
taken as a zero-level for the surface concentration. The
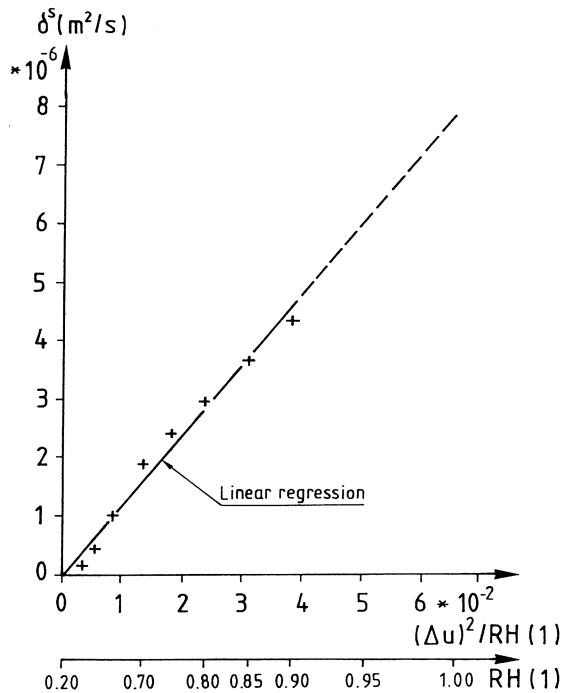desorption isotherm for the first desorption is used.

$\delta^s (m^2/s)$

FIG 13.8 The surface moisture permeability
          dependent on surface flow as function
          of $(\Delta u)^2/RH$. Spruce.

The correlation coefficient in FIG 13.8 for the linear
regression line is 0.994. If the line is extrapolated to 100 %
RH, the dotted line, δ^s will be $7.87*10^{-6}$ m^2/s. The total

moisture permeability is then $(7.87+0.108)*10^{-6} \approx 8.0*10^{-6}$ m^2/s at 100 % RH. At 100 % RH most of the pores are filled with liquid water, and it is of course a simplification to add the gas-phase permeability to the surface permeability to get the total permeability. Spruce is a most complicated material, but the model seems to be applicable.

Hedenblad et al (1991) have measured the moisture permeability for cellular concrete (quality 500) under absorption at +20 °C; see FIG 13.9. The absorption isotherm is taken from Nevander et al (1981), FIG 13.10.
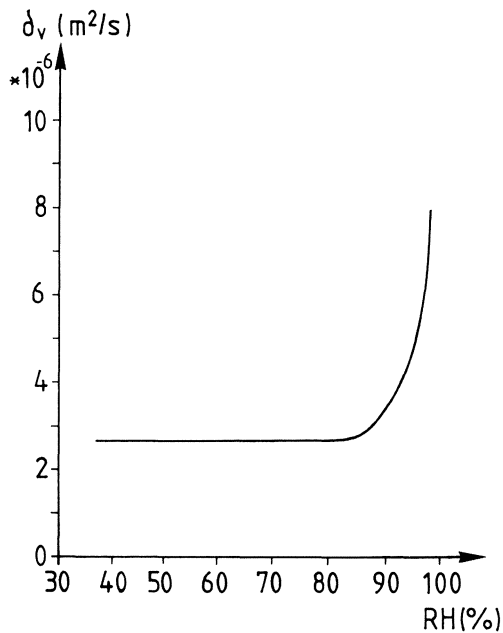
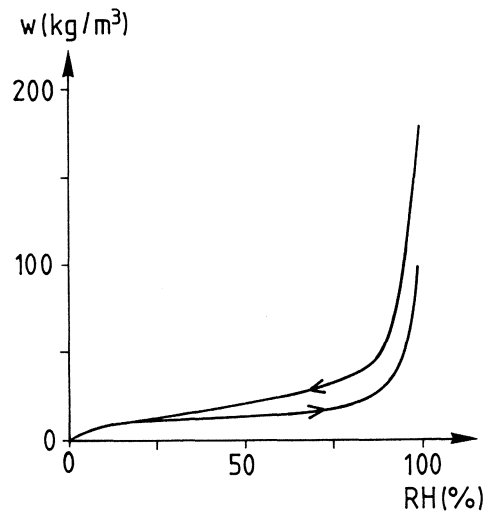FIG 13.9 Moisture permeability for cellular concrete as a function of RH. Hedenblad et al (1991).

FIG 13.10 Sorption isotherms for water in cellular concrete. Nevander et al (1981).

The moisture permeability in FIG 13.9 up to 80 % RH is taken as only dependent on the gas-phase flow as the moisture permeability is constant up to this RH. The moisture content mass by volume (w) at 80 % RH, in FIG 13.10, is taken as the zero-level for the surface concentration. The absorption isotherm is used.
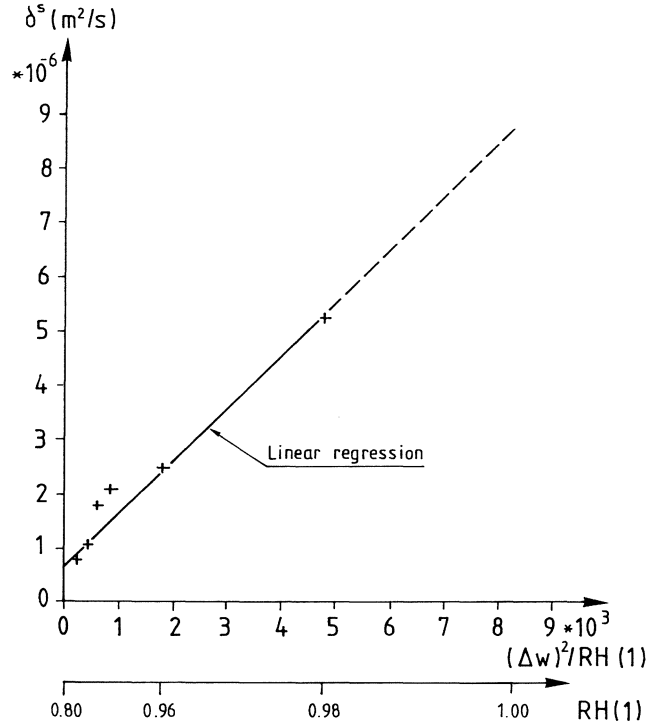

FIG 13.11 The surface moisture permeability dependent on surface flow as function of $(\Delta w)^2/RH$. Cellular concrete.

The correlation coefficient for the linear regression in FIG 13.12 is 0.971. If the line is extrapolated to 100 % RH, δ^s will be $8.75*10^{-6}$ m^2/s. The total moisture permeability, at 100 % RH, is then about $11.4*10^{-6}$ m^2/s. As the measurements of the moisture permeability and the absorption isotherm are not made on the same specimens and not at the same time, the correlation coefficient is not that bad.

128

Sörensen (1980) has measured the moisture permeability and the sorption isotherm for cement paste with w_o/C 0.4; see FIG 13.12 and FIG 13.13.

$\delta_p (g*m^{-1}*hr^{-1}*torr^{-1})$

u (kg/kg)

$*10^{-3}$

0.4 (S) DES
0.4 (S) ADS
0.4 (RT) DES
0.4 (RT) ADS

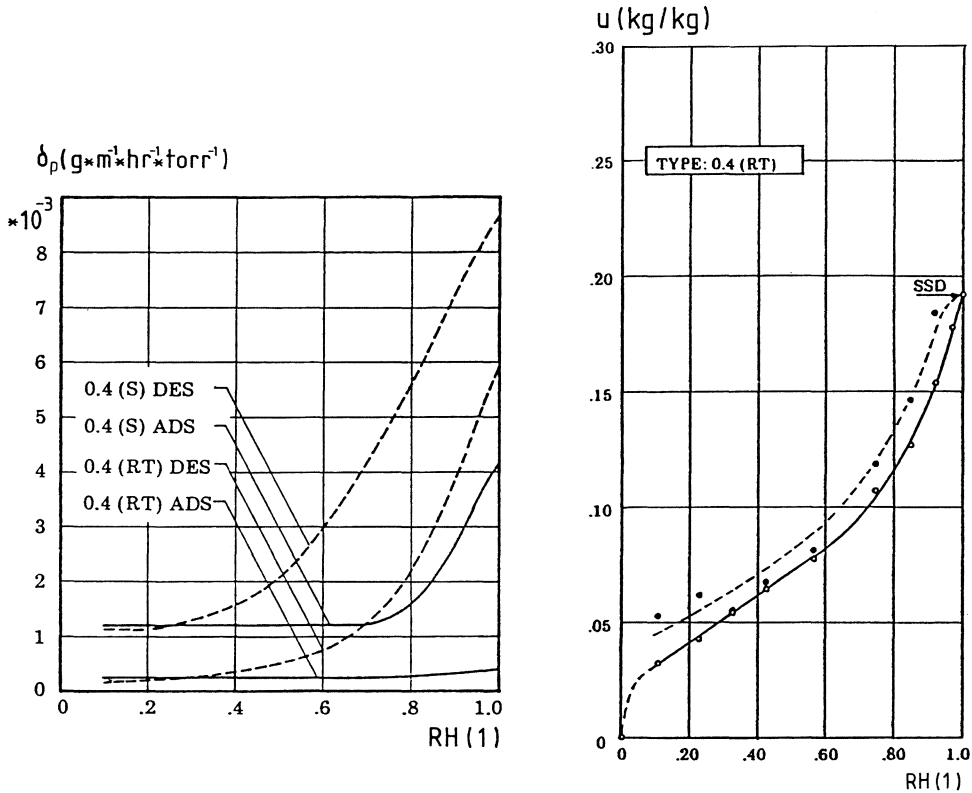TYPE: 0.4 (RT)

SSD

RH (1)

RH (1)

FIG 13.12 Moisture permeability
for cement paste with
w_o/C 0.4 as a function
of RH.
Sörensen (1980).

FIG 13.13 Sorption isotherms
for water in cement
paste with w_o/C 0.4.
Sörensen (1980).

The moisture permeability in FIG 13.12 up to 20 % RH for cement paste under desorption (DES) and at room temperature (RT) is supposed to be only dependent on the gas-phase flow as the moisture permeability is constant below this RH. The moisture content at 20 % RH, in FIG 13.13, is taken as zero-level for the surface concentration.
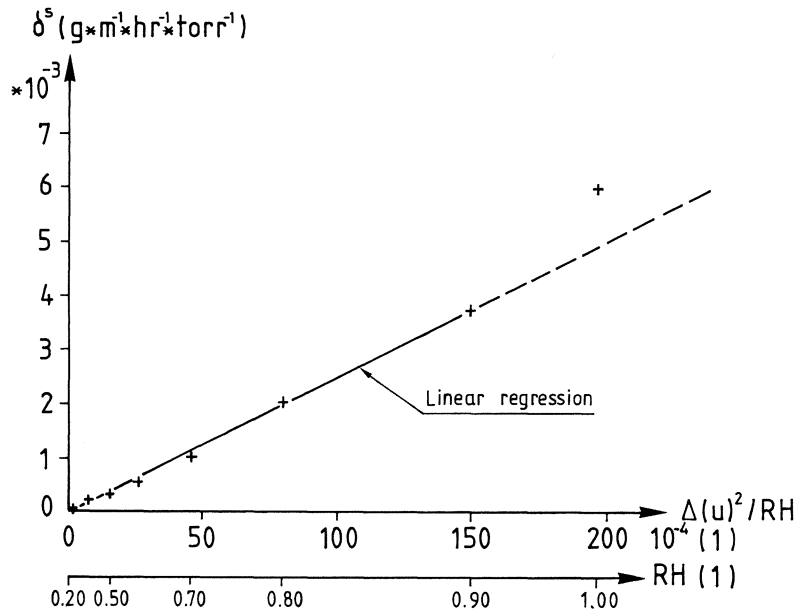
FIG 13.14 The surface moisture permeability
dependent on surface flow as function
of $(\Delta u)^2$/RH. Cement paste w_o/C 0.4

The correlation coefficient of the linear regression in FIG
13.14 is 0.999 if the last point is excluded. This point is
excluded because the desorption isotherm may be somewhat low at
100 % RH, see FIG 13.13.

When the linear regression line is extrapolated up to
$\delta^s = 5.9*10^{-3}$, the u value will be 0.208 instead of 0.192.

The surface flow is of course not only a surface flow in
material with different pore sizes. When the larger pores have
a water surface of a few molecules' thickness, the smaller
pores will be filled with liquid. The larger pores will have
surface flow but in the filled pores the flow is of Poiseuille
type. As a conclusion one can say that the moisture transport

at high relative humidities is well described by the relation
between surface flow and the amount of adsorbed water given by
Gilliland et al (1958).

14 SOME COMPARISONS BETWEEN CALCULATIONS AND DRYING EXPERIMENTS AND FIELD MEASUREMENTS

To see if the reported moisture permeabilities which are measured under stationary conditions in the laboratory can be used in the drying of concrete and cement mortar, some comparisons with drying experiments are made. A comparison is also made with the measured RH-distribution and the measured moisture flow in a concrete slab on the ground.

14.1 The desorption isotherms used

Nilsson (1980) has published desorption isotherms for mature cement paste with different w_0/C. The isotherms go up to 100 % RH. Some revisions of the isotherms have been made by Hedenblad (1988), so that the alkalies in the cement determine the maximum RH (lower than 100 %). FIG 14.1 shows the desorption isotherms from Hedenblad (1988).
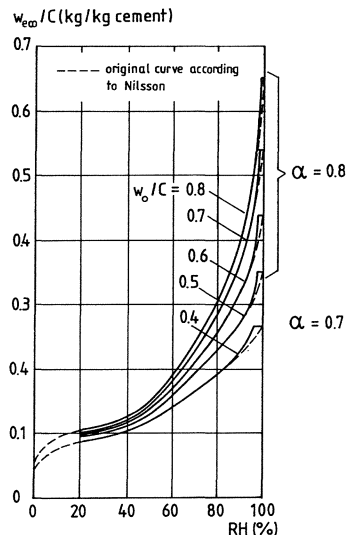

FIG 14.1 Desorption isotherms for mature cement paste with different w_0/C and degrees of hydration. Based on isotherms according to Nilsson (1980).

132

The desorption isotherms in FIG 14.1 must be multiplied by the content of cement in the concrete or the cement mortar to get the isotherm for the material. For the drying experiments in section 14.4 the water-cement ratio is 0.56. For this case a desorption isotherm with w_o/C 0.56 has been constructed with linear interpolation between w_o/C 0.5 and 0.6 in FIG 14.1.

14.2 The moisture permeabilities used

For the drying experiments in section 14.3, with w_o/C 0.6 and 0.7 the average moisture permeabilities for w_o/C 0.6 to 0.8 in TABLE 7.1 have been used between 33 % and 95 % RH. Over 95 % RH the estimated moisture permeabilities in TABLE 7.2 have been used. The mosture permeabilities are for a specimen that is about 0.1 m and drying from one side.

For the drying experiments in section 14.4 the measured δ_V for cement mortar in FIG 8.1 has been used to construct the moisture permeabilities for w_o/C 0.56. The moisture permeabilities between 94 and 96 % RH have been estimated. The δ_V-curve is shown in FIG 14.2.
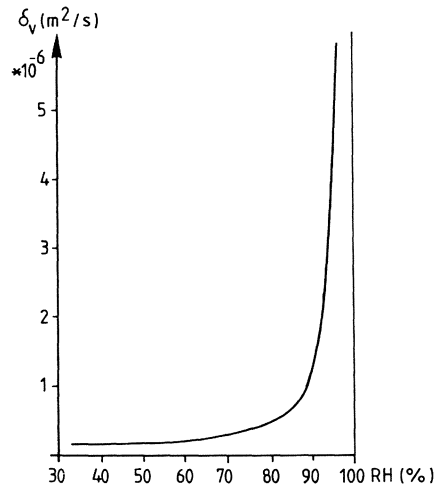

FIG 14.2 The moisture permeability curve for cement mortar with w_o/C 0.56.

For the field measurements in section 14.5, with a concrete slab on the ground, the w_o/C has been estimated at 0.7. The average δ_v-s in TABLE 7.1 have been used between 33 % and 95 % RH. Over 95 % RH the estimated δ_v-s in TABLE 7.2 for w_o/C 0.7 have been used.

14.3 Drying experiments on concrete with w_o/C 0.6 and 0.7

Two specimens, with w_o/C 0.6 and 0.7, from the main investigation were allowed to dry to about 60 % RH. Then they sucked water until they were saturated. The capillary water uptake test is described in Chapter 15. The composition of the tested materials is shown in section 3.2.1.

After the capillary saturation of the two specimens, they were allowed to dry in a climate room with about 60 % RH and 18.5 °C.

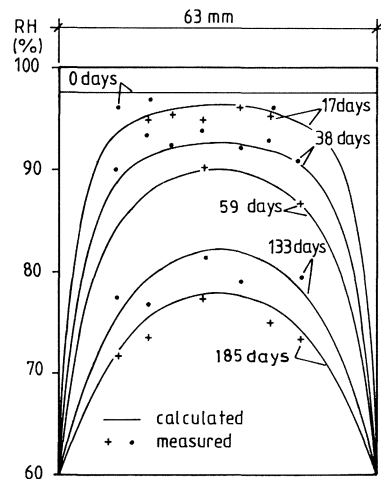The calculated distributions of RH and the measured RH are shown in FIG 14.3 and FIG 14.4.

FIG 14.3   Calculated distribution of RH and measured RH during the drying of a 63 mm thick concrete specimen. w_o/C 0.6.

The relative humidity in the specimen has been measured before
the start of the drying and after 17, 38, 59, 133 and 185 days
of drying. The calculated RH-distributions are shown for the
corresponding times.

In FIG 14.3 it is shown that the RH measured before the start
of the drying was lower than 100 % although the specimen was
capillary-saturated with water.

Separate test results at the different times can deviate from
the calculated RH-distributions by some percent RH. At 133 days
of drying, two test results are about 3 % RH lower than the
calculated RH-distribution. This may depend on a leakage
between the RH-sensor and the specimen. The general impression
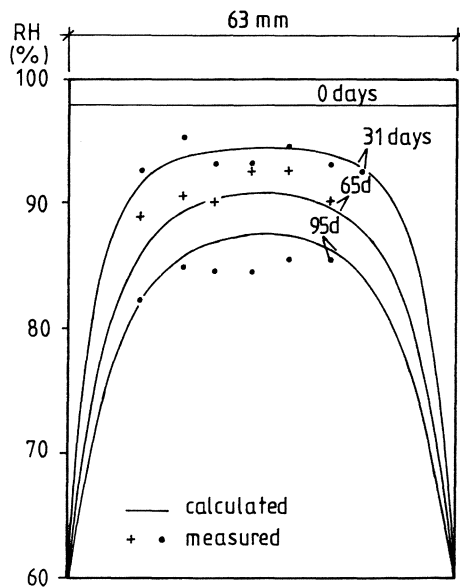is that the calculated and measured RH agree fairly well.

FIG 14.4 Calculated distribution of RH and measured RH during
the drying of a 63 mm thick concrete specimen. w_o/C
0.7.

In FIG 14.4 the calculated RH-distribution is shown after 31, 65 and 95 days of drying. RH in the specimen has been measured at the corresponding times.

At 31 days of drying the maximum difference between calculated RH and measured RH is about 1 % RH.

At 65 days of drying, 5 of 6 test results are higher than the calculated RH-distribution. The maximum difference between measured and calculated RH is about 2.5 % RH.

At 95 days of drying, 5 of 6 test results are lower than the calculated RH-distribution. If the other RH measurement test results are correct, it seems there has been a leakage between the RH-sensor and the specimen for the two points of measuring in the middle.

At higher number of days of drying, a preliminary study shows that the measured RH lies lower than the calculated RH.

14.4 Drying experiments made by Pihlajavaara

Pihlajavaara (1965) has made some drying tests with cement mortar with w_o/C 0.56. Before the drying was started the specimens were stored under sealed conditions for about 10 months. The specimens have the dimensions 40 * 40 * 160 mm. The drying occurred at the end surfaces (40 * 40) of the prisms.

The initial moisture content mass by volume was 166 kg/m^3. Half of the number of specimens dried in a climate room with about 40 % RH and 20 °C. The other half dried in a climate room with about 70 % RH and 20 °C. The equilibrium moisture content mass by volume at 40 % RH was 57 kg/m^3 and at 70 % RH it was 90 kg/m^3.

Pihlajavaara has not mentioned the cement content per m^3 cement mortar. The cement paste – aggregate ratio was 1:1.2 by volume. The maximum particle size was 1.4 mm, and the aggregate was quartz.

An approximative calculation shows that the cement content was about 490 kg per m^3 cement mortar.

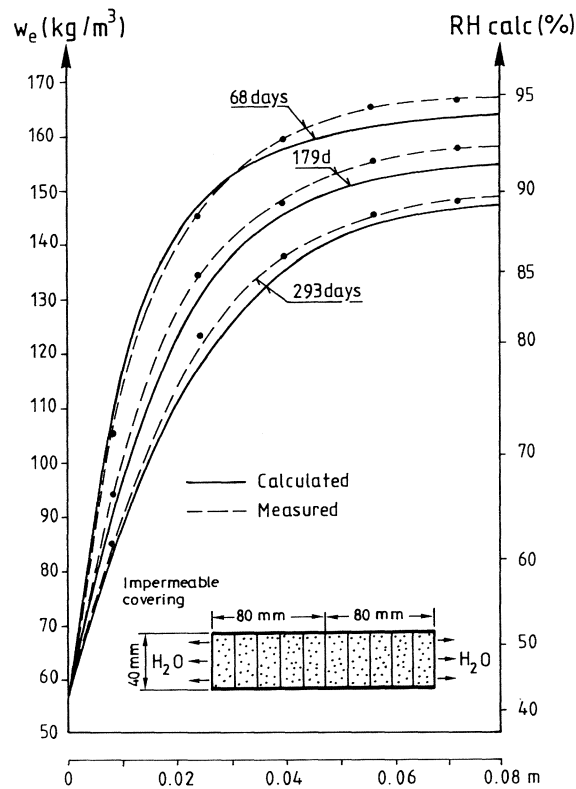In FIG 14.5 and 14.6 the calculated and the measured drying are shown.

FIG 14.5 Measured and calculated distribution of the moisture content mass by volume. Cement mortar with w_o/C 0.56. The measured results are from Pihlajavaara (1965).
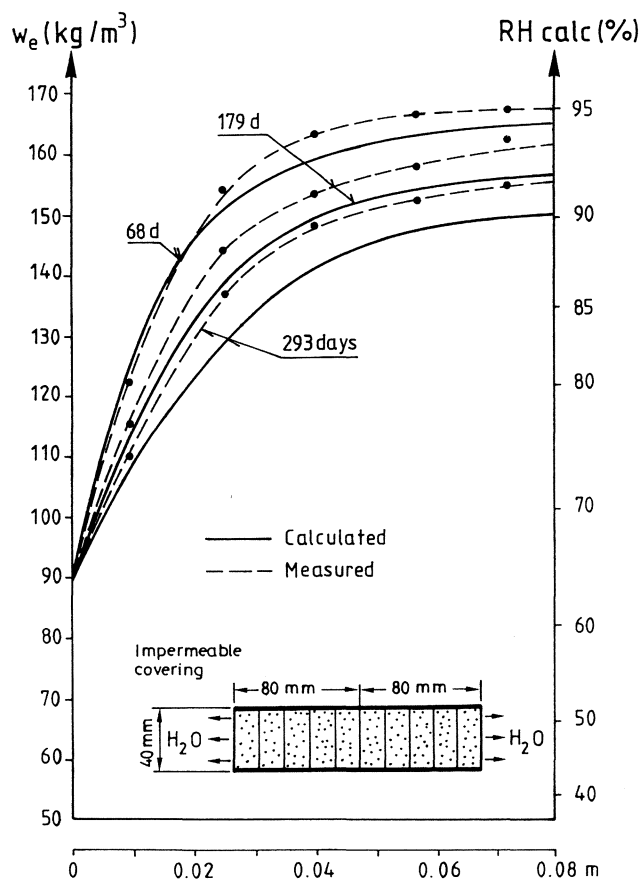
137

FIG 14.6 Measured and calculated distribution of the moisture content mass by volume. Cement mortar with w_o/C 0.56. The measured results are from Pihlajavaara (1965).

The results in FIG 14.5 and FIG 14.6 show that the calculated moisture content mass by volume is somewhat lower than the measured results for all the drying times. But in FIG 14.5 it agrees fairly well.

On the y-axis in FIG 14.5 and FIG 14.6 the calculated RH is also given. In the calculation the sorption isotherms in section 14.1 are used. As is seen in FIG 14.5 and 14.6, the calculated RH at the equlibrium content mass by volume (at the end of the specimens) is not exactly the same RH as reported for the climate rooms. In FIG 14.5 the maximum difference in the calculated RH between the measured curve and the calculated curve is about 1 % RH. In FIG 14.6 the maximum difference is about 2 % RH.

14.5 **Slab on the ground in a cellar**

The inhabitants in a house in Lund felt that they had a moist floor in the cellar. An inspection of the moisture conditions was made by Sahlen (1985). He took samples from different depths in the concrete slab and from the layers under the concrete slab. The construction of the slab on the ground is shown in FIG 14.7. The moisture flow through the slab on the ground was measured with a glass shade with the area 0.2 * 0.25 m, which was placed on the slab. A bowl with a saturated salt solution of potassium iodide, KJ, was placed in the glass shade. The relative humidity of the saturated salt solution is about 69 %, which was about the same as in the cellar (about 60 % RH).
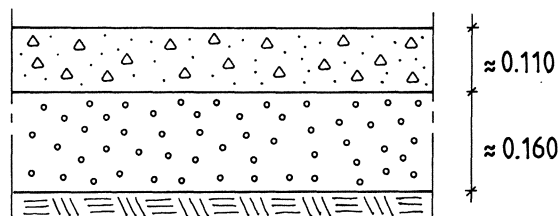

FIG 14.7   Section of the concrete slab on the ground.

The concrete slab is about 0.11 m thick. Under it there is about 0.16 m macadam, which is placed on fine sand. The layer of macadam consists of relatively small macadam, which is mingled with very fine material. This very fine material is on every piece of macadam in such quantity that the judgement was made that the layer of macadam is not capillary breaking.

The measured RH:s are shown in FIG 14.8. Samples were taken at different depths, 0-20, 20-45, 40-60 and 40-90 mm. The relative humidity of the samples was measured in our laboratory.
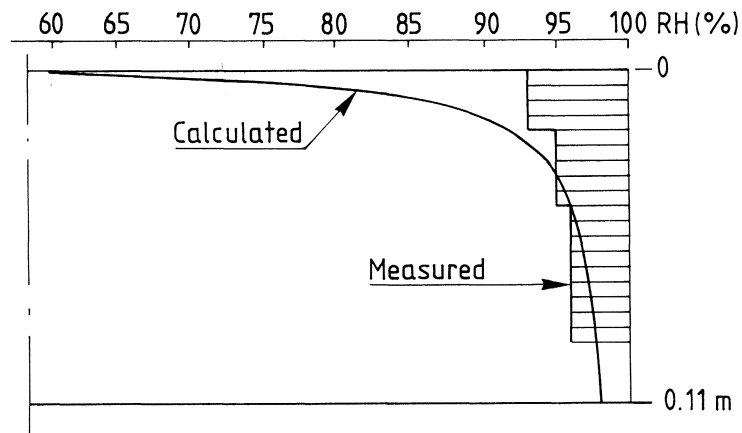

FIG 14.8 Measured and calculated RH in a slab on the ground.

If it is supposed that the macadam does not function as a capillarity breaking layer, and it is supposed that the bottom side of the concrete slab stands in water, then the RH-distribution shown in FIG 14.8 is obtained. w_o/C is assumed to be 0.7. RH on the uppermost side is 60 %. With the above data the calculated moisture flow is 11.5 gram/m^2 day. The measured moisture flow was 10.3 gram/m^2 day, when the RH of the saturated salt solution was 69 %. If RH on the uppermost side in the calculation is changed to 69 % the calculated moisture flow is 11.3 gram/m^2 day. The measured and the calculated moisture flow are in the same magnitude.

Harderup (1991) also had made field measurements of RH in a slab on the ground. The measurements show the same distribution of the relative humidity in the concrete slab as shown in FIG 14.8.

15 CAPILLARY SORPTION OF WATER IN CONCRETE

15.1 Introduction

The water sorption coefficient (A) and the water penetration coefficient (B) for a given material are normally determined by letting a dry specimen suck water from a water surface. An experimental arrangement in principle is shown in FIG 15.1. The methodology for the evaluation of A and B is shown in FIG 15.2.
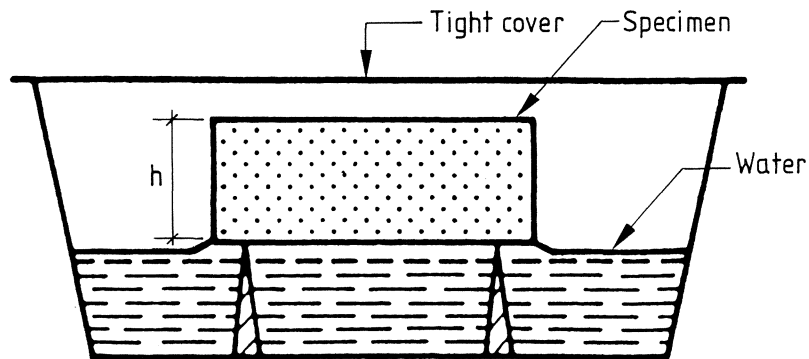

FIG 15.1 Experimental arrangement in principle during capillary sorption experiment.
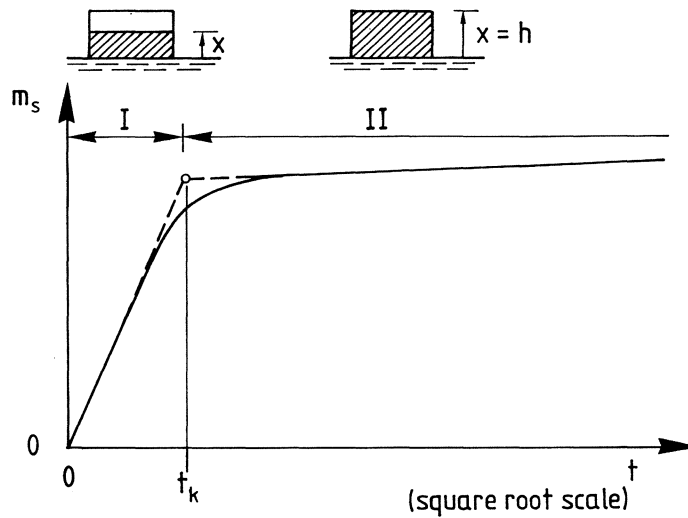Fagerlund (1982).

FIG 15.2 Methodology for the evaluation of the water sorption
and water penetration coefficients.
Fagerlund (1982).

In FIG 15.2 the amount of sucked water has been drawn as
function of the square root of the time. When the water surface
in the specimen has reached the top surface of the specimen,
there is a strong decrease of the water sorption rate. The time
t_k is defined as the point of intersection between phase 1 and
phase 2. In phase 1 the water surface has not reached the top
surface of the specimen. In phase 2 the water surface has
reached the top surface of the specimen. At phase 2 there is a
little increase in the weight of the sorbed water. This
depends, according to Fagerlund (1976), on water filling of
coarse pores.

According to ISO 9346 the following relations are given

$$m_s = A * \sqrt{t} \qquad\qquad\qquad (\ 15.1\ )$$

143

$$x = B * \sqrt{t} \qquad\qquad (15.2)$$

m_s = the mass divided by area of sorbed water from a
water surface $\qquad\qquad$ (kg/ m^2)

t = the time $\qquad\qquad$ (s)

x = the penetration dept of the water front during sorption
from a water surface $\qquad\qquad$ (m)

A = the water sorption coefficient $\qquad\qquad$ (kg/($m^2\sqrt{s}$))

B = the water penetration coefficient $\qquad\qquad$ (m/$\sqrt{s}$)

In Sweden, Eq. (15.2) is normally not used; Eq. (15.3) is used instead.

$$t = m * x^2 \quad m \neq m_s \qquad\qquad (15.3)$$

The quantity that is given in Swedish handbooks is m. It is possible to relate B to m and the relationship is B= $1/\sqrt{m}$.

According to Fagerlund (1982), see FIG 15.2, m is evaluated according to

$$m = t_k/h^2 \qquad\qquad (15.4)$$

and

$$A = m_s/\sqrt{t_k} \qquad\qquad (15.5)$$

h = the height of the specimen

15.2 **Some results**

The results presented in this section are for concrete that is about 5 years old. The specimens have first been used in the experiments which are described in Chapter 3. Thereafter they have dried out and got about the same moisture distribution in the specimen. After the capillary suction tests the specimens are used the drying tests described in Chapter 14. So one can

say that the tests described in this section are a by-product
of the drying experiments in Chapter 14.

Specimens made of concrete with w_o/C 0.7 and 0.6 and dried out
to about 60 % RH were allowed to suck water. The bottom sur-
faces of the specimens are 0.2 x 0.2 m. The height of the
specimens is 0.063 m. In the sides of the specimens there are 7
tubes that are cast in the specimen. Those tubes reduce the
volume by about 5 %. This means that the mass of the sorbed
water is reduced by the same percent.

In FIG 15.3 the mass of the sorbed water is shown as function
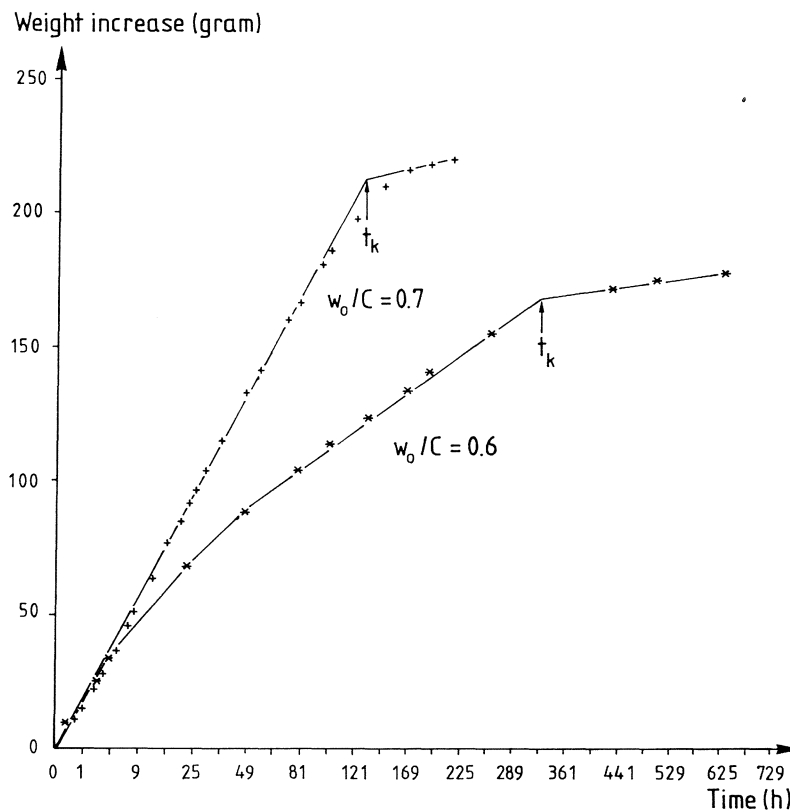of the square root of the time.

FIG 15.3 The mass of the sorbed water as function
              of the square root of the time.

145

For the concrete with w_o/C 0.7, t_k is 130 h. and the amount of the sorbed water, after correction for the dimensions of the bottom surface and the tubes, m_s, is $1.05(0.212/(0.2*0.2)) = 5.565$ kg/m^2. This means that m = $11.7*10^7$ s/m^2 and A = 0.0081 kg/(m^2√s).

For the concrete with w_o/C 0.6 t_k is 324 h. and the amount of the sorbed water, m_s, is $1.05(0.168/(0.2*0.2)) = 4.410$ kg/m^2. This means that m = $29,4*10^7$ s/m^2 and A = 0.0041 kg/(m^2√s). For w_o/C 0.6, the curve in FIG 15.3 is not a straight line up to t_k, but consists of two straight lines. The first part of the line has the same slope as the curve for concrete with w_o/C 0.7. One explanation why the curve, for the specimen with w_o/C 0.6, is not a straight line can be that the outer parts of the specimen were somewhat drier than the rest of the specimen.

The water sorption coefficient, A, is somewhat lower than what is given in Swedish handbooks.

The coefficient m is about 10 times higher than what is given in Swedish handbooks.

On explanation why A and m are different from the handbook values can be that the concretes are about 5 years old and have a high degree of hydration. The bottom surfaces of these two specimens have been in water for several years.

Another explanation is that some carbonation of the bottom surface has occurred and slows down the water transport.

A third explanation is that the specimens are considerably higher than those usually used in capillary sorption tests. Therefore the nick-point is less well-defined than in a normal test.

The moisture permeabilities according to TABLE 7.1 and TABLE 7.2 and the sorption isotherm according to section 14.1 do not

describe the capillary sorption of water. The maximum moisture
permeability measured in the steady state test described in
this thesis must be multiplied with a factor about 10-20 to
describe the capillary water uptake in the concrete in a fair
way.

16 CONCLUSIONS

This study provides the following conclusions.

1. Coefficients for moisture transport through mature
   concrete, cement mortar and cemement paste, under realistic
   conditions, have been established (see Chapters 7, 8 and 9).

2. The size dependence of these coefficients, reported from
   earlier investigations, has been confirmed but not
   explained.

3. The moisture transport coefficients of concrete at low rela-
   tive humidities are nearly independent of the water-cement
   ratio (w_o/C). At high relative humidities they are strongly
   dependent on w_o/C.

4. Most of the moisture transport in concrete at high relative
   humidities takes place along the boundary zone between
   cement paste and aggregate.

6. The moisture transport at high relative humidities is well
   described by the relation between surface flow and the
   amount of absorbed water given by Gilliland et al (1958).

The moisture permeabilities for mature concrete are summarized
in TABLE 16.1.

TABLE 16.1 Moisture permeability for mature concrete with different w_o/C.

RH	$\delta_v * 10^6$ (m²/s)				
%	w_o/C 0.4	w_o/C 0.5	w_o/C 0.6	w_o/C 0.7	w_o/C 0.8
33-65	0.13	0.14	0.17	0.17	0.17
80	0.28	0.33	0.38	0.38	0.38
86	0.39	0.59	0.73	0.73	0.73
90	≈0.53	1.0	1.5	1.5	1.5
93	≈0.6	1.7	3.2	3.2	3.2
95	≈0.7	2.8	7.5	7.5	7.5
96	≈0.7	4.2	8.5	9.5	11
97	-	9	14	17	26
97.6	-	-	22	28	42
98	-	-	-	38	63
98.5	-	-	-	-	130

APPENDIX A

Moisture flow through the specimens

Comments

The measured moisture flow had to be corrected for
 a) the flow through the epoxy resin on the sides of the
    specimen
 b) the influence of the sealing between the specimen and
    the upper box
 c) the influence of the RH-measurement tubes in the specimen
 d) the flow through the building sealant on the outside of the
    specimen.

a), b) and c) are corrected with coefficients of correction and
a total correction is obtained; see below.

The flow through the building sealant on the outside of the
specimen is so small that it only had influence on specimens
with small moisture flows (concrete and cement mortar with w_o/C
0.4).

Coefficients of correction

	Height of specimens (m)		
	0.063	0.100	0.150
a)	1.01	1.02	1.04
b)	1.04	1.03	1.025
c)	1.111	1.107	1.071
Total	1.17	1.16	1.15

The measurement of the moisture flows had been going on for
about 5 years. The moisture flows in this APPENDIX are from
two different times. The first is at about the same time as the
distribution of the relative humidity had been measured,
about 3 years after the test started. The second is about 5
years after the test started.

The bottom surface of the specimens is 0.2*0.2 m.

APPENDIX A(1)
Concrete with different w_o/C

		After about 3 years					After about 5 years			
Speci. number		Meas flow	Flow thr sealant	Corr coef	(1+2)*3	ψ	Meas flow	Flow seal	Corr koef	(6+7)*8
		1	2	3	4	5	6	7	8	9
			gram/day	−	g/day	g/(md)	gram/day		−	g/day
C8	A1	1.00	Neglect	1.17	1.170	1.834	−			
	B1	0.81		1.16	0.940	2.350	−			
	C1	0.58		1.15	0.667	2.501	0.425		1.15	0.489
C7	A1	0.60		1.17	0.702	1.106	−			
	B1	0.42		1.16	0.487	1.218	−			
	C1	−					0.339		1.15	0.390
C6	A1	0.46		1.17	0.538	0.847	−			
	B1	0.27		1.16	0.313	0.783	−			
	C1	0.27		1.15	0.311	1.166	0.176		1.15	0.202
C5	A1	0.24		1.17	0.281	0.443	−			
	B1	0.15		1.16	0.174	0.435	−			
	C1	0.13		1.15	0.150	0.563	0.111		1.15	0.128
C4	A1	0.10	0.002	1.17	0.119	0.187	−			
	B1	0.06	0.002	1.16	0.072	0.180	0.058	0.002	1.16	0.070
	C1	0.06	0.002	1.15	0.071	0.266	0.048	0.002	1.15	0.058
C8	A2	0.28		1.17	0.328	0.517	−			
	B2	0.21		1.16	0.244	0.610	−			
	C2	0.18		1.15	0.207	0.776	0.148		1.15	0.170
C7	A2	0.30		1.17	0.351	0.553	−			
	B2	0.21		1.16	0.244	0.610	−			
	C2	0.21		1.15	0.242	0.908	0.165		1.15	0.190
C6	A2	0.21		1.17	0.246	0.387	−			
	B2	0.18		1.16	0.209	0.523	−			
	C2	0.13		1.15	0.150	0.563	0.121		1.15	0.139
C5	A2	0.16		1.17	0.187	0.295	0.135		1.17	0.158
	B2	0.14		1.16	0.162	0.405	−			
	C2	0.12		1.15	0.138	0.518	0.097		1.15	0.112
C4	A2	0.10	0.002	1.17	0.119	0.187	0.078	0.002	1.17	0.094
	B2	0.07	0.002	1.16	0.084	0.210	0.067	0.002	1.16	0.080
	C2	0.05	0.002	1.15	0.060	0.225	0.045	0.002	1.15	0.054

Specimen number
C = Concrete
8, 7, 6, 5, 4 = 10 * w_o/C
A, B, C = Height of specimen (0,063, 0.100 and 0.150 m)
1 = Specimen bottom in water; 2 = Specimen bottom in moist air

152

Concrete with different amounts of air (Nominal)

Speci. number		Meas flow	Corr coef	1 * 2	Ψ	Meas flow	Corr coef	5 * 6	Ψ
		1	2	3	4	5	6	7	8
		g/day	−	g/day	g/(md)	g/day	−	g/day	g/(md)
4	A1	1.00	1.17	1.170	1.843				
	B1	0.60	1.16	0.696	1.740				
	C1	0.43	1.15	0.495	1.856	0.301	1.15	0.346	1.298
6	A1	0.73	1.17	0.854	1.345				
	B1	0.53	1.16	0.615	1.538				
	C1	0.47	1.15	0.541	2.029	0.349	1.15	0.401	1.504
8	A1	0.95	1.17	1.112	1.751				
	B1	0.65	1.16	0.754	1.885				
	C1	0.55	1.15	0.633	2.374				
10	A1	1.50	1.17	1.755	2.764				
	B1	0.55	1.16	0.638	1.595	0.399	1.16	0.463	1.148
	C1	0.53	1.15	0.610	2.286				
4	A2	0.27	1.17	0.316	0.498	0.236	1.17	0.276	0.435
	B2	0.22	1.16	0.255	0.638	0.170	1.16	0.197	0.493
	C2	0.17	1.15	0.196	0.735	0.137	1.15	0.158	0.593
6	A2	0.27	1.17	0.316	0.498	0.237	1.17	0.277	0.436
	B2	0.28	1.16	0.325	0.813	0.222	1.16	0.258	0.645
	C2	0.18	1.15	0.207	0.776	0.151	1.15	0.174	0.653
8	A2	0.38	1.17	0.445	0.701				
	B2	0.40	1.16	0.464	1.160	0.291	1.16	0.338	0.845
	C2	0.24	1.15	0.276	1.035				
10	A2	−							
	B2	0.23	1.16	0.267	0.668				
	C2	0.23	1.17	0.265	0.994				

Specimen number
4, 6, 8, 10 = Nominal air content (%)
A, B, C = Height of specimen (0.063, 0.100 and 0.150 m)
1 = Specimen bottom in water
2 = Specimen bottom in moist air

APPENDIX A(3)
Concrete with different amounts of aggregate

Speci. number	After about 3 years				After about 5 years			
	Meas flow	Corr coef	1 * 2	Ψ	Meas flow	Corr coef	5 * 6	Ψ
	1	2	3	4	5	6	7	8
	g/day	-	g/day	g/(md)	g/day	-	g/day	g/(md)
1692A1	-							
B1	0.32	1.16	0.371	0.928	0.236	1.16	0.274	0.684
C1	-				0.304	1.15	0.350	1.313
1730A1	-				0.357	1.17	0.418	0.658
B1	0.26	1.16	0.302	0.755	0.221	1.16	0.256	0.641
C1	0.28	1.15	0.322	1.208				
1765A1	-				0.410	1.17	0.480	0.756
B1	0.47	1.16	0.545	1.363	0.384	1.16	0.445	1.114
C1	-				0.349	1.15	0.401	1.505
1827A1	0.65	1.17	0.761	1.199	0.473	1.17	0.553	0.871
B1	0.49	1.16	0.568	1.420	0.348	1.16	0.404	1.009
C1	-				0.339	1.15	0.390	1.462
1854A1	0.81	1.17	0.948	1.493	0.618	1.17	0.723	1.139
B1	0.45	1.16	0.522	1.305	0.319	1.16	0.370	0.925
C1	-				0.385	1.15	0.443	1.660
1692A2	-							
B2	0.18	1.16	0.209	0.523				
C2	0.22	1.15	0.253	0.949				
1730A2	0.21	1.17	0.246	0.387				
B2	0.19	1.16	0.220	0.550	0.153	1.16	0.177	0.444
C2	0.18	1.15	0.207	0.776	0.225	1.15	0.259	0.970
1765A2	-				0.255	1.17	0.298	0.470
B2	0.19	1.16	0.220	0.550				
C2	0.22	1.15	0.253	0.949				
1827A2	0.21	1.17	0.246	0.387				
B2	0.24	1.16	0.278	0.695				
C2	-							
1854A2	0.21	1.17	0.246	0.387				
B2	0.20	1.16	0.232	0.580				
C2	-							

Specimen number
1692 and so on = Aggregate content (kg/m^3)
A, B, C = Height of specimen (0.063, 0.100 and 0.150 m)
1 = Specimen bottom in water
2 = Specimen bottom in moist air

APPENDIX A(4)
Cement mortar with different w_o/C

		After about 3 years					After about 5 years			
Speci. number		Meas flow	Flow thr sealant	Corr coef	(1+2) *3	Ψ	Meas flow	Flow seal	Corr coef	(6+7) *8
		1	2	3	4	5	6	7	8	9
		g/day		–	g/day	g/(md)	g/day		–	g/day
M8	A1	–	Neglect				0.560		1.17	0.655
	B1	–					0.388		1.16	0.450
	C1	0.41		1.15	0.472	1.770	0.319		1.15	0.367
M7	A1	0.39		1.17	0.456	0.718				
	B1	0.32		1.16	0.371	0.928				
	C1	0.30		1.15	0.345	1.294	0.226		1.15	0.260
M6	A1	0.28		1.17	0.328	0.517				
	B1	0.21		1.16	0.244	0.610	0.148		1.16	0.172
	C1	0.21		1.15	0.242	0.908	0.172		1.15	0.198
M5	A1	0.14		1.17	0.164	0.258				
	B1	0.14		1.16	0.162	0.405				
	C1	0.10		1.15	0.115	0.431	0.083		1.15	0.095
M4	A1	0.070	0.002	1.17	0.084	0.132	0.055	0.002	1.17	0.067
	B1	0.047	0.002	1.16	0.057	0.143	0.043	0.002	1.16	0.052
	C1	0.050	0.002	1.15	0.060	0.225	0.035	0.002	1.15	0.043
M8	A2	0.42		1.17	0.491	0.773				
	B2	0.37		1.16	0.429	1.073				
	C2	0.25		1.15	0.288	1.080	0.225		1.15	0.259
M7	A2	0.35		1.17	0.410	0.646				
	B2	0.24		1.16	0.278	0.695				
	C2	0.24		1.15	0.276	1.035	0.189		1.15	0.217
M6	A2	0.21		1.17	0.246	0.387				
	B2	0.22		1.16	0.255	0.638				
	C2	0.165		1.15	0.190	0.713	0.141		1.15	0.162
M5	A2	0.13		1.17	0.152	0.239	0.095		1.17	0.111
	B2	0.12		1.16	0.139	0.348	0.104		1.16	0.121
	C2	0.09		1.15	0.101	0.379	0.076		1.15	0.087
M4	A2	0.065	0.002	1.17	0.078	0.123				
	B2	0.050	0.002	1.16	0.060	0.150	0.039	0.002	1.16	0.048
	C2	0.050	0.002	1.15	0.060	0.225	0.033	0.002	1.15	0.040

Specimen number
M = Cement Mortar
8, 7, 6, 5, 4 = 10 * w_o/C
A, B, C = Height of specimen (0.063, 0.100, 0.150 m)
1 = Specimen bottom in water; 2 = Specimen bottom in moist air

APPENDIX A(5)
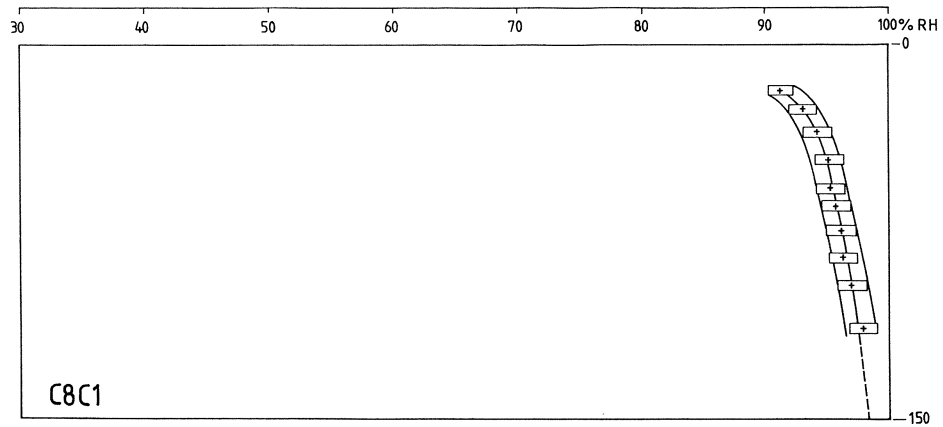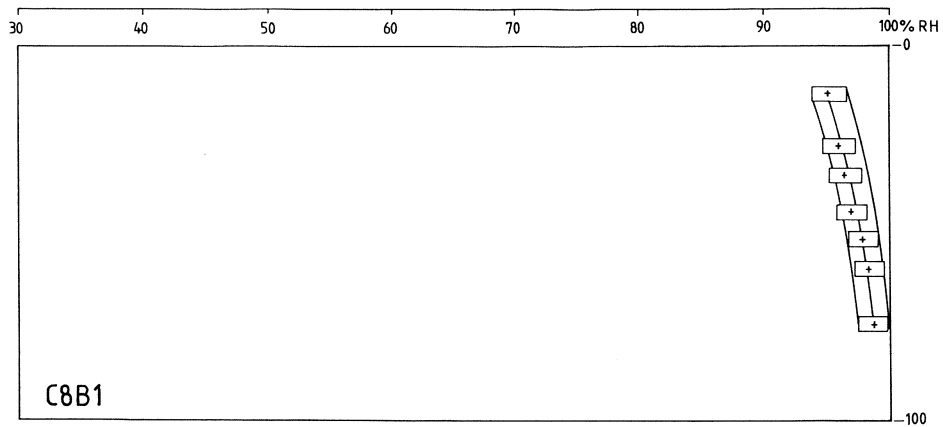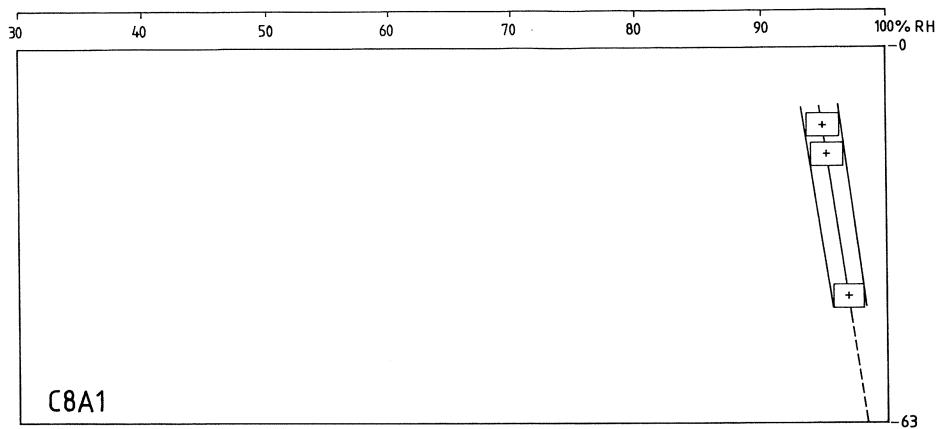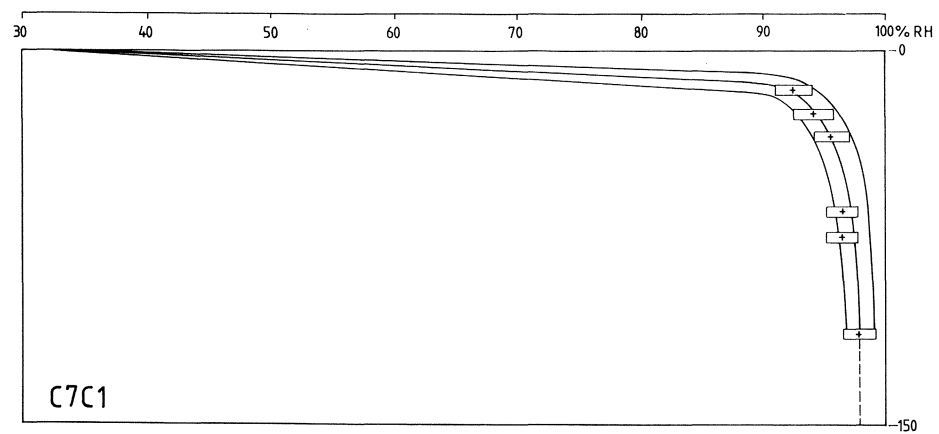
Cement paste with different w_o/C

Speci. number	After about 3 years				After about 5 years			
	Meas flow	Corr coef	1 * 2	ψ	Meas flow	Corr coef	5 * 6	ψ
	1	2	3	4	5	6	7	8
	g/day	–	g/day	g/(md)	g/day	–	g/day	g/(md)
P6 A1	0.84	1.17	0.983	1.548				
B1	0.61	1.16	0.708	1.770	0.507	1.16	0.588	1.470
C1	0.50	1.15	0.575	2.156	0.501	1.15	0.576	2.160
P5 A1	0.55	1.17	0.644	1.014	0.480	1.17	0.562	0.885
B1	0.39	1.16	0.452	1.130	0.355	1.16	0.412	1.030
C1	0.34	1.15	0.391	1.466	0.278	1.15	0.320	1.200
P4 A1	0.17	1.17	0.199	0.313	0.135	1.17	0.158	0.249
B1	–							
C1	0.17	1.15	0.196	0.735	0.101	1.15	0.116	0.435
P6 A2	0.82	1.17	0.959	1.510	0.766	1.17	0.896	1.411
B2	0.78	1.16	0.905	2.263	0.736	1.16	0.854	2.135
C2	0.60	1.15	0.690	2.588	0.550	1.15	0.633	2.374
P5 A2	0.42	1.17	0.491	0.773	0.367	1.17	0.429	0.676
B2	0.42	1.16	0.487	1.218	0.363	1.16	0.421	1.053
C2	0.32	1.15	0.368	1.380	0.263	1.15	0.302	1.133
P4 A2	0.17	1.17	0.199	0.313	0.144	1.17	0.168	0.265
B2	0.17	1.16	0.197	0.493	0.157	1.16	0.182	0.455
C2	–							

Specimen number
P = Cement Paste
6, 5, 4 = 10 * w_o/C
A, B, C = Height of specimen (0.063, 0.100, 0.150 m)
1 = Specimen bottom in water
2 = Specimen bottom in moist air

APPENDIX B

Measured moisture distributions in the specimens

Comments

In this APPENDIX the RH-profiles are shown for different specimens.
The maximum, mean and minimum RH-profiles are shown. The maximum and
minimum curves are obtained when the total error in the RH-measure-
ment is taken in consideration; see Section 5.3. For the specimen
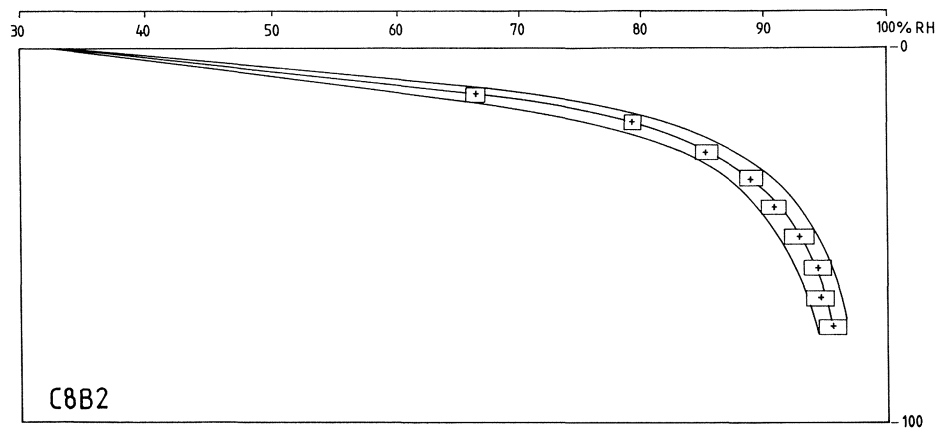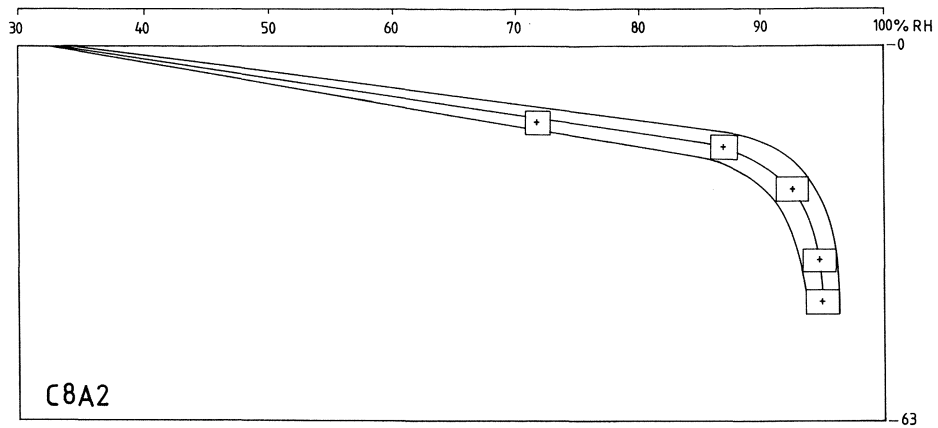number see APPENDIX A.

The dashed curves between the lowest level of the RH-measurement and
the specimen bottom are obtained by letting the mean RH-distribution
curve continue gradually and continuously the measured mean RH-
distribution curve. For most specimens with the bottom in water it
ens at the maximum RH given in section 7.1.3.

C8A1

C8B1

C8C1

159

C7A1

C7B1

C7C1

C6B1

C6C1

C5A1

C5B1

C5C1

162

C8A2

C8B2

C8C2

C7A2

C7B2

C7C2

C6A2

C6B2

C6C2

165

C5B2

C5C2

C4B2

30   40   50   60   70   80   90   100% RH
— 0

4A1

— 63

168

6B1

8B1

8C1

10 B1

10 C 1

4B2

4C2

6B2

1692 B1

1730 A1

1730 B1

1730 C1

176

1765 B1

1827 A1

1827 B1

1854 A1

1854 B1

1692 B2

1692 C2

180

1730 A2

1730 B2

1730 C2

181

1765 A 2

1765 B 2

1827 A2

1827 B2

1854 A2

1854 B2

M8A1

M8B1

M8C1

M7A1

M7B1

M7C1

M6B1

M6C1

M5A1

M5B1

M5C1

188

M4A1

M4B1

M4C1

189

M8A2

M8C2

M7A2

M7B2

M7C2

M6A2

M6B2

M6C2

192

M5A2

M5B2

M5C2

193

M4A2

M4B2

M4C2

P6A1

P6B1

P6C1

P5A1

P5B1

P5C1

P6A2

P6B2

P6C2

P5A2

P5B2

P5C2

198

APPENDIX C

**Measured moisture distributions and the fundamental flow
potential**

Comments

In this APPENDIX the distance from the top of the specimen to
the mean RH-distribution is shown "dimensionless". At the top
of the specimen it is 0 and at the bottom of the specimen it is
1. The value x in this APPENDIX should be multiplied by the
height of the specimen to get the distance to the RH-distri-
bution curve in meters.

The fundamental flow potential (Ψ) is the distance from the top
of the specimen to the mean RH-distribution curve times the
moisture flow; see also Chapter 6. Ψ is in g/(m*day).

APPENDIX C(1)
Concrete w_o/C 0.5

RH	C5A1		C5B1		C5C1	
%	x	ψ	x	ψ	x	ψ
50	0.080	0.035	0.093	0.041	0.080	0.045
60	0.127	0.056	0.147	0.064	0.127	0.071
65	0.147	0.065	0.173	0.076	0.153	0.086
70	0.173	0.076	0.200	0.087	0.180	0.101
75	0.193	0.086	0.233	0.102	0.227	0.127
80	0.220	0.098	0.273	0.119	0.287	0.161
84	0.267	0.118	0.327	0.142	0.347	0.195
86	0.293	0.130	0.353	0.153	0.387	0.218
88	0.333	0.147	0.400	0.174	0.427	0.240
90	0.393	0.174	0.453	0.197	0.473	0.266
91	0.433	0.192	0.493	0.215	0.500	0.281
92	0.480	0.212	0.533	0.232	0.533	0.300
93	0.540	0.239	0.593	0.258	0.567	0.318
94	0.613	0.272	0.660	0.287	0.607	0.341
95	0.700	0.310	0.747	0.325	0.653	0.368
96	(0.800)	(0.354)	(0.860)	(0.374)	(0.733)	(0.412)
97	(1.000)	(0.443)	(1.000)	(0.435)	(1.000)	(0.563)

RH	C5A2		C5B2		C5C2		Mean
%	x	ψ	x	ψ	x	ψ	ψ
50			0.080	0.033			0.039
60			0.127	0.051			0.061
65			0.147	0.059			0.072
70			0.173	0.070			0.084
75			0.193	0.078			0.098
80			0.233	0.094			0.118
84			0.273	0.111			0.142
86			0.307	0.124			0.156
88			0.353	0.143			0.176
90			0.413	0.167			0.201
91			0.460	0.187			0.219
92			0.520	0.210			0.239
93			0.593	0.240			0.264
94			0.693	0.281			0.295
95			0.833	0.337			0.335
96							(0.380)
97							(0.480)

A, B, C in C5A1, C5B1 and C5C1 are the height of the specimens
   (63, 100 and 150 mm).
1 in C5A1 is for specimens with the bottom side in water.
2 in C5A2 is for specimens with the bottom side in moist air.
x is the distance from the top surface to the middle
   RH-distribution curve.
   is the fundamental potential.
( ) is for estimated values, see APPENDIX B

APPENDIX C(2)
Concrete w_o/C 0.6

RH	C6A1		C6B1		C6C1	
%	x	ψ	x	ψ	x	ψ
50			0.047	0.037	0.040	0.046
60			0.073	0.057	0.060	0.070
65			0.080	0.063	0.073	0.086
70			0.093	0.073	0.087	0.101
75			0.107	0.083	0.100	0.117
80			0.120	0.094	0.120	0.139
84			0.140	0.110	0.153	0.179
86			0.160	0.126	0.180	0.210
88			0.187	0.146	0.220	0.256
90			0.227	0.177	0.267	0.311
91			0.253	0.198	0.307	0.358
92			0.280	0.219	0.353	0.412
93			0.320	0.250	0.407	0.474
94			0.387	0.303	0.487	0.567
95			0.527	0.412	0.600	0.700
96			(0.700)	(0.547)	(0.700)	(0.817)
97			(0.893)	(0.699)	(0.873)	(1.018)
97.6			(1.000)	(0.783)	(1.000)	(1.167)

RH	C6A2		C6B2		C6C2		Mean
%	x	ψ	x	ψ	x	ψ	ψ
50	0.087	0.034	0.087	0.045	0.060	0.034	0.039
60	0.133	0.052	0.133	0.069	0.100	0.056	0.061
65	0.160	0.062	0.153	0.080	0.127	0.071	0.072
70	0.187	0.073	0.187	0.097	0.167	0.094	0.088
75	0.213	0.083	0.220	0.115	0.213	0.120	0.104
80	0.233	0.091	0.267	0.140	0.280	0.158	0.124
84	0.280	0.108	0.320	0.168	0.340	0.191	0.151
86	0.313	0.122	0.367	0.192	0.380	0.214	0.173
88	0.367	0.142	0.420	0.220	0.433	0.244	0.202
90	0.453	0.175	0.507	0.265	0.507	0.285	0.243
91	0.513	0.199	0.553	0.289	0.560	0.315	0.272
92	0.593	0.230	0.607	0.317	0.620	0.349	0.305
93			0.673	0.352	0.687	0.386	0.366
94			0.740	0.387	0.773	0.435	0.423
95			0.813	0.425	0.867	0.488	0.506
96			(0.893)	(0.467)	(0.980)	(0.551)	(0.596)
97			(0.987)	(0.515)			(0.744)
97.6							(0.975)

APPENDIX C(3)
Concrete w_o/C 0.7

RH	C7A1		C7B1		C7C1	
%	x	ψ	x	ψ	x	ψ
50	(0.053)		(0.040)			
60	(0.080)		(0.067)			
65	(0.093)		(0.080)			
70	(0.107)		(0.093)			
75	(0.120)		(0.100)			
80	(0.133)		(0.113)			
84	(0.147)		(0.120)			
86	(0.153)		0.127	0.154		
88	(0.160)		0.147	0.178		
90	0.187	0.207	0.180	0.219		
91	0.207	0.228	0.213	0.259		
92	0.233	0.258	0.240	0.292		
93	0.273	0.302	0.287	0.348		
94	0.313	0.346	0.340	0.414		
95	0.373	0.413	0.407	0.495		
96	0.460	0.509	0.500	0.609		
97	0.600	0.663	(0.713)	(0.868)		
98	(1.000)	(1.106)	(1.000)	(1.217)		

RH	C7A2		C7B2		C7C2		Mean
%	x	ψ	x	ψ	x	ψ	ψ
50	0.080	0.044	0.047	0.028	0.040	0.036	0.036
60	0.133	0.074	0.080	0.048	0.073	0.067	0.063
65	0.153	0.085	0.093	0.057	0.087	0.078	0.073
70	0.180	0.099	0.113	0.069	0.107	0.097	0.088
75	0.200	0.111	0.127	0.078	0.133	0.122	0.104
80	0.240	0.133	0.153	0.093	0.173	0.158	0.128
84	0.280	0.155	0.193	0.118	0.227	0.206	0.160
86	0.313	0.173	0.220	0.134	0.260	0.236	0.174
88	0.347	0.191	0.253	0.154	0.307	0.278	0.200
90	0.413	0.229	0.300	0.183	0.373	0.339	0.235
91	0.447	0.247	0.333	0.204	0.420	0.382	0.264
92	0.487	0.269	0.367	0.224	0.473	0.429	0.294
93	0.540	0.298	0.407	0.248	0.533	0.484	0.336
94	0.607	0.336	0.467	0.285	0.593	0.539	0.384
95	0.700	0.387	0.547	0.334			0.407
96	(0.800)	(0.443)	0.660	0.403			0.491
97	(0.960)	(0.531)	0.880	0.537			(0.650)
98							(1.162)

APPENDIX C(4)
Concrete w_o/C 0.8

RH	C8A1		C8B1		C8C1	
%	x	ψ	x	ψ	x	ψ
50						
60						
65						
70						
75						
80						
84						
86						
88						
90						
91						
92					(0.133)	(0.334)
93					(0.167)	(0.417)
94					(0.213)	(0.534)
95	0.213	0.393	0.133	0.313	0.300	0.751
96	0.427	0.787	0.233	0.549	0.453	1.134
97	0.647	1.192	0.367	0.862	0.633	1.585
98	(0.873)	(1.610)	0.540	1.269	(0.847)	(2.118)
98.5			0.813	1.952	(1.000)	(2.501)

RH	C8A2		C8B2		C8C2		Mean
%	x	ψ	x	ψ	x	ψ	ψ
50	0.087	0.045	0.067	0.041	0.067	0.052	0.046
60	0.133	0.069	0.100	0.061	0.107	0.082	0.071
65	0.160	0.082	0.120	0.073	0.120	0.093	0.083
70	0.187	0.097	0.140	0.086	0.147	0.114	0.099
75	0.207	0.107	0.167	0.102	0.173	0.135	0.115
80	0.233	0.120	0.207	0.126	0.220	0.170	0.139
84	0.253	0.131	0.260	0.158	0.267	0.207	0.165
86	0.267	0.138	0.287	0.175	0.300	0.233	0.182
88	0.287	0.148	0.333	0.203	0.333	0.259	0.203
90	0.313	0.162	0.387	0.236	0.380	0.295	0.231
91	0.340	0.176	0.420	0.256	0.407	0.316	0.249
92	0.360	0.185	0.460	0.280	0.453	0.352	0.288
93	0.393	0.203	0.507	0.309	0.500	0.388	0.329
94	0.453	0.234	0.573	0.349	0.567	0.440	0.389
95	0.587	0.303	0.667	0.407	0.673	0.523	0.448
96					(1.000)	(0.777)	0.812
97							1.213
98							(1.666)
98.5							(2.227)

APPENDIX C(5)
cement mortar w_o/C 0.4

RH	M4A1		M4B1		M4C1	
%	x	ψ	x	ψ	x	ψ
50	0.140	0.018	0.133	0.018	0.107	0.023
60	0.260	0.034	0.247	0.034	0.207	0.045
65	0.360	0.046	0.313	0.043	0.260	0.057
70	0.460	0.059	0.400	0.055	0.320	0.070
75	0.560	0.072	0.507	0.070	0.447	0.097
80	0.653	0.084	0.620	0.086	0.573	0.125
84	0.733	0.095	0.720	0.099	0.673	0.147
86			0.773	0.107	0.727	0.158
88			(0.827)	(0.114)	(0.773)	(0.169)
90			(0.880)	(0.121)	(0.827)	(0.180)
91			(0.900)	(0.124)	(0.853)	(0.186)
92			(0.927)	(0.128)	(0.880)	(0.192)
93			(0.953)	(0.132)	(0.913)	(0.199)
94			(0.980)	(0.135)	(0.940)	(0.205)
95					(0.973)	(0.212)
96						
97						

RH	M4A2		M4B2		M4C2		Mean
%	x	ψ	x	ψ	x	ψ	ψ
50	0.180	0.022	0.180	0.026	0.133	0.029	0.023
60	0.307	0.037	0.293	0.043	0.207	0.045	0.040
65	0.367	0.044	0.347	0.050	0.273	0.060	0.050
70	0.433	0.052	0.433	0.063	0.373	0.081	0.063
75	0.540	0.065	0.540	0.078	0.487	0.106	0.081
80	0.660	0.079	0.647	0.094	0.620	0.135	0.101
84	0.760	0.091	0.727	0.105	0.740	0.161	0.116
86	(0.800)	(0.096)	0.767	0.111	0.800	0.174	0.129
88	(0.847)	(0.102)	0.813	0.118	(0.860)	(0.187)	(0.138)
90	(0.900)	(0.108)	0.853	0.124	(0.920)	(0.201)	(0.147)
91	(0.920)	(0.110)	(0.873)	(0.127)	(0.947)	(0.206)	(0.151)
92	(0.947)	(0.114)	(0.893)	(0.130)	(0.980)	(0.214)	(0.156)
93	(0.973)	(0.117)	(0.920)	(0.133)			(0.145)
94	(1.000)	(0.120)	(0.933)	(0.135)			(0.149)
95			(0.960)	(0.139)			(0.176)
96			(0.980)	(0.142)			
97			(1.000)	(0.145)			

APPENDIX C(6)
Cement mortar w_o/C 0.5

RH	M5A1		M5B1		M5C1	
%	x	ψ	x	ψ	x	ψ
50	0.100	0.026	0.060	0.024	0.087	0.037
60	0.160	0.041	0.093	0.038	0.147	0.063
65	0.187	0.048	0.107	0.043	0.180	0.078
70	0.233	0.060	0.153	0.062	0.213	0.092
75	0.287	0.074	0.220	0.089	0.253	0.109
80	0.353	0.091	0.287	0.116	0.313	0.135
84	0.420	0.108	0.367	0.149	0.393	0.169
86	0.460	0.119	0.413	0.167	0.447	0.193
88	0.507	0.131	0.467	0.189	0.493	0.212
90	0.567	0.146	0.527	0.213		
91		(0.157)	0.553	0.224		
92		(0.168)	0.587	0.238		
93		(0.182)	0.620	0.251		
94		(0.198)	0.653	0.264		
95		(0.213)				
96		(0.234)				
97		(0.258)				

RH	M5A2		M5B2		M5C2		Mean
%	x	ψ	x	ψ	x	ψ	ψ
50	0.140	0.033	0.067	0.023	0.087	0.033	0.029
60	0.220	0.053	0.107	0.037	0.167	0.063	0.049
65	0.260	0.062	0.147	0.051	0.207	0.078	0.060
70	0.307	0.073	0.213	0.074	0.247	0.094	0.076
75	0.373	0.089	0.280	0.097	0.307	0.116	0.096
80	0.480	0.115	0.360	0.125	0.413	0.157	0.123
84	0.580	0.139	0.447	0.156	0.513	0.194	0.153
86	0.640	0.153	0.507	0.176	0.573	0.217	0.171
88	0.713	0.170	0.580	0.202	0.633	0.240	0.191
90					0.693	0.263	0.207
91					0.727	0.276	0.219
92					0.767	0.291	0.233
93							(0.217)
94							(0.231)
95							(0.213)
96							(0.234)
97							(0.258)

APPENDIX C(7)
Cement mortar w_o/C 0.6

RH	M6A1		M6B1		M6C1	
%	x	ψ	x	ψ	x	ψ
50	(0.060)				0.040	0.036
60	(0.093)				0.067	0.061
65	(0.113)				0.080	0.073
70	(0.127)				0.107	0.097
75	(0.147)				0.140	0.127
80	(0.167)				0.187	0.170
84	(0.180)				0.240	0.218
86	(0.187)		0.147	0.090	0.280	0.254
88	(0.193)		0.180	0.110	0.333	0.302
90	0.220	0.114	0.227	0.138	0.400	0.363
92	0.240	0.124	0.253	0.154	0.433	0.393
93	0.273	0.141	0.287	0.175	0.473	0.429
94	0.320	0.165	0.333	0.203	0.520	0.472
95	0.373	0.193	0.393	0.240	0.567	0.515
96	0.453	0.234	0.467	0.285	0.647	0.587
97	0.593	0.307	0.587	0.358		
97.6	(0.800)	(0.414)	0.767	0.468		
	(1.000)	(0.517)				

RH	M6A2		M6B2		M6C2		Mean
%	x	ψ	x	ψ	x	ψ	ψ
50	0.087	0.034	0.060	0.038	0.073	0.052	0.040
60	0.140	0.054	0.093	0.059	0.140	0.100	0.069
65	0.167	0.065	0.107	0.068	0.180	0.128	0.084
70	0.207	0.080	0.140	0.089	0.227	0.162	0.107
75	0.267	0.103	0.187	0.119	0.273	0.195	0.136
80	0.340	0.132	0.260	0.166	0.340	0.242	0.178
84	0.407	0.158	0.333	0.212	0.400	0.285	0.218
86	0.440	0.170	0.380	0.242	0.433	0.309	0.213
88	0.487	0.188	0.447	0.285	0.473	0.337	0.244
90	0.533	0.206	0.533	0.340	0.520	0.371	0.255
91	0.560	0.217	0.587	0.375	0.547	0.390	0.276
92	0.593	0.229	0.647	0.413	0.580	0.414	0.300
93	0.633	0.245	0.707	0.451	0.620	0.442	0.330
94	0.673	0.260	0.773	0.493	0.680	0.485	0.364
95			0.853	0.544	0.767	0.547	0.413
96							
97							
97.6							

APPENDIX C(8)
Cement mortar w_o/C 0.7

RH	M7A1		M7B1		M7C1	
%	x	ψ	x	ψ	x	ψ
50						
60						
65						
70						
75						
80					0.147	0.190
84					0.200	0.259
86					0.233	0.302
88	0.213	0.153	0.160	0.148	0.273	0.353
90	0.260	0.187	0.187	0.174	0.327	0.423
91	0.293	0.210	0.213	0.198	0.360	0.466
92	0.333	0.239	0.240	0.223	0.393	0.509
93	0.393	0.282	0.287	0.266	0.440	0.569
94	0.480	0.345	0.333	0.309	0.493	0.638
95			0.393	0.365	0.567	0.734
96			0.487	0.452	0.687	0.889
97			0.633	0.587	(0.800)	(1.035)
98			(1.000)	(0.928)	(1.000)	(1.294)

RH	M7A2		M7B2		M7C2		Mean
%	x	ψ	x	ψ	x	ψ	ψ
50	0.087	0.056	0.040	0.028	0.053	0.055	0.046
60	0.140	0.090	0.067	0.047	0.093	0.096	0.078
65	0.167	0.108	0.080	0.056	0.113	0.117	0.094
70	0.193	0.125	0.093	0.065	0.140	0.145	0.112
75	0.213	0.138	0.140	0.097	0.173	0.179	0.138
80	0.247	0.160	0.207	0.144	0.213	0.220	0.179
84	0.293	0.189	0.267	0.186	0.253	0.262	0.224
86	0.333	0.215	0.307	0.213	0.287	0.297	0.257
88	0.387	0.250	0.340	0.236	0.333	0.345	0.248
90	0.447	0.289	0.380	0.364	0.387	0.401	0.290
91	0.487	0.315	0.407	0.283	0.420	0.435	0.318
92	0.533	0.344	0.440	0.306	0.473	0.490	0.352
93	0.587	0.379	0.480	0.334	0.533	0.552	0.397
94	0.653	0.442	0.533	0.370	0.633	0.655	0.460
95			0.600	0.417			0.505
96			0.693	0.482			0.608
97			0.827	0.575			0.732
98							(1.111)

Cement mortar w_o/C 0.8

RH	M8A1		M8B1		M8C1	
%	x	ψ	x	ψ	x	ψ
50					(0.040)	
60					(0.060)	
65					(0.073)	
70					(0.080)	
75					(0.093)	
80					0.113	0.200
84					0.140	0.248
86					0.160	0.283
88					0.193	0.342
90			0.147		0.240	0.425
91			0.153		0.267	0.473
92			0.160		0.307	0.543
93			0.173		0.360	0.637
94	0.193		0.207		0.420	0.743
95	0.280		0.253		0.513	0.908
96	0.393		0.340		0.700	1.239
97	0.560		0.467			
98	0.813		0.660			
98.5	(1.000)					

RH	M8A2		M8B2		M8C2		Mean
%	x	ψ	x	ψ	x	ψ	ψ
50	0.087	0.067			0.080	0.086	0.077
60	0.147	0.114			0.127	0.137	0.126
65	0.173	0.134			0.147	0.159	0.147
70	0.200	0.155			0.167	0.180	0.168
75	0.227	0.175			0.193	0.208	0.192
80	0.247	0.191			0.227	0.245	0.212
84	0.280	0.216			0.260	0.281	0.248
86	0.300	0.232			0.293	0.316	0.277
88	0.327	0.253			0.333	0.360	0.318
90	0.373	0.288			0.393	0.424	0.379
91	0.413	0.319			0.433	0.468	0.420
92	0.460	0.356			0.480	0.518	0.472
93	0.527	0.407			0.540	0.583	0.542
94	0.613	0.474			0.613	0.662	0.626
95	0.747	0.577			0.707	0.764	0.750
96					0.820	0.886	1.063
97							
98							
98.5							

APPENDIX C(10)
Cement paste w$_o$/C 0.5

RH	P5A1		P5B1		P5C1	
%	x	ψ	x	ψ	x	ψ
50	0.160	0.162	0.153	0.173	0.147	0.216
60	0.247	0.250	0.227	0.257	0.233	0.342
65	0.300	0.304	0.267	0.302	0.273	0.400
70	0.347	0.352	0.300	0.339	0.327	0.479
75	0.393	0.399	0.340	0.384	0.427	0.626
80	0.467	0.474	0.407	0.460	0.540	0.792
84	0.553	0.561	0.507	0.573	0.627	0.919
86	0.600	0.608	0.567	0.641	0.673	0.987
88	0.653	0.662	0.633	0.715		
90	0.707	0.717	0.700	0.791		
91	0.740	0.750	0.733	0.828		
92	(0.773)	(0.784)	(0.773)	(0.873)		
93	(0.807)	(0.818)	(0.813)	(0.919)		
94	(0.847)	(0.859)	(0.853)	(0.964)		
95	(0.887)	(0.899)	(0.900)	(1.017)		
96	(0.940)	(0.953)	(0.953)	(1.077)		
97	(1.000)	(1.014)	(1.000)	(1.130)		

RH	P5A2		P5B2		P5C2		Mean
%	x	ψ	x	ψ	x	ψ	ψ
50	0.193	0.149	0.167	0.203	0.167	0.230	0.188
60	0.280	0.216	0.267	0.325	0.233	0.322	0.285
65	0.320	0.247	0.320	0.390	0.273	0.377	0.337
70	0.367	0.284	0.367	0.447	0.320	0.442	0.391
75	0.480	0.371	0.420	0.512	0.373	0.515	0.468
80			0.480	0.585	0.440	0.607	0.584
84			0.540	0.658			0.678
86			0.573	0.698			0.734
88			0.620	0.755			0.711
90			0.687	0.837			0.782
91			0.727	0.885			0.821
92			0.773	0.942			(0.866)
93			0.833	1.015			(0.917)
94							(0.912)
95							(0.958)
96							(1.015)
97							(1.072)

APPENDIX C(11)
Cementpaste w_o/C 0.6

RH	P6A1		P6B1		P6C1	
%	x	ψ	x	ψ	x	ψ
50	0.133	0.206	0.140	0.248	0.113	0.244
60	0.213	0.330	0.227	0.402	0.187	0.403
65	0.247	0.382	0.273	0.483	0.220	0.474
70	0.287	0.444	0.320	0.566	0.267	0.576
75	0.347	0.537	0.380	0.673	0.313	0.675
80	0.420	0.650	0.453	0.802	0.380	0.819
84	0.493	0.763	0.533	0.943	0.447	0.964
86	0.540	0.836	0.593	1.050	0.493	1.063
88	0.593	0.918	0.660	1.168	0.540	1.164
90	0.660	1.022	0.733	1.297	(0.600)	(1.294)
91	0.693	1.073	0.773	1.368	(0.633)	(1.365)
92	(0.733)	(1.135)	0.813	1.439	(0.667)	(1.438)
93	(0.773)	(1.197)			(0.713)	(1.537)
94	(0.820)	(1.269)			(0.767)	(1.654)
95	(0.867)	(1.342)			(0.820)	(1.768)
96	(0.913)	(1.413)			(0.880)	(1.897)
97	(0.967)	(1.497)			(0.947)	(2.042)
97.6	(1.000)	(1.548)			(1.000)	(2.156)

RH	P6A2		P6B2		P6C2		Mean
%	x	ψ	x	ψ	x	ψ	ψ
50	0.147	0.222	0.107	0.242	0.120	0.311	0.246
60	0.227	0.343	0.173	0.391	0.193	0.499	0.395
65	0.273	0.412	0.200	0.453	0.227	0.587	0.465
70	0.313	0.473	0.233	0.527	0.260	0.673	0.543
75	0.367	0.554	0.267	0.604	0.300	0.776	0.637
80	0.433	0.654	0.307	0.695	0.347	0.898	0.753
84	0.500	0.755	0.353	0.799	0.400	1.035	0.877
86	0.547	0.826	0.393	0.889	0.433	1.121	0.964
88	0.600	0.906	0.433	0.980	0.473	1.224	1.060
90	0.667	1.007	0.480	1.086	0.520	1.346	1.175
91	0.707	1.068	0.513	1.161	0.553	1.431	1.244
92	0.747	1.128	0.553	1.251	0.587	1.519	1.318
93	0.793	1.197	0.600	1.358	0.633	1.638	1.385
94	(0.840)	(1.268)	0.667	1.509	0.700	1.812	(1.502)
95	(0.887)	(1.339)	0.733	1.659	0.773	2.001	(1.622)
96	(0.940)	(1.419)	0.833	1.885	0.880	2.277	(1.778)
97	(1.000)	(1.510)	(0.927)	(2.098)	(1.000)	(2.588)	(1.947)
97.6			(1.000)	(2.263)			(1.989)

APPENDIX D

The fundamental flow potential graphical

In this APPENDIX the fundamental flow potentials are graphical-
ly shown as functions of the relative humidity. The mean, maxi-
mum and minimum fundamental flow potentials for specimens of
the same quality are shown. The mean fundamental flow potential
is the average for up to 6 specimens. The maximum fundamental
flow potential is the highest measured curve for up to 6
specimens. The minimum fundamental flow potential is the lowest
measured fundamental flow potential for up to 6 specimens.

Concrete w_o/C 0.4 (C4)

Ψ (gram/(m * day))

RH (%)

Concrete w_o/C 0.5 (C5)

Ψ (gram/(m * day))

RH (%)

Concrete w_o/C .0.6 (C 6)

Ψ (gram/(m * day))

RH (%)

Mean

Max

Min

Concrete w_o/C 0.7 (C7)

Ψ (gram/(m * day))

Max

Mean

Min

RH (%)

Concrete w_o/C 0.8 (C8)

Ψ (gram/(m*day))

RH (%)

Max

Mean

Min

Concrete w_o/C 0.8 (C8)

Mortar w_o/C 0.4 (M 0.4)

Ψ (gram/(m * day))

RH (%)

Mortar w_o/C 0.5 (M5)

Ψ (gram/(m * day))

RH (%)

Max

Mean

Min

Mortar w_o/C 0.6 (M6)

Ψ (gram/(m * day))

RH (%)

Max

Mean

Min

Mortar w_o/C 0.7 (M7)

Ψ (gram/(m * day))

RH (%)

Max

Mean

Min

Mortar w_o/C 0.8 (M8)

Ψ (gram/(m * day))

RH (%)

Max

Mean

Min

Cement paste w_o/C 0.5 (P5)

$\Psi\ (gram/(m * day))$

RH (%)

Max

Mean

$\bar{x}$(P5A1,P5B1)

Min

Cement paste w_o/C 0.6 (P6)

APPENDIX   E

Composite models of moisture transport in concrete

Hillerborg (1986) has proposed a simple composite model, which is given by Eq. (E.1).

$$\delta^n = V_1 * \delta^n + (1-V_1) * \delta^n \qquad\qquad (\text{ E.1 })$$

δ = the moisture permeability of the composite $\quad (m^2/s)$
δ_1 = the moisture permeability of component 1 $\quad (m^2/s)$
δ_2 = the moisture permeability of component 2 $\quad (m^2/s)$
V_1 = the volume content of component 1 $\quad 0<V_1<1 \quad$ (1)
n = a constant that depends on the ratio δ_1/δ_2,
$\quad$ where δ_1 is for the particle phase and
$\quad \delta_2$ is for the continuous phase

In concrete the cement paste is the continuous phase and the aggregate is the particle phase. Eq.(E.1) can also be used to calculate the coefficient of thermal conductivity or the modulus of elasticity of a composite material.

When a composite material consists of more than two phases you can first calculate δ for two phases. Then you can take this δ and combine with the third phase and so on. The procedure is shown later on.

When $n=1$ the model is the parallel model and with $n=-1$ it is the serial model. Normally n lies between -0.5 and $+0.5$. Hillerborg proposes n-values and they are shown in FIG E.1 as a function of log δ_1/δ_2. Hillerborg's proposed values are marked with +. The continuous lines are used in the calculations later on.
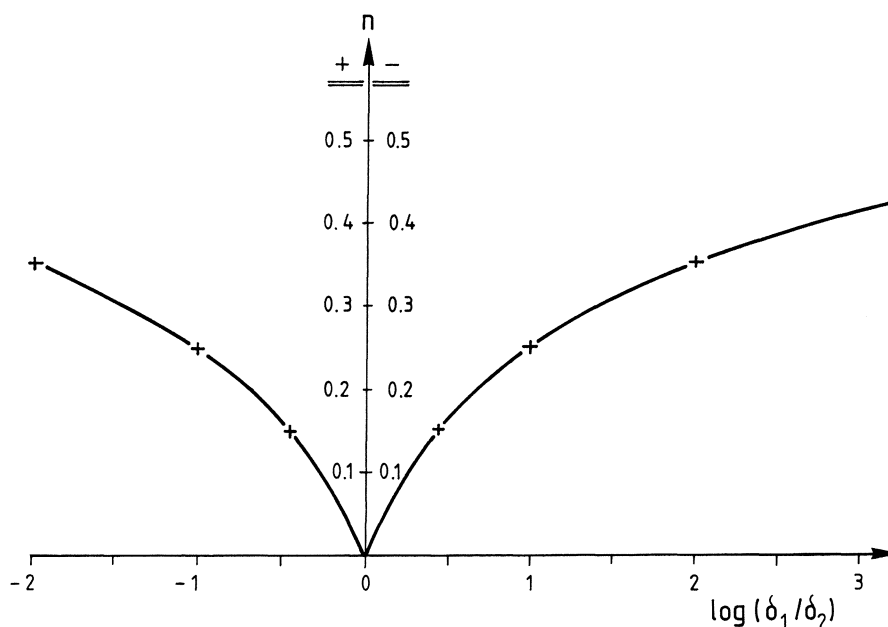
FIG E.1   The values of n as a function of log δ_1/δ_2.

E.1 **Moisture permeability of the aggregate including the interface zone**

The moisture permeability is measured for concrete and cement paste with w_o/C 0.6 as a function of the relative humidity (RH). With Eq. (E.1) it is possible to calculate the moisture permeability of the "aggregate". The moisture permeability of the aggregate is not only of the aggregate but it also includes the moisture permeability of the contact zone between the aggregate and the cement paste. The volume fraction of aggregate in our case is 0.68 (V_1). The moisture permeability for the cement paste is taken from FIG 9.2 and FIG 9.4. The moisture permeability for the concrete is taken from TABLE 7.1 the seventh column (up to 95 % RH) and TABLE 7.2 the fourth column (from 95 % RH). The calculations of the moisture permeabilities of the "aggregate" are shown in TABLE E.1.

TABLE E.1 Calulation of the moisture permeabilities of the "aggregate".

RH %	Paste $\delta_v * 10^6$ (m^2/s)	Concrete $\delta_v * 10^6$ (m^2/s)	n (-)	Aggregate $\delta_v * 10^6$ (m^2/s)	Aggregate $\delta_v/\delta v(33)$ (-)
1	2	3	4	5	6
33	1.0	0.17	0.29	0.046	1
65	1.0	0.17	0.29	0.046	1
70	1.0	0.19	0.28	0.059	1.28
75	1.41	0.27	0.27	0.086	1.87
80	1.83	0.38	0.26	0.13	2.8
84	2.44	0.57	0.25	0.23	5.0
86	2.77	0.73	0.24	0.32	7.0
88	3.42	0.98	0.22	0.47	10.2
90	4.3	1.5	0.20	0.84	18.3
91	4.7	1.9	0.18	1.17	25.4
92	5.7	2.4	0.17	1.5	33
93	6.4	3.2	0.13	2.3	50
94	7	4.8	0.09	4	87
95	8.5	7.5	0.06	7	152
96	10	8.5	0.04	8	172
97	13.5	14	-0.03	14	309
97.6	16.8	22.5	-0.09	26	563

In column 4 the chosen values of n are according to FIG 5.1. In column 5 the calculated δ_v are of the "aggregate". When comparing columns 2 and 5 it is seen that at low RH:s δ_v of the "aggregate" is much lower than δ_v of the cement paste (about 5 %). At saturation (97.6 % RH) δ_v of the "aggregate" is in the same magnitude as δ_v of the cement paste. This means that the "aggregate" is as permeable as the cement paste. In column 6 is the quotient between the actual δ_v and δ_v at 33 % RH of the "aggregate". At saturation the quotient is about 600.

E.2 A model for the moisture permeability of concrete

The solid aggregate is considered to be impermeable and all
moisture transport in connection with the aggregate takes place
in the contact zone between the aggregate and the cement paste.
One aggregate grain with its boundary zone is shown in FIG E.2.
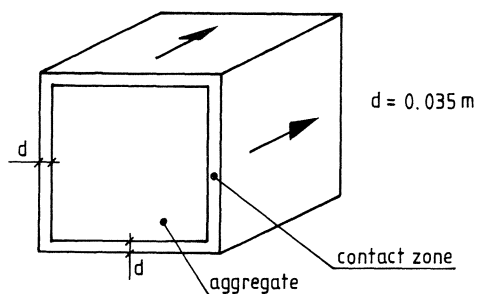
FIG E.2 A cubical aggregate with its contact zone.

All the aggregates are assumed cubic. In FIG 12.4 the porosity
and thickness of the interfacial zone for a 10-week-old
specimen with w_o/C 0.5 are shown. The same values of the
porosity and the thickness are assumed for w_o/C 0.6. The
average porosity is 17 %. All the different sizes of aggregates
are supposed to have the same thickness of the interfacial zone
(d=0.035 mm.). The moisture flow in the interfacial zone is
considered as unidimensional and takes place on 4 sides of the
6 sides of the aggregate (4/6 in Eq. (E.2)). There are pores in
the contact zone and only 1/3 of them are considered to be in
the flow direction. (1/3 in Eq. (E.2)). The other 2/3 of the
pores in the contact zone are considered to be in the
perpendicular directions. In TABLE E.2 the calculated
properties of the "aggregate" are shown.

TABLE E.2 Calculated properties of the "aggregate".

Sieve size mm.	% mater. pass. each sieve (M)	ΔM %	Weight kg/m^3	Porosity in the flow direct. (P) –	P –	$\delta_v * 10^6$ m^2/s	Volume fract. –	Fract number
1	2	3	4	5	6	7	8	9
0.125	4	4		0.0278				
		11	109		0.0238	0.595	0.0411	1
0.25	15			0.0198				
		17	168		0.0161	0.403	0.0634	2
0.5	32			0.0123				
		20	198		0.00962	0.241	0.0747	3
1	52			0.00694				
		20	198		0.00532	0.133	0.0747	4
2	72			0.00370				
		15	149		0.00281	0.0703	0.0562	5
4	87			0.00192				
		13	129		0.00145	0.0363	0.0487	6
8	100			0.00098				
8	0			0.00098				
		50	405		0.00081	0.0204	0.1528	7
12	≈50			0.00065				
		50	405		0.00055	0.0136	0.1528	8
18	100			0.00044				

The porosity in the flow direction is calculated as

$$P = \frac{(\text{sieve size}+2d)^3 - (\text{sieve size})^3}{(\text{sieve size}+2d)^2} \quad 4/6 * 0.17 * 1/3 \quad (E.2))$$

The moisture permeability of the aggregate is calculated with the parallel model

$$\delta_v = \Delta P * \delta_v(\text{contact zone}) \qquad\qquad (E.3)$$

The moisture permeability in the interfacial zone at low RH is the same as in air ($25 * 10^{-6}$). From 70 % RH the calculated δ_V at 33 % RH is increased with the factor given in TABLE E.1 column 6. This is done because at higher RH:s there are also other transport mechanisms than pure diffusion.

The moisture permeability of the concrete is calculated with Eq.(E.1). First the resulting δ_V of the cement paste and fraction number 1 is calculated. With this δ_V and δ_V of fraction 2 the resulting δ_V is calculated and so on. The results of the calculations are shown in TABLE E.3.

TABLE E.3 "Theoretical" moisture permeability of concrete with w_o/C 0.6.

Fract. number	V_1 in eq. (E.1)	$\delta_V * 10^6$ (m^2/s) RH (%)					
		65	80	86	90	93	95
C-past		1.0	1.83	2.77	4.3	6.4	8.5
1	0.109	0.946	1.811	2.895	4.737	7.374	10.40
2	0.144	0.840	1.692	2.884	5.046	8.455	12.95
3	0.145	0.711	1.492	2.683	4.949	8.899	14.93
4	0.127	0.591	1.275	2.369	4.539	8.579	15.52
5	0.087	0.509	1.113	2.106	4.109	7.975	15.03
6	0.070	0.444	0.980	1.874	3.695	7.285	14.08
7	0.180	0.301	0.675	1.319	2.662	5.423	11.07
8	0.153	0.22	0.49	0.98	2.0	4.2	8.9

The model used in the calculations is very simple, but it gives a qualitative understanding. At low RH, below about 80 %, all fractions of aggregate decrease the moisture permeability. When RH is over about 80 % the smallest aggregates (the contact zone) are more permeable than the cement paste. The higher RH is, the more permeable the aggregates are.

In FIG E.3 the measured moisture permeabilities of cement paste and concrete with w_o/C 0.6 are shown. The "theoretical" δ_v according to TABLE E.3 is also shown.
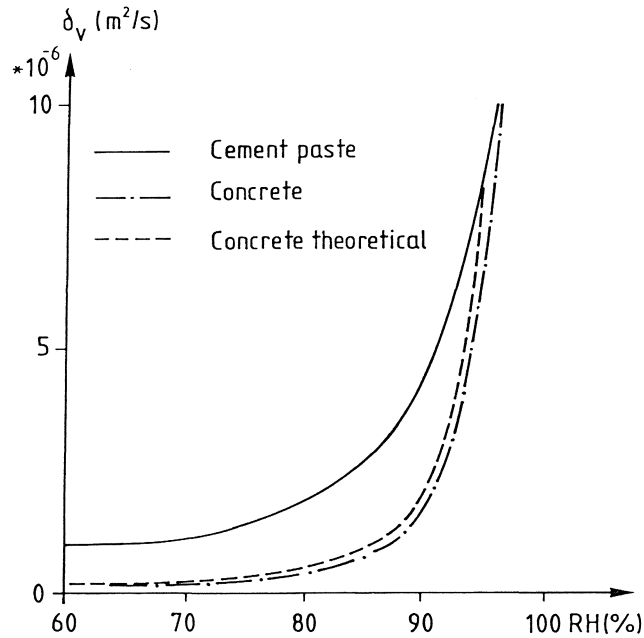
FIG E.3   Moisture permeabilities of concrete and cement paste
as functions of the relative humidity. Measured and
theoretical curves. w_o/C 0.6.

In FIG E.3 it is shown that δ_v of cement paste at low RH is about 5 times bigger than δ_v of concrete. About 95 % RH δ_v of concrete and cement paste are the same. The theoretical δ_v of concrete closely follows the measured curve. The theoretical δ_v is not purely "theoretical" since the quotients in column 6 in TABLE E.1 are used as input data in the calculation of δ_v and the quotients are calculated from measured δ_v of concrete and cement paste.

E.3 Effect of different amounts of air in the concrete

In section E.2 it was assumed that the moisture permeability of
the aggregate is proportional to the average porosity of the
interfacial zone. In normal concrete the air content is about 2
%, which is the same as 6.25 % air content of the cement paste.
This amount of air will probably influence the interfacial zone
equally. The average porosity of the interfacial zone is 17 %.
If it is assumed that 6.25 % of this porosity depends on the
air content, there is about 11 % porosity in the contact zone
when it has no air.

In concrete with 10 % air the air content in the cement paste
is 31 %. It is assumed that this air content is equally
distributed in the cement paste including the contact zone. The
porosity of the contact zone is then 31+11=42 %. As the
moisture permeability of the aggregate is assumed to be
proportional to the porosity in the interfacial zone, the
permeability of the aggregate is multiplied by 42/17 when
comparing 10 % air with 2 % air.

The moisture permeability of the cement paste is also
calculated with Eq. (E.1). δ_v of the air is $25 * 10^{-6}$ m^2/s. The
water-cement ratio of the concrete is 0.7. It is supposed that
the contact zone has the same porosity when w_o/c is 0.7
compared to w_o/C 0.5.

First the moisture permeability of the cement paste is
calculated when it has 6.25 % air and then with no air. δ_v of
the aggregate and the cement paste with different amounts of
air are then calculated. The results are shown in TABLE E.4.

TABLE E.4 Calculated δ_V in concrete with different amounts of air.

RH	$\delta_V * 10^6$ (m²/s)				Increase in δ_V (%)		
%	air 2%	air 6%	air 8%	air 10%	air 6%	air 8%	air 10%
33	0.17	0.25	0.30	0.35	50	75	105
65	0.17	0.25	0.30	0.35	50	75	105
70	0.19	0.28	0.33	0.39	50	76	108
75	0.27	0.40	0.48	0.56	50	77	108
80	0.38	0.57	0.68	0.79	50	77	107
84	0.57	0.85	1.00	1.16	50	77	104
86	0.73	1.10	1.29	1.49	50	76	104
88	0.98	1.47	1.72	1.99	50	76	104
90	1.51	2.3	2.7	3.1	50	76	103
92	2.4	3.6	4.2	4.9	50	76	101
94	4.8	7.3	8.5	9.7	51	76	102
96	9.5	14.1	16.5	18.4	49	71	94
97	17.5	25.5	29	32	45	65	84
97.6	28.5	42	46	51	43	61	80
98	37.5	53	60	65	42	59	75

In TABLE E.4 it is shown that δ_V increases about 25 % when the air content of the concrete increases 2 %. At high RH (about 96 to 98 %) the increases in δ_V are not so big as for lower RH. $\delta_V^{mean,1}$ as a function of the air content in the concrete is calculated with δ_V according to TABLE E.4 and the results are shown in FIG 7.11. The results of the calculations are adjusted to coincide with the linear regression line at 2 % air content of the concrete.

APPENDIX F

A complete set of moisture data for concrete with different water-cement ratios

The moisture data presented in this Appendix are for the concrete qualities shown in TABLE 3.1.

The moisture data are for concrete with about 0.1 m thickness in the flow direction and drying from one side. For other dimensions, see Chapter 10.

Note; different scales in the figures.

δv = moisture permeability with regard to humidity by volume in the pores of the specimen

RH = relative humidity

w_e = evaporable moisture content mass by volume

ψ = fundamental flow potential

C_ψ = moisture capacity factor; $(C(\psi) = dw/d\psi$

Concrete w_o/C 0.4 (C4)

w_e (kg/m³)

$(kg/(m*s))$

$40 * 10^{-10}$ 30 20 10   0 10 20 30 40 50 60 70 80 90 100 (%)

ψ

ϕ

$* 10^9$ $* 10^{-6}$

$C_\psi (s/m^2)$ $d_v (m^2/s)$

239

Concrete w_o/C 0.5 (C5)

w_e (kg/m³)

$(kg/(m*s))$

$80*10^{-10}$ 60   40   20   10   20   30   40   50   60   70   80   90   100 (%)

ψ

ϕ

$C_\psi(s/m^2)$ $\delta_v(m^2/s)$

240

Concrete w_o/C .0.6 (C6)

w_e (kg/m³)

$(kg/(m*s))$

ψ

ϕ

$C_\psi(s/m^2)$

δ_v (m²/s)

241

Concrete w_o/C 0.7 (C7)

w_e (kg / m^3)

(kg /(m*s))

Ψ

ϕ (%)

C_Ψ(s/m^2) δ_v(m^2/s)

Concrete w_o/C 0.8 (C8)

w_e (kg/m³)

(kg/(m*s))

ψ

C_ψ (s/m²) δ_v (m²/s)

243
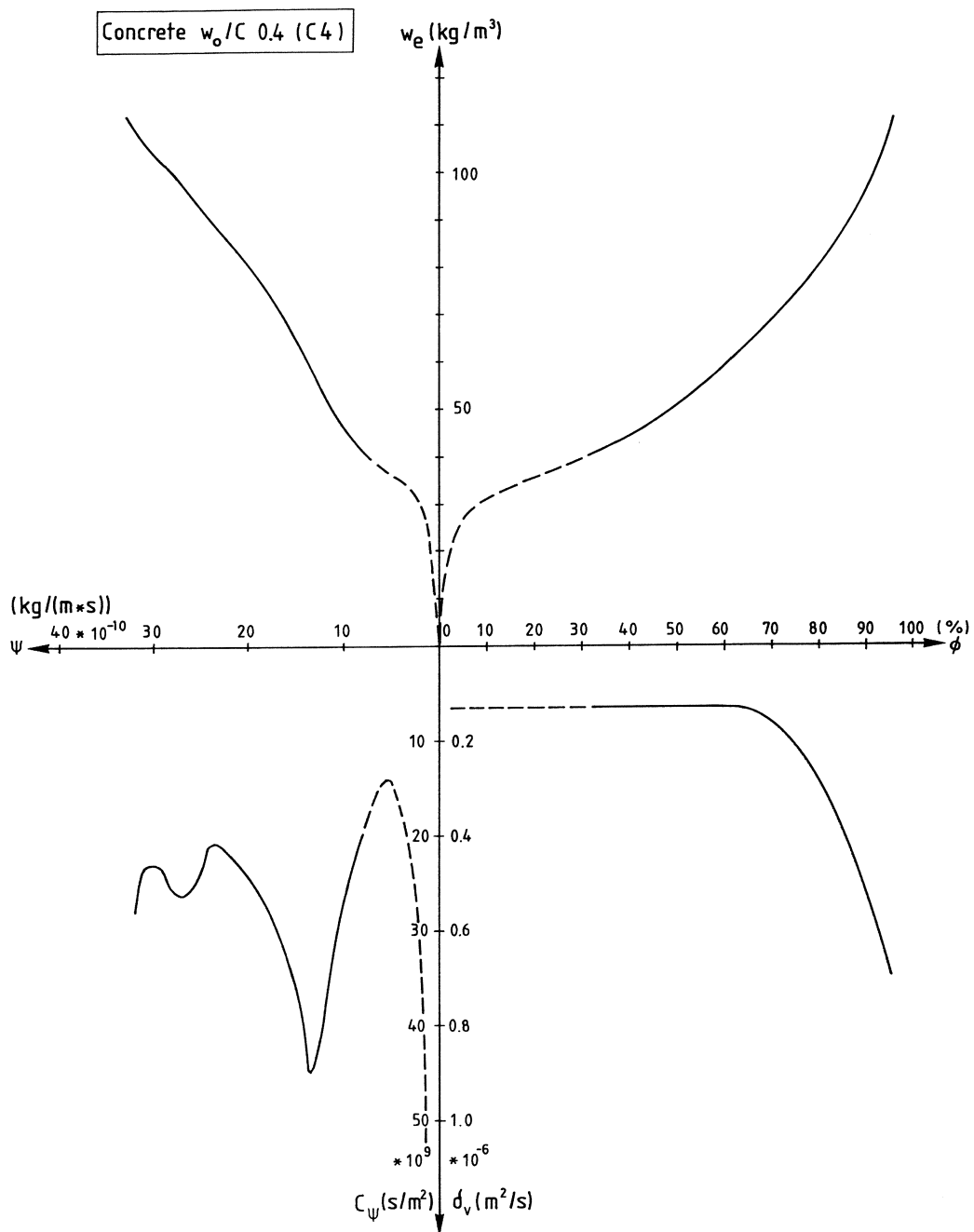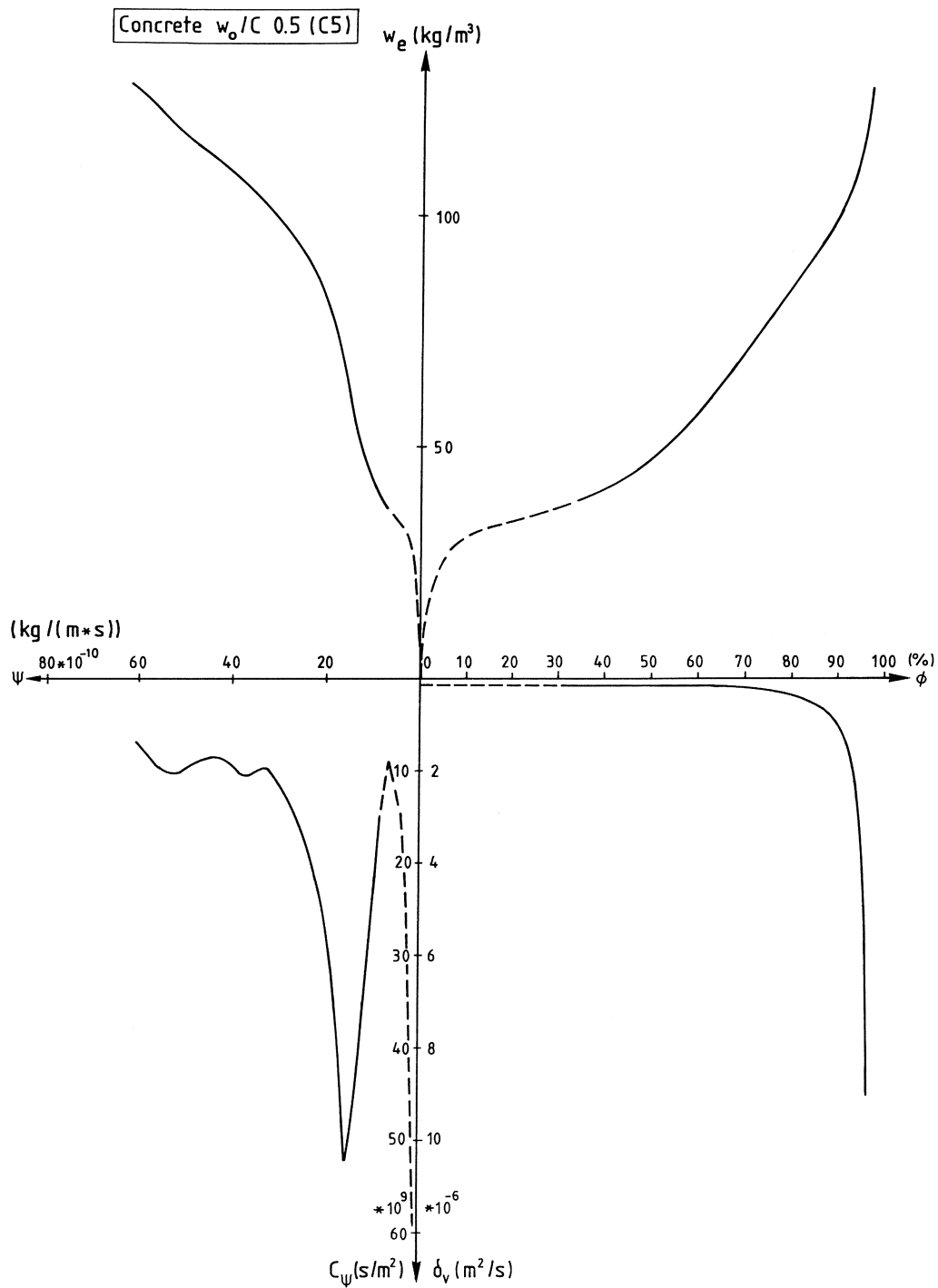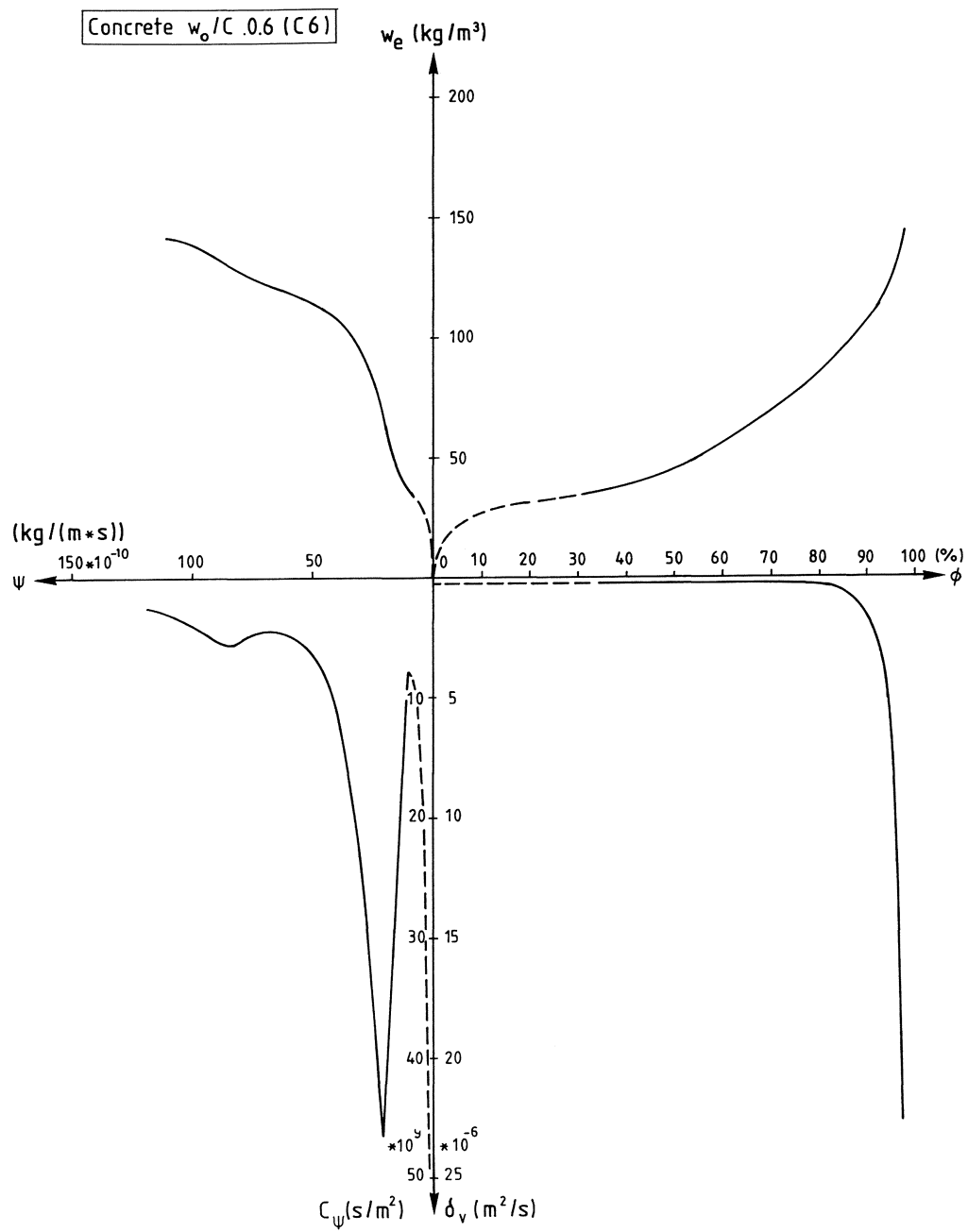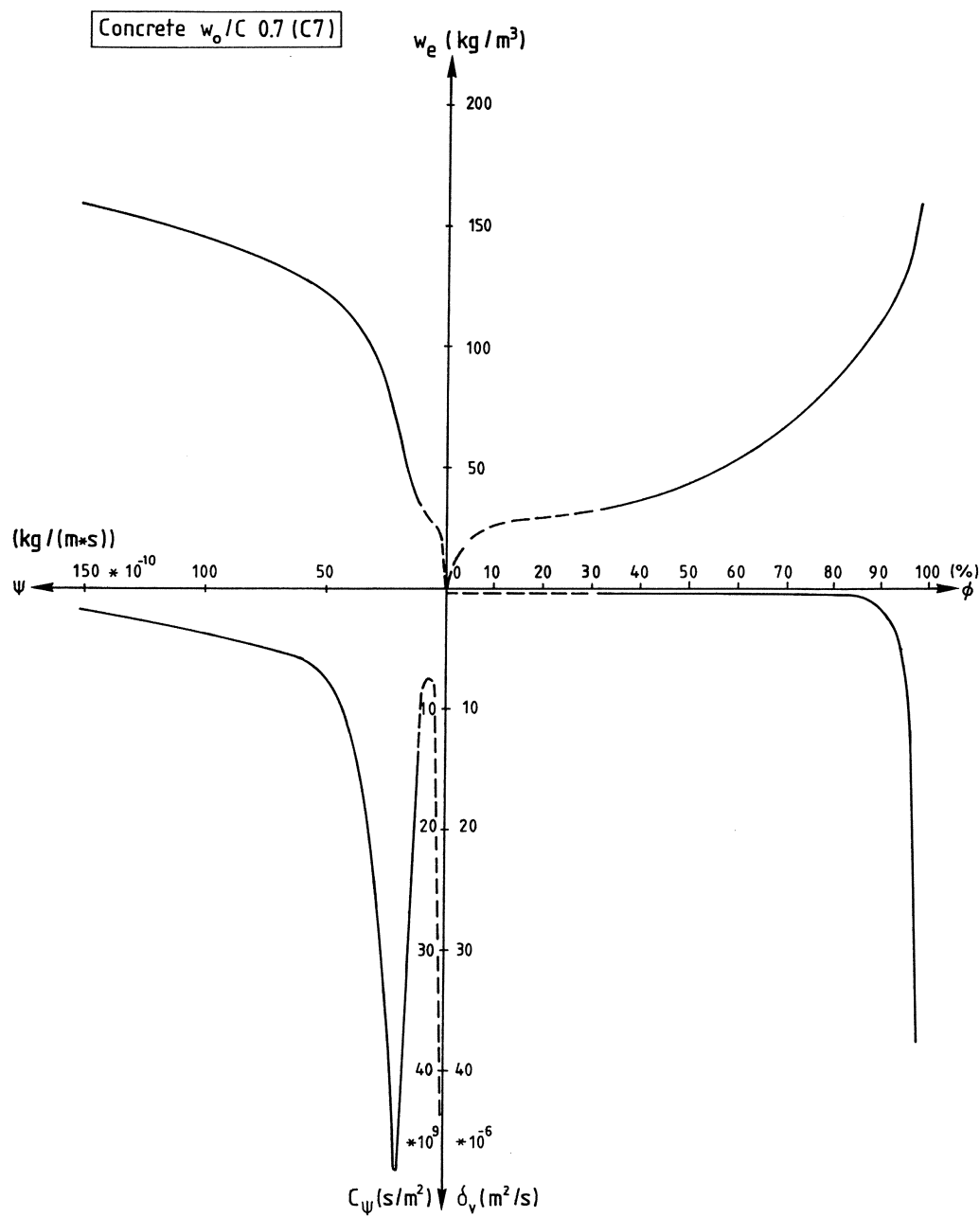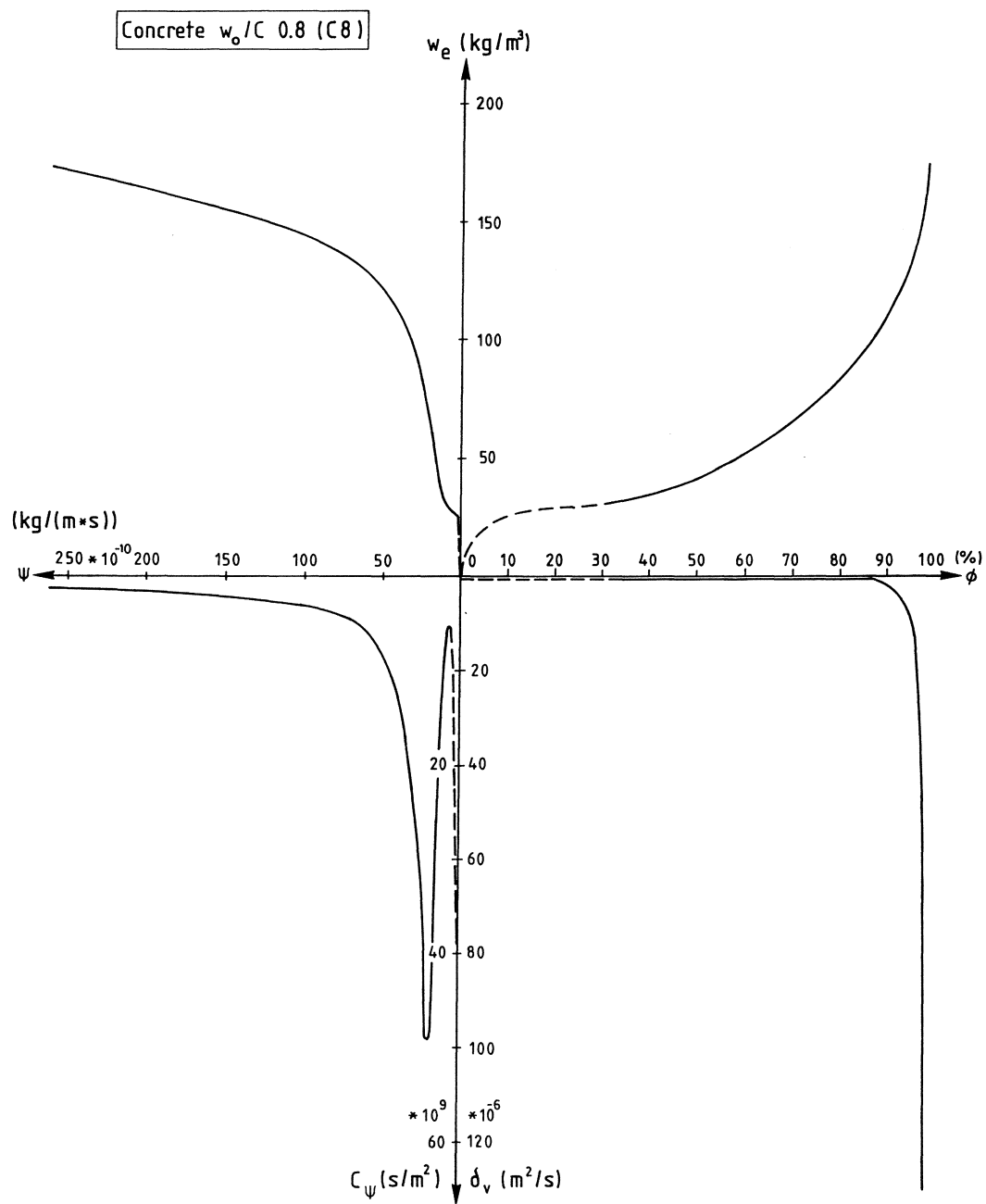
REFERENCES

Andersson, A.-C. (1985) Verification of calculation methods for moisture transport in porous building materials. Swedish Council for Building Research, Stockholm, Document D6:1985.

Arfvidsson, J. (1989) Computer model for two-dimensional moisture transport, Manual for JAM-2. Lund Institute of Technology, Dept. of Building Technology, Lund.

Arfvidsson, J. & Claesson, J. (1989) A PC-based method to calculate moisture transport, heat and mass transfer in building materials and structures, editors Chaddock, J. B. & Todorvic, B. Hemisphere Publishing Corporation.

Bažant, Z. P. & Najjar, L. J. (1972) Nonlinear water diffusion in nonsaturated concrete, Matr. & Constr. Vol.5 No 25, pp 3-20.

Bertelsen, N. H. (1983) Diffusion measurements on European spruce with the cup method (in Danish). Technical University of Denmark, Building Materials Laboratory, Technical Report 129/83.

Carman, P. C. (1956) Flow of gases through porous media, Butterworths Scientific Publications, London.

Claesson, J. (1987), Notes on potentials to moisture flow, Lund Institute of Technology, Dept. of Building Technology, Lund.

Claesson, J. (1990) Private communication.

Crank, J. (1975) The mathematics of diffusion, Oxford University Press, Oxford, UK.

Dacey, J. R. (1965) Surface diffusion of adsorbed molecules,
     Industrial and engineering chemistry, Vol 57, No 6,
     pp 26-33.

Dullien, F. A. L. (1979) Porous media fluid transport and pore
     structure, Academic Press.

Eisenhart, C. (1963) Realistic evaluation of the precision and
     accuracy of instrument calibration systems, J. Res. Nat.
     Bur. stand.-c (v.s.), Engineering and Instrumentation,
     vol. 67 c, No 2, pp 161-187.

Eisenhart, C. (1968) Expression of uncertainties of final
     results, Science, Vol 160, No 3833, pp 1201-4.

Fagerlund, G. (1976) The critical degree of saturation method -
     a general method of estimating the frost resistance of
     material and structures (in Swedish). Swedish Cement and
     Concrete Research Institute, Stockholm, report 12:76.

Fagerlund, G. (1982) Concrete Handbook (in Swedish), Part:
     Material, AB Svensk Byggtjänst, Stockholm.

Flood, E. A., Tomlinson, R. H. & Leger, A. E. (1952) The flow
     of fluids through activated carbon rods, Part I to III,
     Canadian Journal of Chemistry, Vol. 30, pp 348-410.

Garrecht, H., Hilsdorf, H. K. Kropp, J. (1990) Hygroscopic
     salt influence on the moisture behaviour of structural
     elements, Durability of building materials and components,
     Proceedings of the Fifth International Conference held in
     Brighton, UK, 7-9 November 1990. E & F. N. SPON, An
     imprint of Chapman and Hall.

Gilliland, E. R. Baddour & Russel, J. L. (1958) Rates of flow
     through microporous solids, American Institute of Chemical
     Eng. 4/1958, pp 90-96.

Greaves, P. (1986) Calibration to salt systems for RH measurement. Humidity sensors end their calibration, Conference Proceedings, National Physical Laboratory, UK.

Greenspan, L. (1977) Humidity fixed points of binary saturated aqueous solutions. J. Res. Nat. Bur. Stand., (U.S.), Vol. 81 A, No 1, pp 89-96.

Grove, D. M. (1967) Permeability and flow studies, Porous carbon solids, Edited by Bond, R. L., Academic press, London.

Hagentoft, C.-E. (1989) Numerical studies on the edge-effect, private notes.

Harderup, L.-E. (1991) Concrete slab on the ground and moisture control. Lund Institute of Technology, Department of Building Physics, Lund, Report TVBM-1005.

Hedenblad, G. (1988) Effect of soluble salt on the sorption isotherm, Lund Institute of Technology, Division of Building Materials, Lund, Report TVBM-3035.

Hedenblad, G. & Roszak, W. (1991) Coefficients of moisture transport of some building materials, preliminary (in Swedish), Internal report, Lund Institute of Technology, Division of Building Materials, Lund.

Hillerborg, A. (1986) Compendium of building materials FK (in Swedish), Lund Institute of Technology, Division of Building Materials, Lund.

Hägg, G. (1963) Common and inorganic chemistry (in Swedish), Almqvist & Wiksell, Stockholm.

Joy, F. A. & Wilson, A. G. (1965) Standardization of the dish method for measuring water vapour transmission, Humidity and Moisture, editor Wexler, A., Reinhold Publ., New York,

Vol. 4, pp 259-270.

Kohonen, R. (1984), A method to analyze the transient hygro-
    thermal behaviour of building materials and components,
    VTT Technical Research Centre of Finland, Publ. 21.

Kropp, J. (1983) Carbonation and transport in cement paste (in
    German), Thesis, Universität Karlsruhe.

Lafarie, J. P. (1988) Accuracy of relative humidity instru-
    ments, Energy Engineering, Vol. 85, nr 2 pp 42-49.

Mehta, K. (1986) Concrete; structure, properties and materials,
    Prentice-Hall, USA.

Monteiro, P. J. M., Maso, J. C., Ollivier, J. P. (1985) The
    aggregate-mortar interface, Cement and Concrete Research,
    Vol. 15, pp 953-958.

Nevander, L.-E. & Elmarsson, B. (1981) Moisture handbook (in
    Swedish). AB Svensk Byggtjänst, Stockholm.

Nilsson, L.-O. (1977) Moisture problems in concrete floors (in
    Swedish), Lund Institute of Technology, Division of Buil-
    ding Materials, Lund, Report TVBM-3002.

Nilsson, L.-O. (1980) Hygroscopic Moisture in Concrete -
    Drying, measurements and related material properties. Lund
    Institute of Technology, Division of Building Materials,
    Lund, Report TVBM-1003.

Nilsson, L.-O. (1987) Temperature effects in relative humidity
    measurements on concrete - some preliminary studies. Lund
    Institute of Technology, Dept. of Building Science, Lund,
    Fuktgruppen informerar 1987:1, pp 79-85

Peterson, O. (1987) Estimation of basicity in portland cement concrete, Internal report (in Swedish), Lund Institute of Technology, Division of Building Materials, Lund.

Pihlajavaara, S. E. (1965) On the main features and methods of investigation of drying and related phenomena in concrete. State Inst. for Techn. Research, Helsinki, Ph.D. Thesis, Publ. No 100.

Powers, T. C. (1960) Physical properties of cement paste, Proceedings of the Fourth International Symposium on the chemistry of cement, paper v-1, pp 577-613.

Quenard, D. (1989) Adsorption and moisture transfer in hygroscopic materials (in French), Thesis, Institut National Polytechnique de Toulouse, France, No 290.

Radjy, F. (1974) Moisture transport in microporous substances, Part 1, Journal of Materials Science 9, pp 744-752.

Robinson & Stokes (1955) Electrolyte solutions. Butterworth, London.

Sahlén, S. (1985) Examination of the moisture state of the cellar floor at Bredgatan, Lund. (In Swedish). Internal report. Lund Institute of Technology, Division of Building Materials, Lund.

Sakata, K. (1983) A Study on moisture diffusion in drying and drying shrinkage of concrete, Cement & Concrete Research, Vol. 13, No 2, pp 216-224.

Scrivener, K. L. (1989) The microstructure of concrete, Materials Science of Concrete, editated by Skalny, J. P., The American Ceramic Society, Inc., (USA).

Sörensen, E. G. (1980) Water vapour permeability of hardened
    cement paste, Technical University of Denmark, Department
    of Civil Engineering, Building Materials Laboratory, Tech-
    nical report 83/80.

Vos, B. H. & van Minnen, J. (1966) Moisture transport in porous
    materials, Institute TNO for Building Materials and Buil-
    ding Structures, Netherlands, Report II-11/23 n 5.

Wadsö, L. (1992) A critical review on anomalous or non-Fickian
    vapour sorption, Lund Institute of Technology, Division of
    Building Materials, Lund, report TVBM-7017.

Wallenten, P. (1989) SCTRANS a Schwarz-Christoffel transform
    finding program. Notes on heat Transfer 5-88, Lund Insti-
    tute of Technology, Dept. of Building Technology, Lund.

Wierig, H.-J. (1965) The permeability of cement mortar and
    concrete to water vapour (in German), Zement-Kalk-Gips
    Nr 9/1965.

Zimbelmann, R. (1985) A contribution to the problem of cement-
    aggregate bond, Cement and Concrete Research. Vol 15,
    pp 801-808.

"Absolute certainty is a privilege of uneducted
minds and fanatics. It is, for scientific folk,
an unattainable ideal."

(Keyser)